

N67-31305

FACILITY FORM 902

(ACCESSION NUMBER)

123

(PAGES)

CR-85873

(NASA CR OR TMX OR AD NUMBER)

(THRU)

1

(CODE)

07

(CATEGORY)


Report No. P67-82
HAC Ref. No. A7747

Sixth Quarterly Report
for
PARAMETRIC ANALYSIS OF MICROWAVE AND LASER SYSTEMS
FOR COMMUNICATION AND TRACKING

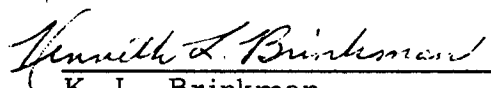
(6 December 1966 – 6 March 1967)

Contract No. NAS 5-9637

Prepared by
Aerospace Group
Hughes Aircraft Company
Culver City, California



L. S. Stokes
Program Manager



K. L. Brinkman
Associate Program Manager

for
Goddard Space Flight Center
Greenbelt, Maryland

HUGHES AIRCRAFT COMPANY
COPYRIGHT © 1967

CONTENTS

		Current Issue
SUMMARY	iii	6 March 67
1.0 INTRODUCTION	1-1	6 March 67
2.0 COMMUNICATION SYSTEMS OPTIMIZATION METHODOLOGY APPENDICES	A2.1-1	6 March 67
14.0 HEAT REJECTION SYSTEMS	14-1	6 March 67

SUMMARY

PROGRAM STATUS

The National Aeronautics and Space Administration, in its space exploration program, has promoted space communications through hardware development and technical studies. August 6, 1965, the Goddard Space Flight Center, NASA, awarded the Hughes Aircraft Company a study contract for Parametric Analysis of Microwave and Laser Systems for Communications and Tracking, NAS 5-9637.

This study contract has three basic purposes: first, to collect the information and conclusions of previous studies and present them in a readily accessible form. Secondly, to formulate a "Reference Data for Advanced Space Communications and Tracking Systems" which will contain: (1) a methodology for solving space communication and tracking problems, (2) parametric studies of the parameters involved in the methodology and, (3) a state-of-the-art documentation of the parameter values. Finally, the third major purpose of the study is to evaluate the capability and amenability to modification of the available world-wide communication and tracking system to the increased performance requirements of future microwave and optical communications systems.

The Parametric Analysis of Microwave and Laser Systems for Communication and Tracking is to be conducted in two phases. Phase I had a six-month duration and Phase II has a thirty-three month duration. The study is presently at the twelve-month point of Phase II. The present program plan for the study is indicated in Figure 1. For calendar 1966 and 1968 this plan indicates periodic updating and enlargement of the first issue of "Reference Data for Advanced Space Communication and Tracking Systems." During 1967 the majority of the low level program effort will be devoted to determining optimum solutions of space communication configurations.

SIXTH QUARTER EFFORT

During the sixth quarter effort was expended on refinement of portions of the Methodology section and updating of the "Heat Radiator Systems" section.

	1966				1967				1968			
	1	2	3	4	1	2	3	4	1	2	3	4
PHASE II PROGRAM PLAN SUBMITTED	Δ											
PHASE II GO-AHEAD	Δ											
UPDATING OF "REFERENCE DATA FOR ADVANCED SPACE COMMUNICATION AND TRACKING SYSTEMS"												
METHODOLOGY				*				*				*
MISSION ANALYSIS		*		*						*		*
COMMUNICATION THEORY			*							*		
TRANSMITTING POWER SOURCES		*							*		*	
DETECTORS			*							*		
MODULATORS		*							*		*	
ACQUISITION AND TRACKING		*	*							*	*	
RADIO FREQUENCY ANTENNAS			*								*	
OPTICS				*					*			*
PRIME POWER				*								
RADIATION BACKGROUND AND ATMOSPHERIC PROPAGATION		*								*		
GROUND RECEIVING SITES				*								*
HEAT RADIATORS					*				*			
SYSTEMS IMPLEMENTATION			*						*		*	*
COMMUNICATION SYSTEM PROBLEM SOLUTIONS												
QUARTERLY REPORTS				Δ	Δ	Δ	Δ	Δ	Δ	Δ	Δ	Δ
QUARTERLY REVIEW MEETINGS				Δ	Δ	Δ	Δ	Δ	Δ	Δ	Δ	Δ
FINAL REPORT												Δ

* TECHNICAL SECTION UPDATED

Figure 1. Program plan for Parametric Analysis of Microwave and Laser Systems for Communications and Tracking.

The Methodology, as given in the 6 December 1966 issue, provided a means of determining an optimum centerline design for a communications system. Optimization to date has been made on the basis of minimized cost.* However optimization on the basis of weight is easily implemented in the computer programmed optimization procedure by setting certain parameters to zero. The computer program accuracy is, of course, critically dependent upon the input data it receives. Much of this data is empirical. For example, the relationship between an antenna weight and its diameter is given the computer by the relationship

$$W_{d_T} = K_{d_T} (d_T)^{n_T} + W_{K_T}$$

* Since a dominant cost of space hardware is putting the payload in space, optimizing on the basis of cost, in essence, minimizes payload weight.

where

W_{d_T} is the antenna weight

d_T is the antenna diameter

n_T is a constant but not necessarily an integer

W_{K_T} is a fixed weight

The constants of this equation are determined empirically and programmed into the computer. During the past quarter better empirical data has been gathered for parameter values such as the antenna weight noted above. Perhaps more significant is the successful operation of three computer programs with the fractional exponents, e.g., $n_T = 2.3$. These programs are: (1) the optical direct, thermal noise limited, detection (TOP), (2) optical heterodyne detection (HOP), and (3) the radio receiver program (ROP). The Fortran IV computer printouts of these programs are given in this report in Appendices A2.5, A2.6, and A2.7 of Section 2.0, Methodology. Additional updated material is given as Methodology appendices in Appendices A2.1, Nomenclature; A2.2, Input Data Program; A2.3, Output Data Program.

The TOP, HOP, and ROP optimization programs have been used to calculate optimum system parameters for a Jupiter communication link. This was done for a carrier wavelength of 10.6 microns and a radio frequency of 2.3 GHz. While the data from these computer calculations must still be regarded as preliminary since sensitivity of the output data has not been correlated with input data and since the constants of the computer program input data have not yet been fully reviewed in all the technology areas, the data does provide very interesting comparisons and shows general trends.

The TOP, HOP, and ROP data is given in Figure 2, 3, and 4 and in Table 1. Figure 2 is a total cost comparison of the three systems made on the basis of an optimized minimum cost system. Booster cost and ground receiving system costs were considered in the optimization but only the spaceborne costs are shown in Figure 2. Figure 3 is a comparison of the spaceborne weights of these three systems which were selected on the basis of minimum cost. Figure 4 gives the variable parameter

values for the cost optimized systems. Figures 2, 3, and 4 are all plotted as a function of bit rate and assume a 14 db receiver signal to noise ratio.

Table 1 contains a tabulation of the weights of the three systems. The total weight noted in Table 1 corresponds to the values given in Figure 3.

The second major area of emphasis during the past quarter has been the updating and revising of Section 14.0, Heat Radiator Systems. The material of this section has been revised to incorporate more data into the graphics and now includes weight and cost burden relationships. These are being used in the Methodology to determine optimum communications systems configuration based upon minimum cost or minimum weight systems.

Cost and weight burden relationships for technology areas other than Heat Radiator Systems have been examined during the last quarter. These will be incorporated in future reports with the complete updating of the corresponding technology section.

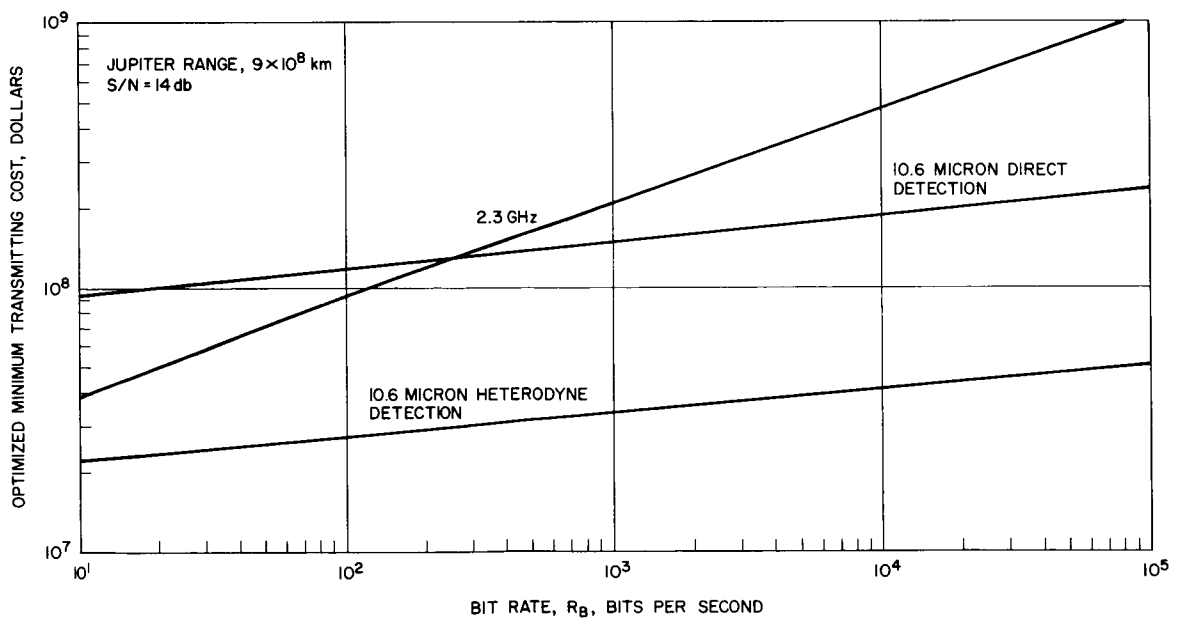


Figure 2. Spaceborne transmitting cost versus bit rate for an optimized minimum cost communication system at Jupiter range.

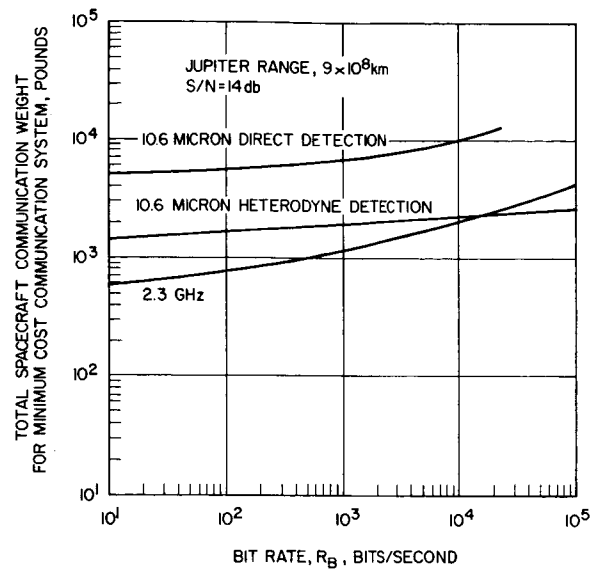
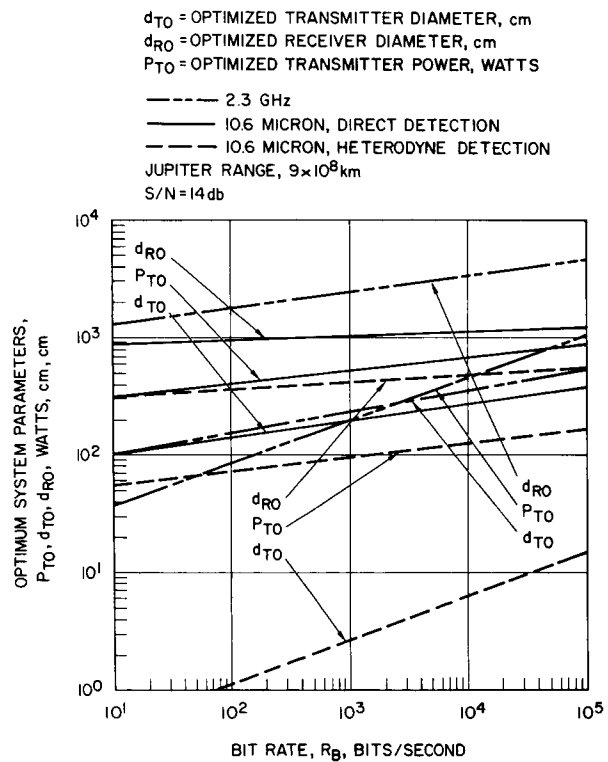


Figure 3. Total spaceborne weight of an optimized minimum cost communication system at Jupiter range.

Figure 4. System parameters versus bit rate for optimized minimum cost communication system at Jupiter range.



Bit Rate, R_B , bits/sec	Optimized Values (See Figure 3)			Telescope Weight, W_{dT} , lb	Transmitter Weight, W_T , lb	Power Supply Weight, W_{ST} , lb	Heat Exchanger Weight, W_H , lb	Acq. and Track System Weight, W_{QT} , lb	Modulator Weight, W_M , lb	Total Spacecraft Communication System, Weight, W_A , lb
	Transmitter Diameter, d_{TO} , cm	Receiver Diameter, d_{RO} , cm	Transmitted Power, P_{TO} , watts							
1.04×10^7	1263	8618	5608	689	566	17,711	416	527	0	19,908
1.55×10^6	893	6667	2804	344	285	9,087	208	268	0	10,193
1.26×10^5	565	4748	1122	138	117	3,912	83	113	0	4,363
1.02×10^4	357	3382	449	55	50	1,842	33	51	0	2,032
1.53×10^3	252	2616	224	28	27	1,152	17	31	0	1,254
695	219	2351	168	21	22	980	13	25	0	1,060
229	178	2023	112	14	16	807	8	20	0	866
34	126	1565	56	7	11	635	4	15	0	672

a. 2.3 GHz system.

Table 1. Optimum system parameters, weight, and total space communications system weight — Jupiter mission.

Bit Rate, R_B , bits/sec	Optimized Values (See Figure 3)			Telescope Weight, W_{dT} , lb	Transmitter Weight, W_T , lb	Power Supply Weight, W_{ST} , lb	Heat Exchanger Weight, W_H , lb	Acq. and Track System Weight, W_{QT} , lb	Modulator Weight, W_M , lb	Total Spacecraft Communication System, Weight, W_A , lb
	Transmitter Diameter, d_{TO} , cm	Receiver Diameter, d_{RO} , cm	Transmitted Power, P_{TO} , watts							
14,000	285	1226	702	835	1428	5758	442	2258	20	10,742
3,290	238	1115	590	590	1205	4835	372	1713	20	8,734
562	188	1003	484	377	992	3977	305	1242	20	6,913
61.5	136	891	387	209	799	3218	244	869	20	5,359
3.62	85.8	784	303	99	631	2594	191	623	20	4,158

b. 10.6 micron direct detection system.

Table 1. (continued)

Bit Rate, R_B , bits/sec	Optimized Values (See Figure 3)			Telescope Weight W_{dT} , lb	Transmitter Weight, W_T , lb	Power Supply Weight, W_{ST} , lb	Heat Exchanger Weight, W_H , lb	Acq. and Track System Weight, W_{QT} , lb	Modulator Weight, W_M , lb	Total Spacecraft Communication System, W_A , lb
	Transmitter Diameter, d_{TO} , cm	Receiver Diameter, d_{RO} , cm	Transmitted Power, P_{TO} , watts							
6.72×10^8	285	1226	702	835	1428	5758	442	2258	20	10,742
3.26×10^8	238	1115	590	590	1205	4835	372	1713	20	8,734
1.35×10^8	188	1003	484	377	992	3977	305	1242	20	6,913
4.46×10^7	136	891	387	209	799	3218	244	869	20	5,359
1.08×10^7	85.8	784	303	99	631	2594	191	623	20	4,158
1.71×10^6	44.5	685	234	45	492	2110	147	504	20	3,318
1.47×10^6	17.7	588	173	28	372	1718	109	467	20	2,714
4.49×10^3	4.63	479	116	25	257	1357	73	460	20	2,193
11.	0.464	339	58.7	25	142	998	37	460	20	1,682

c. 10.6 micron heterodyne detection system.

Table 1. (continued)

Report No. P67-82

FIFTH ISSUE

REFERENCE DATA FOR ADVANCED SPACE COMMUNICATION
AND TRACKING SYSTEMS

6 March 1967

Contract No. NAS 5-9637

Prepared by

Aerospace Group
Hughes Aircraft Company
Culver City, California

for

Goddard Space Flight Center
Greenbelt, Maryland

PRECEDING PAGE BLANK NOT FILMED.

CONTENTS

		Current Issue
1.0	INTRODUCTION	1-1 6 Mar 67
1.1	Purpose	1-1
1.2	Reference Data Format	1-2
1.2.1	Introduction	1-3
1.2.2	Theory	1-3
1.2.3	Performance	1-3
1.2.4	Burden Relationships	1-3
1.2.5	Nomenclature	1-3
1.2.6	References	1-4
1.3	Front Matter	1-4
2.0	COMMUNICATION SYSTEMS OPTIMIZATION METHODOLOGY	2-1 6 Dec 66
2.1	Introduction	2-1
2.2	Communication Components Analysis	2-1
2.3	Communication Systems Analysis	2-17
2.4	Systems Evaluation	2-18
2.5	Optical Communication Systems Optimization Example	2-36
2.6	Radio Communication Systems Optimization Example	2-61
APPENDICES		6 Mar 67
A2.1	Nomenclature	A2.1-1
A2.2	Input Data Program	A2.2-1
A2.3	Output Data Program	A2.3-1
A2.4	Shot Noise Limited Direct Detection Optical Receiver Optimization Program without Component Stops (SOP).	2-106
A2.5	Thermal Noise Limited Direct Detection Optical Receiver Optimization Program (TOP) without Component Stops	A2.5-1

A2.6	Heterodyne Detection Optical Receiver Optimization Program (HOP) without Component Stops	A2.6-1	
A2.7	Radio Receiver Optimization Program (ROP) without Component Stops	A2.7-1	
A2.8	Shot Noise Limited Direct Detection Optical Receiver Optimization Program with Component Stops (SOPS)	2-118	
A2.9	Thermal Noise Limited Direct Detection Optical Receiver Optimization Program (TOPS) with Component Stops	2-122	
A2.10	Heterodyne Detection Optical Receiver Optimization Program (HOPS) with Component Stops	2-123	
A2.11	Radio Receiver Optimization Program (ROPS) with Component Stops	2-124	
A2.12	Verification of Computer Optimization Procedure for a Shot Noise Limited Direct Detection Optical Receiver	2-125	
3.0	MISSION ANALYSIS	3-1	6 Dec 66
3.1	Introduction	3-1	
3.2	Probable Mission Objectives	3-1	
3.2.1	Unmanned Missions	3-1	
3.2.2	Manned Missions	3-1	
3.3	Communication System Requirements for Projected Missions	3-6	
3.3.1	Data Transmission Requirements	3-12	
3.3.2	Pointing Accuracy Requirements	3-17	
3.3.3	Communication Range	3-18	
3.3.4	Mission Duration	3-18	
3.3.5	Communication System Weight Restrictions	3-27	
3.4	Conclusion	3-29	
3.5	References	3-30	

		Current Issue
4.0	COMMUNICATION THEORY	4-1 6 Sept 66
	Preface	4-1
	Introduction	4-1
4.1	Detection	4-3
4.1.1	Detection Methods	4-3
4.1.2	Detection Noise	4-5
4.1.3	Detection Statistics	4-16
4.1.4	Optical Direct Detection	4-19
4.1.5	Optical Heterodyne Detection	4-23
4.1.6	Optical Homodyne Detection	4-31
4.2	Modulation	4-34
4.2.1	Modulation Methods	4-34
4.2.2	Optical Intensity Modulation	4-37
4.2.3	Optical Frequency Modulation	4-40
4.2.4	Optical PCM Intensity Modulation	4-40
4.2.5	Optical PCM Polarization Modulation	4-42
4.2.6	Optical PCM Frequency Modulation	4-45
4.2.7	Optical PPM Intensity Modulation	4-47
4.2.8	Radio Amplitude Modulation	4-50
4.2.9	Radio Frequency Modulation	4-50
4.2.10	Radio PCM Amplitude Modulation	4-50
4.2.11	Radio PCM Frequency Modulation	4-52
4.2.12	Radio PCM Phase Modulation	4-54
4.3	Communication Coding	4-55
4.3.1	Data Compression	4-55
4.3.2	Data Representation	4-57
4.3.3	Synchronization	4-58
4.4	Nomenclature	4-62
4.5	References	4-70

5.0	TRANSMITTING POWER SOURCES	5-1
5.1	Introduction	5-1
5.2	Radio Frequency Sources	5-1
5.2.1	Radio Frequency Source Theory	5-2
5.2.2	Available Source Performance	5-9
5.2.3	Power-Burden Relationships	5-26
5.3	Optical Frequency Transmitting Sources	5-29
5.3.1	Optical Frequency Source Theory	5-29
5.3.2	Theory of the Argon Ion Laser	5-33
5.3.3	Characteristics of Mode-Coupled Gas Lasers	5-48
5.3.4	Laser Stabilization	5-54
5.3.5	The CO ₂ Laser	5-79
5.3.6	Available Optical Source Performance	5-93
5.3.7	Power/Burden Relationships	5-104
5.4	Nomenclature	5-109
5.5	References	5-113
6.0	DETECTORS	6-1
6.1	Introduction	6-1
6.2	Radio Frequency Detectors	6-1
6.2.1	Micro/Millimeter-Wave Detectors	6-1
6.2.2	Detectivity/Burden Relationships	6-8
6.3	Detectors in the Submillimeter Range	6-9
6.4	Comparison and Evaluation of Detectors	6-10
6.4.1	Figures of Merit	6-10
6.4.2	Available Detector Performance	6-11
6.4.3	Detectivity/Burden Relationships	6-13
6.4.4	I-F Amplifiers	6-14

6.5	Optical Frequency Detectors	6-14	
6.5.1	Introduction	6-14	
6.5.2	Theory	6-22	
6.5.3	Available Detector Performance	6-41	
6.6	Nomenclature	6-55	
6.7	References	6-58	
7.0	OPTICAL MODULATORS	7-1	6 June 66
7.1	Introduction	7-2	
7.2	Electro-Optic Modulation	7-4	
7.2.1	Theory of Electro-Optic Modulation	7-4	
7.2.2	Design of Intensity Modulators	7-8	
7.2.3	Design of Optical Frequency Translators	7-17	
7.2.4	Design of Phase Modulators	7-29	
7.2.5	Design of Polarization Modulators	7-31	
7.3	Elasto-Optic Modulation	7-32	
7.3.1	Theory of the Elasto-Optic Effect	7-32	
7.3.2	Theory of Ultrasonic Diffraction of Light	7-36	
7.3.3	Modulation Techniques	7-38	
7.3.4	Properties of Ultrasonic Modulators	7-41	
7.4	Internal Modulation	7-47	
7.4.1	Internal Polarization Modulation	7-47	
7.4.2	Other Methods of Internal Modulation	7-49	
7.5	Modulator Performance-Modulator/ Burden Relationships	7-52	
7.6	Nomenclature	7-55	
7.7	References	7-58	

8.0	ACQUISITION AND TRACKING	8-1	6 Sept 66
8.1	Introduction	8-1	
8.2	General Acquisition and Tracking System Considerations	8-3	
8.2.1	Mission Associated Considerations	8-3	
8.2.2	Receiver Location Considerations	8-13	
8.3	Acquisition and Tracking System Performance Analysis	8-21	
8.3.1	The Acquisition Subsystem Operational Considerations	8-22	
8.3.2	The Tracking Subsystem	8-28	
8.3.3	Signal-to-Noise Analysis of Optical Tracking Systems	8-53	
8.3.4	Acquisition	8-78	
8.3.5	Detection Theory	8-84	
8.3.6	Angle Noise Error in Optical Tracking Systems	8-91	
8.4	Component Performance and Burden Relationships	8-118	
8.4.1	Attitude and Tracking Sensors	8-118	
8.4.2	Attitude Control Techniques	8-133	
8.5	Nomenclature	8-156	
8.6	References	8-165	
9.0	RADIO FREQUENCY ANTENNAS	9-1	6 Sept 66
9.1	Introduction	9-1	
9.2	Antenna Theory for Large Apertures	9-2	
9.2.1	General	9-2	
9.2.2	Gain Degradation Due to Predictable Systematic (Non Random) Phase Errors	9-4	
9.2.3	Gain Degradation Due to Random Errors	9-8	
9.3	Available Antenna Types	9-17	
9.3.1	Reflector-Type Antenna	9-17	
9.3.2	Lens-Type Antenna	9-18	

			Current Issue
	9.3.3	Multiple-Beam Antennas . . .	9-21
	9.3.4	Self-Phased and Adaptive Arrays	9-26
	9.3.5	Phase Array	9-36
	9.3.6	Frequency Scanned Array . . .	9-37
9.4		Burden Relationships	9-37
	9.4.1	Cost Estimate of Antenna Arrays	9-37
9.5		Nomenclature	9-42
9.6		References	9-44
10.0		OPTICS	10-1 6 Dec 66
	10.1	Introduction	10-1
	10.2	Optical Implementation Choices . . .	10-1
	10.3	Optical Parameters/Burden Relationships	10-8
		10.3.1 Optical Manufacturability . . .	10-8
		10.3.2 Mechanical Manufacturability . . .	10-18
		10.3.3 Alignment	10-22
	10.4	Nomenclature	10-27
	10.5	References	10-28
11.0		PRIME POWER SYSTEMS	11-1 6 Dec 66
	11.1	Introduction	11-1
	11.2	Solar Power Systems	11-1
		11.2.1 Solar Photovoltaic	11-1
		11.2.2 Solar Thermal Systems	11-9
	11.3	Nuclear Power Systems	11-10
		11.3.1 Reactor Power Systems	11-10
		11.3.2 Radioisotope Power Systems . . .	11-20
	11.4	Chemical Power Systems	11-22
		11.4.1 Fuel Cell Systems	11-22
		11.4.2 Batteries	11-24
	11.5	References	11-28

		Current Issue
12.0	BACKGROUND RADIATION AND ATMOSPHERIC PROPAGATION	12-1 6 June 66
12.1	Introduction	12-1
12.2	Radio Frequency Background	12-1
	12.2.1 Comparison of Radio Frequency Noise Sources	12-1
12.3	Cosmic Background Radiation	12-9
	12.3.1 Diffuse Background	12-9
	12.3.2 Radio Stars	12-14
	12.3.3 Hydrogen Line Emission by Interstellar Gas Clouds	12-14
	12.3.4 Solar System Background	12-18
	12.3.5 Terrestrial Atmospheric Radiation	12-25
12.4	Optical Background	12-26
	12.4.1 Cosmic Background Radiation	12-26
	12.4.2 Solar System Background	12-26
	12.4.3 Terrestrial Atmospheric Background	12-37
12.5	Propagation of Radio Frequency Radiation through the Terrestrial Atmosphere	12-47
	12.5.1 Attenuation	12-47
	12.5.2 Turbulence Effects	12-47
12.6	Propagation of Optical Frequency Radiation in the Terrestrial Atmosphere	12-51
	12.6.1 Attenuation	12-51
	12.6.2 Turbulence effects	12-54
	12.6.3 Loss of Spatial Coherence	12-55
	12.6.4 Scintillation	12-59
	12.6.5 Beam Steering	12-61
12.7	References	12-69
13.0	GROUND RECEIVING FACILITIES	13-1 6 Dec 66
13.1	Introduction	13-1
13.2	Radio Frequency Facilities	13-1
	13.2.1 Deep Space Network	13-2
	13.2.2 The Manned Space Flight Network	13-13

13.2.3	The Satellite Tracking and Data Acquisition Network (STADAN) . . .	13-24	
13.3	Optical Receiving Site Considerations . . .	13-34	
13.3.1	Geometric Considerations . . .	13-34	
13.3.2	Weather Considerations . . .	13-37	
13.3.3	Use of Existing Observatories . . .	13-47	
13.4	References	13-53	
14.0	HEAT REJECTION SYSTEMS	14-1	6 Mar 67
14.1	Introduction	14-1	
14.2	Communication System Heat Rejection Requirements	14-1	
14.2.1	General Considerations	14-1	
14.2.2	Transmitter Source Characteristics	14-2	
14.3	General Heat Rejection System Considerations	14-4	
14.4	Active Heat Rejection Systems	14-4	
14.4.1	Radiative Heat Transfer	14-5	
14.4.2	Radiator Area Requirements	14-9	
14.4.3	Pressure Drops	14-13	
14.5	Passive Heat Rejection Systems	14-18	
14.6	Nomenclature	14-20	
14.7	References	14-22	
15.0	SYSTEMS IMPLEMENTATION	15-1	6 Sept 66
15.1	Introduction	15-1	
15.2	Mariner Mars 1964 Telemetry and Command System	15-1	
15.2.1	Radio Subsystem	15-2	
15.2.2	Telemetry Subsystem: Basic Technique	15-9	
15.2.3	Command Subsystem	15-14	
15.2.4	Performance	15-14	
15.3	Surveyor Telecommunications	15-17	
15.3.1	Introduction	15-17	
15.3.2	General Telecommunications Requirements	15-17	
15.3.3	Individual Subsystems	15-21	
15.3.4	Telecommunications Performance	15-28	
15.4	Nomenclature	15-32	
15.5	References	15-33	

ILLUSTRATIONS

Figure 2-1.	Systems optimization flow chart	2-2
Figure 2-2.	Communication components analysis flow chart	2-2
Figure 2-3.	Communication systems analysis flow chart	2-19
Figure 2-4.	Systems evaluation flow chart	2-19
Figure 2-5.	Transmitter optics weight	2-37
Figure 2-6.	Transmitter optics fabrication cost	2-37
Figure 2-7.	Receiver optics weight	2-37
Figure 2-8.	Receiver optics fabrication cost	2-37
Figure 2-9.	Transmitter acquisition and track system weight	2-38
Figure 2-10.	Transmitter acquisition and track system fabrication cost	2-38
Figure 2-11.	Receiver acquisition and track system weight	2-38
Figure 2-12.	Receiver acquisition and track system fabrication cost	2-38
Figure 2-13.	Transmitter fabrication cost	2-39
Figure 2-14.	Transmitter weight	2-39
Figure 2-15.	Transmitter fabrication cost	2-39
Figure 2-16.	Transmitter weight	2-39
Figure 2-17.	Transmitter fabrication cost	2-40
Figure 2-18.	Transmitter weight	2-40
Figure 2-19.	Transmitter fabrication cost	2-40
Figure 2-20.	Transmitter weight	2-40
Figure 2-21.	Transmitter fabrication cost	2-41
Figure 2-22.	Transmitter weight	2-41
Figure 2-23.	Modulation equipment fabrication cost	2-41
Figure 2-24.	Modulation equipment weight	2-41
Figure 2-25.	Demodulation equipment fabrication cost	2-42
Figure 2-26.	Demodulation equipment weight	2-42
Figure 2-27.	Transmitter power supply fabrication cost	2-42
Figure 2-28.	Transmitter power supply weight	2-42

ILLUSTRATIONS (Continued)

Figure 2-29.	Receiver power supply fabrication cost . . .	2-43
Figure 2-30.	Receiver power supply weight	2-43
Figure 2-31.	Transmitter aperture system cost	2-47
Figure 2-32.	Receiver field of view cost	2-48
Figure 2-33.	Receiver aperture system cost	2-48
Figure 2-34.	Transmitter system cost	2-48
Figure 2-35.	Transmitter system cost	2-49
Figure 2-36.	Transmitter system cost	2-49
Figure 2-37.	Transmitter system cost	2-49
Figure 2-38.	Transmitter system cost	2-49
Figure 2-39.	Optimization cost as a function of information rate and transmission wavelength for direct detection and heterodyne detection communication systems with optimum system parameters operating at a Mars range of 10^8 KM . . .	2-54
Figure 2-40.	Optimization cost as a function of information rate and transmission wavelength for direct detection and heterodyne detection communication systems with optimum system parameters operating at a Jupiter range of 9×10^8 KM . . .	2-55
Figure 2-41.	Optimization cost as a function of information rate and range for a transmission wavelength of 0.51 microns for a direct detection and heterodyne detection communication system with optimum system parameters . . .	2-56
Figure 2-42	Optimization cost and system parameters costs as a function of information rate for a transmission wavelength of 0.51 microns for direct and heterodyne detection communication systems with optimum system parameters operating at a Mars range of 10^8 KM	2-57
Figure 2-43.	Optimization cost and system parameters costs as a function of information rate for a transmission wavelength of 10.6 microns for direct and heterodyne detection communication systems with optimum system parameters operating at a Mars range of 10^8 KM	2-58

ILLUSTRATIONS (Continued)

Figure 2-44.	Optimum system parameters as a function of information rate for a transmission wavelength of 0.51 microns for direct and heterodyne detection communication systems operating at a Mars range of 10^8 KM	2-59
Figure 2-45.	Optimum system parameters as a function of information rate for a transmission wavelength of 10.6 microns for direct and heterodyne detection communication systems operating at a Mars range of 10^8 KM	2-60
Figure 2-46.	Transmitter antenna weight — 2.3 GHz system	2-62
Figure 2-47.	Transmitter antenna fabrication cost — 2.3 GHz system	2-63
Figure 2-48.	Transmitter acquisition and track system weight — 2.3 GHz system	2-64
Figure 2-49.	Transmitter acquisition and track system fabrication cost — 2.3 GHz system	2-65
Figure 2-50.	Transmitter and heat exchanger weight — 2.3 GHz system	2-66
Figure 2-51.	Transmitter and heat exchanger fabrication cost — 2.3 GHz system	2-67
Figure 2-52.	Power supply weight — 2.3 GHz system	2-68
Figure 2-53.	Power supply fabrication cost — 2.3 GHz system	2-69
Figure 2-54.	Transmitter aperture system cost — 2.3 GHz system	2-71
Figure 2-55.	Transmitter system cost — 2.3 GHz system	2-72
Figure 2-56.	Optimization cost as a function of information rate for a transmission frequency of 2.3 GHz for a heterodyne detection radio communication system with optimum system parameters operating at a Mars range of 10^8 KM	2-74
Figure 2-57.	Optimum system parameters as a function of information rate for a transmission frequency of 2.3 GHz for a heterodyne detection radio communication system operating at a Mars range of 10^8 KM	2-75

ILLUSTRATIONS (Continued)

Exhibit A2.2-1.	Optimization Methodology Input Data Program	A2.2-2
Exhibit A2.3-1.	Optimization Methodology Output Data Program	A2.3-3
Exhibit A2.4-1.	Shot Noise Limited Direct Detection Optical Receiver Optimization Program without Component Stops (SOP)	2-107
Exhibit A2.5-1.	Thermal Noise Limited Direct Detection Optical Receiver Optimization Program without Component Stops (TOP)	A2.5-3
Exhibit A2.6-1.	Heterodyne Detection Optical Receiver Optimization Program without Component Stops (HOP)	A2.6-3
Exhibit A2.7-1.	Radio Receiver Optimization Program without Component Stops (ROP)	A2.7-3
Exhibit A2.8-1.	Shot Noise Limited Direct Detection Optical Receiver Optimization Program with Component Stops (SOPS)	2-119
Figure A2.12-1.	Ratios of system parameter costs to optimization cost as a function of information rate for a transmission wavelength of 0.51 microns for a direct detection communication system with optimum system parameters operating at a Mars range of 10^8 KM.	2-130
Figure 3-1.	Timetable of future manned space missions	3-7
Figure 3-2.	Project technology growth in technology areas critical to manned space flight	3-9
Figure 3-3.	Television bandwidth requirements	3-14
Figure 3-4.	Projected communication requirements for near planets	3-15
Figure 3-5.	Increases in communication capability from Mars resulting from anticipated technological improvements	3-16
Figure 3-6.	Variation in parameters which determine pointing accuracy for various missions	3-19
Figure 3-7.	Mercury 1968: time of flight versus launch date	3-21
Figure 3-8.	Venus 1970: time of flight versus launch date	3-22
Figure 3-9.	Mars 1973: time of flight versus launch date	3-23

ILLUSTRATIONS (Continued)

Figure 3-10.	Jupiter 1973: time of flight versus launch date, Type I	3-23
Figure 3-11.	Mercury 1968: Earth-Mercury communication distance versus launch date	3-24
Figure 3-12.	Venus 1970: Earth-Venus communication distance versus launch date	3-24
Figure 3-13.	Mars 1973: Earth-Mars communication distance versus launch date	3-25
Figure 3-14.	Jupiter 1973: Earth-Jupiter communication distance versus launch date, Type I	3-25
Figure 3-15.	Jupiter gravity assisted Saturn fly-by mission	3-26
Figure 3-16.	Comparison of one-way flight times to the outer planets using ballistic gravity assisted, and thrust trajectories	3-26
Figure 3-17.	Launch vehicle capabilities — payloads and destination	3-28
Figure 4-1.	Communication system model	4-2
Figure 4-2.	Photodetector with capacitor filter thermal noise model	4-7
Figure 4-3.	Likelihood ratio test threshold for PCM/IM laser communication system	4-20
Figure 4-4.	PPM/IM likelihood ratio test threshold	4-20
Figure 4-5.	Direct detection model	4-21
Figure 4-6.	Local oscillator reference heterodyne detection model	4-24
Figure 4-7.	Spatial combination of carrier and local oscillator	4-24
Figure 4-8.	Local oscillator reference homodyne detection model	4-32
Figure 4-9.	Probability of error for PCM/IM laser communication system	4-43
Figure 4-10.	Difference channel detection method	4-43
Figure 4-11.	Probability of detection error for PCM/PL laser communication system	4-46
Figure 4-12.	Probability of detection error for PCM/FM laser communication system	4-48
Figure 4-13.	Probability of detection error for PPM/IM threshold detection laser communication system	4-51

ILLUSTRATIONS (Continued)

Figure 4-14.	Probability of detection error for PCM radio communication systems	4-53
Figure 4-15.	Communication coding	4-56
Figure 4-16.	Bit representative forms	4-59
Figure 5-1.	Power limitations for a single twt	5-10
Figure 5-2.	Required manufacturing tolerances in twt as a function of frequency	5-11
Figure 5-3.	Power characteristics of available low-power backward-wave oscillators. Sperry and Bendix use Karp structure, and CSF uses the vane line. In general, these tubes use low operating voltages and are suited for local oscillator and laboratory source use	5-12
Figure 5-4.	Power characteristics of available low-power klystrons. All tubes are reflex klystrons and are light in weight since they use no magnetic focusing fields. They are particularly suited as pump, local oscillator, and laboratory signal sources	5-13
Figure 5-5.	Power characteristics of available high-power cw sources. Most significant is 35 percent efficiency achieved in the 813H and marked increase in available power which has occurred since 1960. The letter - A stands for amplifier and the letter - O signifies oscillator	5-16
Figure 5-6.	State of the art of the power output of primary transistor oscillators and transistor varactor-multipliers versus output frequency	5-19
Figure 5-7.	Typical P-N junction in reverse bias (conditions at avalanche)	5-21
Figure 5-8.	Equivalent circuit for avalanche diode at small transit angle	5-21
Figure 5-9.	Frequency dependence of the real and imaginary parts of the diode impedance	5-21
Figure 5-10.	IMPATT performance	5-23
Figure 5-11.	Gunn oscillator performance	5-27
Figure 5-12.	Figure of merit for spaceborne cw transmitter	5-29

ILLUSTRATIONS (Continued)

Figure 5-13.	Figure of merit for ground based cw transmitter	5-30
Figure 5-14.	Schematic energy level diagram and processes for singly ionized atoms . . .	5-34
Figure 5-15.	Gain curves for right and left hand circular polarization as a function of magnetic field strength	5-36
Figure 5-16.	Index of refraction for right and left hand components with and without magnetic field . .	5-38
Figure 5-17.	Typical gain saturation characteristic for a laser amplifier	5-40
Figure 5-18.	Comparison of (a) inhomogeneous interaction (hole burning) and (b) homogeneous interaction with a single frequency	5-41
Figure 5-19.	Nonoverlapping holes burned in the gain line by a multimode laser	5-42
Figure 5-20.	Gain line "burned off" by a multimode laser	5-42
Figure 5-21.	Schematic representation of the change in power with different discharge and cavity lengths	5-45
Figure 5-22.	Fractional stability required as a function of desired absolute stability	5-56
Figure 5-23.	Fractional stability resulting from a given temperature fluctuation, δT , for several common materials suitable for cavity fabrication	5-60
Figure 5-24.	Schematic representation of an optical discriminant	5-63
Figure 5-25.	Typical feedback laser frequency control system	5-63
Figure 5-26.	Typical Fabry-Perot transmission characteristic. Numerical values typical of gas lasers are given in parentheses . . .	5-65
Figure 5-27.	Simple stabilized laser using a Fabry-Perot cavity as a reference	5-67
Figure 5-28.	Discriminant characteristics	5-67
Figure 5-29.	Dither method of locking a laser to a Fabry-Perot cavity resonance	5-67
Figure 5-30.	Discriminant characteristics	5-68

ILLUSTRATIONS (Continued)

Figure 5-31.	Two-beam interferometer balanced discriminator frequency stabilizing system (after Kaminow ³)	5-69
Figure 5-32.	Optical discriminant obtained from a two-beam interferometer with path length difference of $L_a - L_b$	5-72
Figure 5-33.	Schematic representation of the laser transition gain and power output profiles, showing line center, ν_0 , doppler width, $\Delta\nu_D$, and loss line which determines threshold of oscillation	5-72
Figure 5-34.	Discriminant derivation	5-73
Figure 5-35.	Discriminant characteristics	5-76
Figure 5-36.	One variation of the Zeeman effect derived discriminator stabilization system	5-77
Figure 5-37.	Energy level diagram showing pertinent levels in CO_2 and N_2	5-80
Figure 5-38.	Variation of laser power per unit volume of discharge and laser power per unit length of discharge and discharge diameter	5-89
Figure 5-39.	Variation of axial electric field with discharge tube diameter	5-89
Figure 5-40.	Variation of optimum discharge current with discharge tube diameter	5-89
Figure 5-41.	Schematic illustration of pumping and detection scheme for sun-pumped laser	5-100
Figure 5-42.	A cone-sphere condenser	5-100
Figure 5-43.	Experimental optical setup for pumping laser rod and detecting laser output	5-100
Figure 5-44.	Comparison of lasers for spacecraft transmitter	5-107
Figure 5-45.	Comparison of lasers for ground based transmitter	5-107
Figure 6-1.	Crystal noise ratio versus local oscillator power	6-5
Figure 6-2.	Conversion loss versus local oscillator power and bias	6-5
Figure 6-3.	Noise temperature	6-8

ILLUSTRATIONS (Continued)

Figure 6-4.	Detectivity versus wavelength of photoconductive and thermal millimeter and submillimeter detectors	6-15
Figure 6-5.	Spectral response of various photographs	6-26
Figure 6-6.	Signal and noise equivalent circuits of photomultiplier and idealized receiver	6-27
Figure 6-7.	Microwave phototube	6-28
Figure 6-8.	Physical configuration of electron multiplication system	6-30
Figure 6-9.	Three modes of operation of solid state photodetectors	6-33
Figure 6-10.	Operating circuits of photodiode and photoconductor detectors	6-33
Figure 6-11.	Representative current-voltage characteristics of a photodiode (upper) and a photoconductor (lower) for various values of incident flux. Arrows indicate directions of increasing photon flux, i. e., $F_2 > F_1 > F_0$	6-34
Figure 6-12.	Constant current equivalent circuits of the photodiode (upper) and photoconductor (lower)	6-34
Figure 6-13.	Noise equivalent circuit for the photodiode and photoconductor. $\bar{v}_R^2 \Delta f$ represents excess noise arising in the preamplifier and has been neglected in the text	6-37
Figure 6-14.	Bandwidth of traveling wave phototubes using thermionic cathodes	6-46
Figure 6-15.	Monochromatic detectivity as a function of wavelength for several extrinsic photoconductors	6-50
Figure 6-16.	Blackbody detectivity as a function of temperature for several extrinsic photoconductors	6-51
Figure 6-17.	Detectivity versus wavelength for the best detectors	6-54
Figure 7-1.	Multielement optical modulator	7-11
Figure 7-2.	Sixteen-element KDP crystal modulator	7-11
Figure 7-3.	Two-element parallel-strip modulator	7-13

ILLUSTRATIONS (Continued)

Figure 7-4.	Strip-line traveling-wave modulator configuration.	7-15
Figure 7-5.	Low frequency one-element optical frequency translator	7-20
Figure 7-6.	A possible microwave optical frequency translator	7-20
Figure 7-7.	Two-element KDP optical frequency translator for SSBSC modulator	7-21
Figure 7-8.	Frequency components at the output of a two-element frequency translator	7-27
Figure 7-9.	Cross sectional view of parallel strip transmission line ADP phase modulator	7-29
Figure 7-10.	Modulator for PCM/PL system.	7-31
Figure 7-11.	Ultrasonic diffraction geometry	7-37
Figure 7-12.	Laser oscillator with internal polarization modulation	7-49
Figure 7-13.	Laser with coupling modulation by internal frequency shifting.	7-50
Figure 7-14.	Internal SSBSC modulator	7-51
Figure 8-1.	Earth and DSV line-of-sight geometry	8-4
Figure 8-2.	Lead angle, tracking rate, and tracking acceleration curves for a 174-day Mars trajectory	8-8
Figure 8-3.	Deep space vehicle communication control system block diagram for a manned mission communication "satellite"	8-12
Figure 8-4.	Deep space vehicle communication control system block diagram for an unmanned mission	8-12
Figure 8-5.	Longitude coverage and probability of cloud-free operation for eight selected sights	8-14
Figure 8-6.	Unmanned DSV roll control system	8-23
Figure 8-7.	Unmanned DSV pitch or yaw control system	8-23
Figure 8-8.	DSV acquisition signal flow diagram	8-25
Figure 8-9.	Error in predicted pointing angle versus time between successive communication interrogations	8-27

ILLUSTRATIONS (Continued)

Figure 8-10.	Simplified relationships of servo loops and angle error sources	8-29
Figure 8-11.	Relation of pointing error to track system quantities	8-34
Figure 8-12.	Quadrant detector boresight errors	8-40
Figure 8-13.	Pio's method of pictorial representation of coordinate transformations	8-40
Figure 8-14.	Error vector "Pio-gram"	8-43
Figure 8-15.	Typical outer gimbal servo loop with inertial stabilization	8-46
Figure 8-16.	Parametric relationship	8-54
Figure 8-17.	NEFD versus slit width	8-67
Figure 8-18.	SNR versus slit width	8-68
Figure 8-19.	Field of view versus spectral irradiance	8-72
Figure 8-20.	Sunlight reflection off a planet	8-74
Figure 8-21.	Optimum detector	8-86
Figure 8-22.	Detection probability	8-86
Figure 8-23.	Threshold as a function of average number of events in time t	8-90
Figure 8-24.	Threshold as a function of average number of noise events in time t	8-92
Figure 8-25.	Monopulse tracking	8-95
Figure 8-26.	Boresight error produced by PMT gain unbalance	8-99
Figure 8-27.	Block diagram of monopulse quadrant tracking system	8-101
Figure 8-28.	Beam lobing PPM tracking system	8-109
Figure 8-29.	AM tracking system	8-112
Figure 8-30.	Simple AM reticle	8-112
Figure 8-31.	Radiation signal after modulation by AM reticle	8-113
Figure 8-32.	Space and frequency spectrum of signal	8-113
Figure 8-33.	FM precessional reticle	8-115
Figure 8-34.	Instantaneous frequency as function of rotation of reticle axis about boresight	8-115
Figure 8-35.	Angle noise versus slit width, third magnitude star	8-117

ILLUSTRATIONS (Continued)

Figure 8-36.	Sensor accuracy	8-119
Figure 8-37.	Simple shadow mask sun sensor	8-119
Figure 8-38.	Simple lens type sun sensor	8-119
Figure 8-39.	Critical angle prism sensor design	8-121
Figure 8-40.	Digital-type sun sensors	8-121
Figure 8-41.	Scanning mirror star sensors	8-123
Figure 8-42.	Vibrating reed star sensor	8-124
Figure 8-43.	Star sensor weight versus accuracy	8-125
Figure 8-44.	Image dissector star sensor	8-126
Figure 8-45.	Schematic diagram of a quadrant photomultiplier type of star sensor	8-129
Figure 8-46.	Operating principle of horizon scanners	8-129
Figure 8-47.	Edge tracker implementation	8-130
Figure 8-48.	Operating principle of edge tracker devices	8-131
Figure 8-49.	Attitude control system accuracy	8-133
Figure 8-50.	Solar radiation torque as a function of lever arm effective length	8-137
Figure 8-51.	Gravity gradient forces	8-138
Figure 8-52.	Field intensity versus altitude for earth's magnetic field	8-140
Figure 8-53.	Maximum torque versus altitude (at magnetic equator)	8-142
Figure 8-54.	ARDC 1959 standard atmosphere	8-143
Figure 8-55.	Weight versus momentum storage (max) in reaction wheel	8-145
Figure 8-56.	Weight as a function of speed for 5-day reaction wheels	8-146
Figure 8-57.	Weight as a function of speed for 1-day reaction wheel dumping	8-146
Figure 8-58.	Momentum capacity as a function of time for a constant torque	8-146
Figure 8-59.	Momentum wheel system weight and angular momentum versus wheel speed for constant wheel diameter (5 feet)	8-149
Figure 8-60.	Momentum wheel system weight versus wheel diameter for constant wheel speed (500 rpm) and angular momentum (13.24 foot-pound-seconds)	8-150

ILLUSTRATIONS (Continued)

Figure 8-61.	Attitude control system weights versus total impulse	8-154
Figure 8-62.	Minimum impulse bit versus thrust	8-154
Figure 8-63.	Thrust range of mass expulsive systems	8-154
Figure 8-64.	Specific impulse of propellants	8-154
Figure 9-1.	Antenna half-power beamwidths versus aperture widths for rectangular apertures	9-6
Figure 9-2.	Antenna half-power beamwidths versus aperture width for circular or elliptical apertures	9-6
Figure 9-3.	Bending of an array supported at one fourth the array length from each end.	9-7
Figure 9-4.	Antenna gain degradation due to random phase errors in aperture illumination	9-12
Figure 9-5.	Antenna gain degradation due to random phase errors in aperture illumination	9-13
Figure 9-6.	Antenna gain degradation due to random phase errors in aperture illumination	9-14
Figure 9-7.	Gain loss due to reflector tolerance	9-14
Figure 9-8.	Gain of large paraboloids (based on published estimates)	9-18
Figure 9-9.	Typical ray in an ideal Luneberg lens	9-19
Figure 9-10.	Approximate theoretical electromagnetic field near the focus point of a 10-inch Luneberg lens ($f = 6$ GHz, $kq = 15.971$)	9-22
Figure 9-11.	Experimental far field radiation pattern of a 10-inch Luneberg lens ($f = 6$ GHz, $kq = 15.971$)	9-22
Figure 9-12.	Trans-Directive array	9-24
Figure 9-13.	Specific configuration for a Trans-Directive array	9-27
Figure 9-14.	Van Atta array. (Van Atta, 1959)	9-28
Figure 9-15.	Retrodirective array techniques	9-29
Figure 9-16.	Electronic beam-forming techniques	9-31
Figure 9-17.	Adaptive retrodirective antenna module	9-32
Figure 9-18.	Active Van Atta system with separate arrays for reception and retransmission	9-32
Figure 9-19.	Modulated Van Atta array	9-33

ILLUSTRATIONS (Continued)

Figure 9-20.	Specific configuration for a retrodirective array	9-35
Figure 9-21.	Block diagram of the active adaptive antenna array system simulator. (Gangi, 1963).	9-35
Figure 9-22.	Acquisition time of the 8-channel antenna array simulator versus mixer output voltage. (Gangi, 1963)	9-36
Figure 9-23.	Oscillograms showing the adaptiveness of the phase-locked system. (Gangi, 1963)	9-36
Figure 9-24.	Occultation time versus first sidelobe level	9-41
Figure 10-1.	Diffraction limited resolving power for all types of telescopes versus aperture for NaD light	10-2
Figure 10-2.	Aberrations of a parabolic reflector off axis, versus f number	10-5
Figure 10-3.	Geometric blur of various types versus field of view	10-6
Figure 10-4.	The limiting photo magnitude of a telescope as a function of its aperture and focal ratio	10-9
Figure 10-5.	Approximate mirror weight of beryllium sandwich mirrors	10-10
Figure 10-6.	Approximate cost of beryllium sandwich mirrors	10-11
Figure 10-7.	Approximate mirror weight of fused silica sandwich mirrors	10-12
Figure 10-8.	Approximate cost of fused silica sandwich mirrors	10-13
Figure 10-9.	Combined defocusing and wave front errors	10-14
Figure 10-10.	A typical expansivity curve for low expansion Cer-Vit mirror material	10-16
Figure 10-11.	Transmission curve of the Lick 36-inch refractor and its photographic correcting lens	10-18
Figure 10-12.	Reflectivity of evaporated aluminum and chemically deposited silver	10-20
Figure 10-13.	The reflectances of aluminum and silver for different angles of incidence, when the plane of polarization is parallel (R_p) and perpendicular (R_s) to the plane of incidence	10-20

ILLUSTRATIONS (Continued)

Figure 10-14.	Preliminary weight estimate for the telescope mechanical and optical structure using beryllium optical components . . .	10-21
Figure 10-15.	Preliminary cost estimate for mechanical and optical structure using beryllium optical components	10-23
Figure 10-16.	Components of a Cassegrain system . . .	10-24
Figure 10-17.	Tolerance on axial position of the secondary mirror of a Cassegrain telescope . . .	10-25
Figure 10-18.	Focal ratio — primary mirror	10-26
Figure 11-1.	Power system range of application at near-Earth solar distance	11-2
Figure 11-2.	Solar cell array specific weight	11-3
Figure 11-3.	Oriented planar solar cell array specific power	11-3
Figure 11-4.	Temperature dependency of solar cell efficiency	11-4
Figure 11-5.	Solar power with conventional solar panels — silicon cells	11-5
Figure 11-6.	Solar power with conventional solar panels — gallium arsenide cells	11-5
Figure 11-7.	Actual arrangement of a basic thermoelectric couple	11-11
Figure 11-8.	Direct-radiating thermoelectric module . . .	11-12
Figure 11-9.	Reactor-thermoelectric system schematic . . .	11-13
Figure 11-10.	Thermoelectric reactor power system (2 kwe)	11-14
Figure 11-11.	A thermionic converter of heat to electrical energy	11-14
Figure 11-12.	Nuclear thermionic system weight versus operating temperature	11-16
Figure 11-13.	Comparison of nuclear thermionic systems (General Electric)	11-16
Figure 11-14.	Brayton cycle dynamic power system . . .	11-18
Figure 11-15.	Rankine cycle dynamic power system . . .	11-20
Figure 11-16.	Schematic of hydrogen-oxygen fuel cell . . .	11-23

ILLUSTRATIONS (Continued)

Figure 11-17.	Hydrox fuel cell system specific weight as a function of power requirement for missions of various length	11-23
Figure 11-18.	Production cost of fuel cell electrical power subsystems	11-25
Figure 11-19.	Secondary battery energy density versus discharge rate	11-25
Figure 11-20.	Secondary battery capacity versus cycle life	11-27
Figure 12-1.	Map of the radio sky background at 64 mc (after Hey, Parsons, and Phillips). The contours give the absolute brightness temperature of the radio sky in degrees Kelvin	12-10
Figure 12-2.	Map of the radio sky background at 81 mc (after Baldwin). The contours give the absolute temperature of the radio sky in degrees Kelvin	12-10
Figure 12-3.	Map of the radio sky background at 100 mc (after Bolton and Westfold). The contours give the absolute temperature of the radio sky in degrees Kelvin	12-10
Figure 12-4.	Map of the radio sky background at 160 mc (after Reber). The contours give the absolute brightness temperature of the radio sky in degrees Kelvin	12-10
Figure 12-5.	Map of the radio sky background at 250 mc (After Ko and Kraus). The contours give the absolute brightness temperature of the radio sky in degrees Kelvin	12-11
Figure 12-6.	Map of the radio sky background at 480 mc (after Reber). The contours give the absolute brightness temperature of the radio sky in degrees Kelvin	12-11
Figure 12-7.	Map of the radio sky background at 600 mc (after Piddington and Trent). The contours give the absolute temperature of the radio sky in degrees Kelvin	12-11
Figure 12-8.	Map of the radio sky background at 910 mc (after Denisse, Leroux, and Steinberg). The contours give the absolute brightness temperature of the radio sky in degrees Kelvin	12-11

ILLUSTRATIONS (Continued)

Figure 12-9.	Galactic noise temperature	12-13
Figure 12-10.	Galactic noise along the ecliptic at three frequencies. The 600-mc peak extends to a height of 21 units and the 81-mc peak to 27 units	12-14
Figure 12-11.	Radio stars in 378 mc	12-15
Figure 12-12.	The most prominent radio stars superimposed on the radio sky background map at 250 mc. (Brightness temperatures of the isophotes are in degrees Kelvin)	12-16
Figure 12-13.	Spectra of the most prominent radio stars	12-17
Figure 12-14.	Sun noise temperature versus frequency	12-20
Figure 12-15.	The predicted intensity of planetary thermal radio radiation when the planet is near closest approach to the earth (dashed lines), and the measured intensity of radiation from the planets, the moon, and the nonthermal radio source, Cassiopeia A (solid lines and points)	12-22
Figure 12-16.	The brightness temperature of the center of the disk of the moon as a function of the phase of solar illumination. Long dashes — brightness temperature corresponding to the infrared radiation as approximated by the calculated surface temperature of Wesselink (Bull. Astron. Inst. Neth., Vol. 10, pp. 351-363; April 1948). Solid line—brightness temperature corresponding to the 8.6-mm radiation measured by Gibson (proc. IRE, vol. 46, pp. 280-286; January 1958). Short dashes — brightness temperature corresponding to the 3.15 cm radiation measured by Mayer, McCullough, and Sloanaker ("Planets and Satellites," University of Chicago Press, Chicago, Ill., Ch. 12; 1961). Reproduced from "Planets and Satellites," G. P. Kuiper and B. M. Middlehurst, Eds., University of Chicago Press, Chicago, Ill., 1961; copyright 1961 by the University of Chicago	12-24

ILLUSTRATIONS (Continued)

Figure 12-17.	Sky noise temperature due to oxygen and water vapor	12-27
Figure 12-18.	Spectral irradiance of brightest stars outside the terrestrial atmosphere . .	12-27
Figure 12-19.	Solar spectral irradiance outside the earth's atmosphere	12-29
Figure 12-20.	Calculated planetary spectral irradiance outside the terrestrial atmosphere . .	12-32
Figure 12-21.	Full moon spectral irradiance outside the terrestrial atmosphere	12-33
Figure 12-22.	Spectral albedo versus wavelength . .	12-33
Figure 12-23.	Position of Mercury and Venus at greatest elongation ($\alpha = 90^\circ$)	12-34
Figure 12-24.	Solar and terrestrial radiation. Reflected solar and total earth radiation to space values should be divided by π to obtain the radiance for each case. T_S is the surface temperature and T_A is the effective radiating air temperature . .	12-36
Figure 12-25.	Illumination factor as a function of altitude for parametric values of bistatic angle, σ	12-38
Figure 12-26.	Clear sky radiance at Colorado Springs, Colorado; sun angle = 45 degrees . .	12-39
Figure 12-27.	Diffuse component of typical background radiance from 30 km and sea level zenith angle 45 degrees and excellent visibility	12-40
Figure 12-28.	Estimated average diffuse radiation from zenith night sky. Average diffuse radiation from zenith, 0.3 to 1.3 microns . .	12-42
Figure 12-29.	Spectral radiance in the infrared of a clear sky for several elevation angles above the horizon. These spectra were measured at an elevation of 11,750 feet, at night, with an ambient temperature of 8°C	12-43
Figure 12-30.	Zenith twilight intensity	12-44
Figure 12-31.	Zenith moonlight intensity	12-45
Figure 12-32.	Correction factor for moon phase . .	12-46

ILLUSTRATIONS (Continued)

Figure 12-33.	Ionospheric attenuation for a source at 1000-km height	12-48
Figure 12-34.	One-way attenuation through the standard summer atmosphere due to oxygen and water vapor	12-48
Figure 12-35.	Total attenuation for one-way transmission through the atmosphere. (Proc. IEEE, p. 488, April 1966) . . .	12-49
Figure 12-36.	Atmospheric attenuation summary . . .	12-50
Figure 12-37.	Atmospheric distortion of RF wavefront based on NBS Maui data	12-52
Figure 12-38.	Atmospheric transmission, 0.3 to 1.3 microns	12-52
Figure 12-39.	Atmospheric transmission, 1.2 to 5.0 microns	12-53
Figure 12-40.	Fog-rain attenuation, $\lambda = 0.63\mu$	12-56
Figure 12-41.	Power reduction caused in an optical heterodyne receiver caused by loss of phase coherence (after Fried). . . .	12-56
Figure 12-42.	Dependence of coherence length, γ_0 on zenith angle, ϕ , and wavelength λ_μ (after Fried)	12-58
Figure 12-43.	Geometry for optical heterodyne receiver in the atmosphere (after Fried) . .	12-58
Figure 12-44.	Dependence of the amount of quivering of stellar images on the zenith distance. . .	12-60
Figure 12-45.	Empirical dependence of the amount of star twinkling on the diameter of the telescope diaphragm (1, winter; 2, summer)	12-62
Figure 12-46.	Dependence of the amount of star twinkling on the zenith distance when the telescope diaphragm has a diameter of three inches	12-62
Figure 12-47.	Dependence of the amount of star twinkling on the zenith distance when the telescope diaphragm has a diameter of 12.5 inches	12-62
Figure 12-48.	Mean-square deviation in log-level of intensity, X_I^2	12-63

ILLUSTRATIONS (Continued)

Figure 12-49.	Mean-square deviation on log-level of intensity, X_I^2	12-63
Figure 12-50.	Mean-square deviation in log-level of intensity, X_I^2	12-65
Figure 12-51.	Geometry of propagation through a turbulent blob	12-65
Figure 12-52.	Mean-square variation (Δn^2) versus altitude, h	12-67
Figure 12-53.	Correlation distance, L_O versus altitude, h	12-67
Figure 13-1.	Typical MSFN remote site block diagram	13-25
Figure 13-2.	MSFN and STADAN visibility contours for typical orbital altitude of 200 nm at 5° elevation	13-27
Figure 13-3.	Altitudes (THSDS of FT MSL) above which there is 95% probability of having <1/10 sky cover, July	13-39
Figure 13-4.	Altitudes (THSDS of FT MSL) above which there is 60% probability of having <1/10 sky cover, July	13-40
Figure 13-5.	Altitudes (THSDS of FT MSL) above which there is 95% probability of having <1/10 sky cover, October	13-41
Figure 13-6.	Altitudes (THSDS of FT MSL) above which there is 60% probability of having <1/10 sky cover, October	13-42
Figure 13-7.	Mean cloudiness in fractional cloud cover, July	13-43
Figure 13-8.	Mean cloudiness in fractional cloud cover, September	13-44
Figure 13-9.	Probability of no clouds at one or more sites, $P(C)$, versus number of sites, n	13-46
Figure 14-1.	Schematic diagram showing basic parts of a traveling-wave tube	14-3
Figure 14-2.	Fin effectiveness versus radiation modulus	14-8
Figure 14-3.	Specific heat dissipation capacity versus radiator temperature	14-8
Figure 14-4.	Area requirements for non-condensing radiator	14-11

ILLUSTRATIONS (Continued)

Figure 14-5.	Fin and tube radiator weight, W_H (pounds), versus heat dissipation capacity at various radiator temperatures, T_R . . .	14-12
Figure 14-6.	Fin and tube radiator cost, C_H , versus heat dissipation capacity at various radiator temperatures, T_R	14-14
Figure 14-7.	Coefficient relating the pressure gradient for two-phase flow with those for single-phase flows	14-16
Figure 14-8.	Specific heat dissipation capacity versus temperature of radiators in direct sunlight at various solar distances	14-19
Figure 15-1.	Mariner 1964 spacecraft telecommunication system	15-3
Figure 15-2.	Mariner IV spacecraft	15-6
Figure 15-3.	Received signal level vs time, spacecraft to earth	15-16
Figure 15-4.	Telemetry performance margin vs time. Diplexed tracking antenna with maser, 8-1/3 b/s	15-16
Figure 15-5.	Received signal level vs time, earth to spacecraft. Ground transmission power = 10 kw, command modulation on .	15-16
Figure 15-6.	Command performance margin vs time. Ground transmission power = 10 kw . . .	15-18
Figure 15-7.	Surveyor spacecraft	15-18
Figure 15-8.	Electronic system elements	15-22

TABLES

Table 3-1.	Mariner Mars mission comparisons . . .	3-2
Table 3-2.	Preliminary design results, Voyager spacecraft system . . .	3-3
Table 3-3.	Present and contemplated unmanned interplanetary missions . . .	3-4
Table 3-4.	Description and status of future manned space missions . . .	3-5
Table 3-5.	Communications subsystem summary table . . .	3-10
Table 3-6.	Planetary fly-by scientific payload . . .	3-12
Table 3-7.	Typical data requirements . . .	3-13
Table 3-8.	Near future goals . . .	3-20
Table 3-9.	Typical mission durations . . .	3-27
Table 4-1.	Detection techniques . . .	4-3
Table 4-2.	Signal-to-noise ratio expressions . . .	4-4
Table 4-3.	Power spectral densities of major sources of optical detection noise . . .	4-16
Table 4-4.	Laser modulation techniques . . .	4-34
Table 4-5.	Probability of error expressions . . .	4-38
Table 4-6.	Source bit rate reduction . . .	4-57
Table 5-1.	Negative grid tube characteristics . . .	5-3
Table 5-2.	Type classification of microwave tubes-oscillators and amplifiers . . .	5-4
Table 5-3.	Klystron characteristics . . .	5-5
Table 5-4.	Traveling wave tube characteristics . . .	5-6
Table 5-5.	Crossed-Field tube characteristics . . .	5-7
Table 5-6.	Spontaneous radiative transition probabilities in CO ₂ . . .	5-81
Table 5-7.	Continuous wave laser oscillation wavelengths in the 00°1 to 10°0 band of CO ₂ . . .	5-87
Table 5-8.	State-of-the-art CO ₂ lasers (May 1966) . . .	5-91
Table 5-9.	CW laser oscillators . . .	5-92

TABLES (Continued)

Table 5-10.	Typical high energy laser oscillators . . .	5-96'
Table 5-11.	High peak power laser oscillators . . .	5-97
Table 5-12.	High repetition frequency laser oscillators . .	5-98
Table 5-13.	Figure of merit for several gas lasers . . .	5-106
Table 6-1.	Best measured conversion loss reported for millimeter wave mixers using various "point-contact" diodes.	6-6
Table 6-2.	Detector characteristics	6-16
Table 6-3.	Quantum efficiencies and responsivities of red-sensitive photosurfaces	6-43
Table 6-4.	Wavelengths of peak response and Engstrom's factors	6-43
Table 6-5.	Noise in photomultiplier tubes	6-43
Table 6-6.	NEP in one-cycle band at 6328 Å and 6943 Å for several photomultipliers	6-44
Table 6-7.	Traveling wave phototube parameters	6-45
Table 6-8.	Traveling wave phototube sensitivity	6-46
Table 6-9.	High-speed photodiode characteristics	6-47
Table 6-10.	Characteristics of semiconductor materials for 10.6μ detector	6-49
Table 7-1.	Optical and electrical constants of KDP	7-8
Table 7-2.	Properties of some typical electro-optic materials	7-9
Table 7-3.	Elasto-optic performance parameters for selected crystals	7-46
Table 7-4.	Characteristics of some electro-optic modulators - June 1966	7-54
Table 8-1.	Probability of clear view	8-15
Table 8-2.	Refraction angle versus apparent zenith angle . .	8-16
Table 8-3.	Comparison between optical receiver sites . . .	8-20
Table 8-4.	Pointing error causes and means of correction .	8-31
Table 8-5.	Attitude sensing techniques summary	8-32
Table 8-6.	Stabilization and control system torquing techniques summary	8-34
Table 8-7.	Comparison matrix of star sensors	8-127
Table 8-8.	Comparison matrix of horizon scanners	8-132
Table 8-9.	Comparison matrix of attitude control techniques.	8-134

TABLES (Continued)

Table 8-10.	Coefficient of radiation	8-136
Table 8-11.	Momentum storage devices	8-148
Table 9-1.	Secondary pattern characteristics produced by various types of aperture distributions	9-5
Table 9-2.	Number of elemental paraboloids required for 70 and 80 db gain	9-39
Table 9-3.	Selected costs	9-40
Table 9-4.	Station costs	9-40
Table 10-1.	Effect of wave front errors in energy density at the center of the beam	10-3
Table 10-2.	Optical materials	10-19
Table 11-1.	Solar photovoltaic power system production cost	11-6
Table 11-2.	Solar array degradation in Earth-Mars transit by solar flare activity n/p silicon cells with 30-mil quartz covers.	11-7
Table 11-3.	Solar array degradation in Earth-Mars transit by solar flare activity n/p silicon cells with 45-mil quartz covers	11-8
Table 11-4.	Reactor thermoelectric system performance (1/2 to 20 kw)	11-12
Table 11-5.	Primary space batteries	11-26
Table 12-1.	Planetary radiation	12-21
Table 13-1.	Deep space instrumentation facility locations	13-4
Table 13-2.	DSIF range and range rate measurement accuracy.	13-6
Table 13-3.	DSIF frequencies	13-8
Table 13-4.	DSIF receiver capabilities	13-11
Table 13-5.	210-foot altitude/azimuth antenna performance	13-14
Table 13-6.	MSFN ground station system equipment	13-15
Table 13-7.	MSFN USBS-equipped ground station data handling capability.	13-18
Table 13-8.	LEM down-link MSFN S-band transmission summary	13-20
Table 13-9.	CSM to MSFN S-band transmission combination summary (FM modes).	13-21
Table 13-10.	CSM to MSFN S-band transmission combination summary (PM-mode)	13-22

TABLES (Continued)

Table 13-11.	LEM up-link S-band transmission combinations summary	13-23
Table 13-12.	MSFN to CSM S-band transmission combinations summary	13-23
Table 13-13.	STADAN ground stations system equipment	13-28
Table 13-14.	Refraction angle versus apparent zenith angle	13-35
Table 13-15.	Maximum angular excursion of beam from normal for M ground stations	13-37
Table 13-16.	Baker Nunn sites showing percent of time lost due to clouds	13-48
Table 13-17.	Astronomical optical telescopes, Aperture \geq 20 inches or 50 GM	13-50
Table 13-18.	Selected sites for optical observations	13-53
Table 15-1.	Spacecraft radio transmission parameters (2998 MHz)	15-8
Table 15-2.	Spacecraft radio reception parameters (2116 MHz)	15-8
Table 15-3.	Registered events.	15-12
Table 15-4.	Video storage characteristics	15-13
Table 15-5.	Telemetry parameters	15-13
Table 15-6.	Command parameters	15-15
Table 15-7.	Communication system requirements	15-20
Table 15-8.	DSIF parameters	15-20
Table 15-9.	Surveyor receiver specifications	15-24
Table 15-10.	Surveyor transmitter specifications.	15-24
Table 15-11.	TV capabilities for the survey cameras	15-29
Table 15-12.	Earth to spacecraft transmission (lunar phase command mode)	15-30
Table 15-13.	Spacecraft to earth transmission (television transmission - primary mode)	15-31

1.0 INTRODUCTION

1.1 PURPOSE

"Reference Data for Advanced Space Communications and Tracking Systems" is being produced for the Goddard Space Flight Center by the Hughes Aircraft Company under NASA Contract NAS 5-9637. The purpose of this contract is to perform a parametric study with the following goals:

1. Perform overall systems tradeoff studies in sufficient detail to identify those missions which will make the best use of laser/optical, microwave, or a combination of microwave and laser/optical communication and tracking systems.
2. Provide a plan for optimum integrating such future microwave and/or laser/optical communication and tracking systems into present and future world-wide systems.
3. Provide overall systems design criteria or specifications for microwave and/or laser/optical communication and tracking systems.

The first issue of "Reference Data for Advanced Space Communication and Tracking" provided preliminary data for the achievement of these goals. This data was presented in 13 technical sections, in addition to the introductory material. These technical sections were designed to meet the contract goals listed above, as follows:

- The Methodology section provides a basis for determining the optimum communication and tracking system configuration, whether it be at microwave, millimeter waves, or optical frequencies. The Methodology section, in its detailed documentation of functional relationships, also establishes the parametric studies which must be performed in each technological area.
- Two sections of the Reference Data will dominate in establishing a means of integrating future space communication systems with existing and future ground facilities. These

are Mission Analysis and Ground Receiving Sites. Mission Analysis is concerned with overall future space mission goals and the facilities for their achievement. Present Ground Receiving Sites are documented in the 6 December 1966 report. The final report will contain a refinement of this data and give criteria for future receiving systems.

- The basis for system design criteria is found in the remaining technical sections. They are: Communication Theory, Transmitting Power Sources, Detectors, Optical Modulators, Acquisition and Tracking, Radio Frequency Antennas, Optics, Spacecraft Prime Power Generation, Background Radiation and Atmospheric Attenuation, and Heat Transfer Systems.

In this sixth quarterly report of "Parametric Analysis of Microwave and Laser Systems for Communications and Tracking" the Heat Radiator Section has been updated. It completely replaces the earlier edition dated 6 February 1966. In addition, several Appendices of the Methodology have been revised and replace earlier editions dated 6 December 1966.

1.2 REFERENCE DATA FORMAT

Each Reference Data Section is formed of six basic subsections. They are:

- Introduction
- Theory
- Performance
- Burden Relationships
- Nomenclature
- References

Each subsection of this basic structure is used in the component technology sections. However, some sections are not completely amenable to this organization of material and variations are allowed. The intent of the subsections is as follows.

1.2.1 Introduction

This subsection introduces the material of the section. The status of the section in relation to its ultimate development may be noted.

1.2.2 Theory

This subsection is designed to introduce the reader to the theory of the technological area being discussed. Basic relationships are given but extensive derivations are avoided. The theory is presented as a guide for using the material of the section and as a means to project parameter capabilities.

1.2.3 Performance

This subsection contains the documented state of the art of the technology. It lists new variants of the technology and tabulated parameters and performance.

1.2.4 Burden Relationships

This subsection contains the parametric relationships of the section technology. Of particular concern is the relationship of parameter values as a function of weight, cost, size, etc. Ancillary equipment required by the technology are also described in this subsection.

1.2.5 Nomenclature

A nomenclature subsection was introduced in the 6 June 1966 issue of "Reference Data for Advanced Space Communication and Tracking Systems." It is intended to apply only to the section of which it is a part. It will form the basis for a complete and uniform nomenclature for the entire volume.

1.2.6 References

This subsection lists references used in the section proper. The references are not intended as an extensive bibliography but rather to direct the reader to the source of the documented material.

1.3 FRONT MATTER

The Table of Contents, List of Illustrations and List of Tables is complete for the entire volume of "Reference Data for Advanced Space Communication and Tracking Systems." The date of last issue for each section is given in the Table of Contents. Text material for sections not updated in this issue may be found in the second issue dated 6 June 1966, Report Number P66-135, in the third issue dated 6 September 1966, Report Number P66-213, and in the fourth dated 6 December 1966, Report Number P67-09. (Note that the first issue dated 6 February 1966, Report Number P66-16, has now been completely replaced by subsequent editions.)

APPENDIX A2.1
NOMENCLATURE

Computer Symbol	Text Symbol	Description <u>System Parameters</u>
PT	P_T	= transmitter power
DT	d_T	= transmitter aperture diameter
DR	d_R	= receiver aperture diameter
THER	θ_R	= receiver field of view
RB	R_B	= information rate
PT ϕ	P_{TO}	= optimum value of P_T
DT ϕ	d_{TO}	= optimum value of d_T
DR ϕ	d_{RO}	= optimum value of d_R
THER ϕ	θ_{RO}	= optimum value of θ_R
PTI	P_{TI}	= initial program value of P_T
DTI	d_{TI}	= initial program value of d_T
DRI	d_{RI}	= initial program value of d_R
THRI	θ_{RI}	= initial program value of θ_R
PTB	P_{TB}	= limit value of P_T
DTB	d_{TB}	= limit value of d_T
DRB	d_{RB}	= limit value of d_R
THERB	θ_{RB}	= limit value of θ_R
PTM	P_{TM}	= fixed value of P_T (= 0 for no constraint)
DTM	d_{TM}	= fixed value of d_T (= 0 for no constraint)
DRM	d_{RM}	= fixed value of d_R (= 0 for no constraint)
THERM	θ_{RM}	= fixed value of θ_R (= 0 for no constraint)

Computer Symbol	Text Symbol	Description <u>System Costs</u>	
CDT	C_{d_T}	=	transmitter antenna cost
CDR	C_{d_R}	=	receiver antenna cost
CAT	C_{AT}	=	transmitter acquisition and track equipment fabrication cost independent of transmitter beamwidth
CTHT	C_{θ_T}	=	transmitter antenna fabrication cost
CTHR	C_{θ_R}	=	receiver antenna fabrication cost
CQT	C_{QT}	=	transmitter acquisition and track equipment cost
CNT	C_{NT}	=	transmitter acquisition and track equipment fabrication cost
CAR	C_{AR}	=	receiver acquisition and track equip- ment fabrication cost independent of receiver field of view
CQR	C_{QR}	=	receiver acquisition and track equipment cost
CNR	C_{NR}	=	receiver acquisition and track equipment fabrication cost
CFL	C_{FL}	=	transmitter fabrication cost
CPT	C_{P_T}	=	transmitter cost
CM	C_M	=	modulation equipment cost
CD	C_D	=	demodulation equipment cost
CFM	C_{FM}	=	modulation equipment fabrication cost
CFD	C_{FD}	=	demodulation equipment fabrication cost
CKT	C_{KT}	=	transmitter antenna fabrication cost independent of transmitter aperture diameter
CKR	C_{KR}	=	receiver antenna fabrication cost inde- pendent of receiver aperture diameter

Computer Symbol	Text Symbol	Description
CKH	C_{KH}	= transmitter heat exchanger fabrication cost independent of transmitter power dissipation
CST	C_{ST}	= transmitter power supply cost
CSR	C_{SR}	= receiver power supply cost
CH	C_H	= heat exchanger fabrication cost
CFT	C_{FT}	= transmitter power supply fabrication cost
CFR	C_{FR}	= receiver power supply fabrication cost
CKP	C_{KP}	= transmitter fabrication cost independent of transmitter power
CKM	C_{KM}	= modulation equipment fabrication cost independent of information rate
CKD	C_{KD}	= demodulation equipment fabrication cost independent of information rate
CKE	C_{KE}	= transmitter power supply fabrication cost independent of transmitter power requirement
CKF	C_{KF}	= receiver power supply fabrication cost independent of receiver power requirement
CS	C_S	= total system cost
CV	C_V	= variable part of total system cost (optimization cost)
CFA	C_{FA}	= fixed part of total transmitter cost
CFB	C_{FB}	= fixed part of total receiver cost
CG	C_G	= cost of transmitter, transmitter power supply, and transmitter heat exchanger which is dependent upon transmitter power

Computer Symbol	Text Symbol	Description
CT	C_T	= cost of transmitter antenna, transmitter acquisition and track equipment, and associated power supply which is dependent upon transmitter aperture diameter
CQ	C_Q	= cost of receiver acquisition and track equipment which is dependent upon receiver field of view
CR	C_R	= cost of receiver antenna, receiver acquisition and track equipment, and associated power supply which is dependent upon receiver aperture diameter
CFA	C_{FA}	= total transmitter fabrication costs for optimum system parameters
CFB	C_{FB}	= total receiver fabrication costs for optimum system parameters
CA	C_A	= total transmitter cost for optimum system parameters
CB	C_{BO}	= total receiver cost for optimum system parameters
$CT\phi$	C_{TO}	= value of C_T for optimum system parameters
$CR\phi$	C_{RO}	= value of C_R for optimum system parameters
$CG\phi$	C_{GO}	= value of C_G for optimum system parameters
$CQ\phi$	C_{QO}	= value of C_Q for optimum system parameters
$CV\phi$	C_{VO}	= value of C_V for optimum system parameters

Computer Symbol	Text Symbol	Description <u>System Weights</u>	
WDT	W_{dT}	=	transmitter antenna weight
WDR	W_{dR}	=	receiver antenna weight
WQT	W_{QT}	=	transmitter acquisition and track equipment weight
WBT	W_{BT}	=	transmitter acquisition and track equipment weight independent of transmitter beamwidth
WQR	W_{QR}	=	receiver acquisition and track equipment weight
WBR	W_{BR}	=	receiver acquisition and track equipment weight independent of receiver field of view.
WT	W_T	=	transmitter weight
WM	W_M	=	modulation equipment weight
WD	W_D	=	demodulation equipment weight
WSR	W_{SR}	=	receiver power supply weight
WST	W_{ST}	=	transmitter power supply weight
WH	W_H	=	transmitter heat exchanger weight
WKT	W_{KT}	=	transmitter antenna weight independent of transmitter aperture diameter
WKR	W_{KR}	=	receiver antenna weight independent of receiver aperture diameter
WKP	W_{KP}	=	transmitter weight independent of transmitter power
WKH	W_{KH}	=	transmitter heat exchanger weight inde- pendent of transmitter power dissipation

Computer Symbol	Text Symbol	Description
WKM	W_{KM} =	modulation equipment weight independent of information rate
WKD	W_{KD} =	demodulation equipment weight independent of information rate
WKE	W_{KE} =	transmitter power supply weight independent of transmitter power requirement
WKF	W_{KF} =	receiver power supply weight independent of receiver power requirement
WA	W_A =	total transmitter weight for optimum system parameters
WB	W_B =	total receiver weight for optimum system parameters

Computer Symbol	Text Symbol	Description	
		<u>System Power Requirements</u>	
PQT	P_{QT}	=	transmitter acquisition and track equipment power requirement
PQR	P_{QR}	=	receiver acquisition and track equipment power requirement
PPT	P_{PT}	=	transmitter power requirement
PM	P_M	=	modulation equipment power requirement
PD	P_D	=	demodulation equipment power requirement
PST	P_{ST}	=	transmitter power supply power requirement
PSR	P_{SR}	=	receiver power supply power requirement
PA	P_A	=	total transmitter power requirement for optimum system parameters
PB	P_B	=	total receiver power requirement for optimum system parameters

Computer Symbol	Text Symbol	Description
<u>System Constants of Proportionality</u>		
KDT	K_{d_t}	= constant relating transmitter antenna weight to transmitter aperture diameter
KTHT	K_{θ_T}	= constant relating transmitter antenna fabrication cost to transmitter aperture diameter
KS	K_S	= cost per unit weight for spaceborne equipment
KDR	K_{d_R}	= constant relating receiver antenna weight to receiver aperture diameter
KTHR	K_{θ_R}	= constant relating receiver antenna fabrication cost to receiver aperture diameter
KAT	K_{AT}	= constant relating transmitter tracking equipment fabrication cost to transmitter beamwidth
KWAT	$K_{W_{AT}}$	= constant relating transmitter tracking equipment weight to transmitter antenna weight
KPQT	$K_{P_{QT}}$	= constant relating transmitter acquisition and track equipment power requirement to equipment weight
KAR	K_{AR}	= constant relating receiver tracking equipment fabrication cost to receiver field of view
KWAR	$K_{W_{AR}}$	= constant relating receiver tracking equipment weight to receiver antenna weight
KPQR	$K_{P_{QR}}$	= constant relating receiver acquisition and track equipment power requirement to equipment weight
KWT	K_{W_T}	= constant relating transmitter weight to transmitter power
KPT	K_{P_T}	= constant relating transmitter fabrication cost to transmitter power

Computer Symbol	Text Symbol		Description
KPM	K_{P_M}	=	constant relating modulation equipment power requirement to equipment weight
KPD	K_{P_D}	=	constant relating demodulation equipment power requirement to equipment weight
KST	K_{ST}	=	constant relating transmitter power supply fabrication cost to power requirement
KWST	$K_{W_{ST}}$	=	constant relating transmitter power supply weight to power requirement
KSR	K_{SR}	=	constant relating receiver power supply fabrication cost to power requirement
KWR	K_{WR}	=	constant relating receiver power supply weight to power requirement
KH	K_H	=	constant relating transmitter heat exchanger fabrication cost to transmitter power dissipation
KX	K_X	=	constant relating transmitter heat exchanger weight to transmitter power dissipation
KM	K_M	=	constant relating modulation equipment weight to information rate
KFM	K_{FM}	=	constant relating modulation equipment fabrication cost to information rate
KD	K_D	=	constant relating demodulation equipment weight to information rate
KFD	K_{FD}	=	constant relating demodulation equipment fabrication cost to information rate
KQT	K_{q_T}	=	constant defined in text
KMT	K_{m_T}	=	constant defined in text

Computer Symbol	Text Symbol		Description
KNT	K_{n_T}	=	constant defined in text
KQR	K_{q_R}	=	constant defined in text
KMR	K_{m_R}	=	constant defined in text
KNR	K_{n_R}	=	constant defined in text
KGT	K_{g_T}	=	constant defined in text
KHT	K_{h_T}	=	constant defined in text
KJT	K_{j_T}	=	constant defined in text
QT	q_T	=	constant
MT	m_T	=	constant
NT	n_T	=	constant
QR	q_R	=	constant
MR	m_R	=	constant
NR	n_R	=	constant
GT	g_T	=	constant
HT	h_T	=	constant
KN	K_N	=	SNR constant for shot noise limited direct and heterodyne detection optical receiver
K	K	=	SNR constant for shot noise limited direct detection optical receiver
KT	K_M	=	SNR constant for thermal noise limited direct detection optical receiver
KR	K_R	=	SNR constant for radio receiver
KE	k_e	=	transmitter power efficiency

Computer Symbol	Text Symbol		Description
R	R	=	transmission range
LMBDI	λ_i	=	receiver input filter bandwidth in wavelength units
	B_O	=	receiver output filter bandwidth in frequency units
	Λ	=	optimization dummy variable
	Q	=	optimization dummy variable
	G	=	detector current gain
	I_D	=	detector dark current
TAUT	τ_t	=	transmitter transmissivity
TAUR	τ_r	=	receiver transmissivity
TAUA	τ_a	=	atmospheric transmissivity
ETA	η	=	detector quantum efficiency
QB	Q_B	=	background radiation photon spectral radiance
LAMBDA	λ	=	transmission wavelength
RL	R_L	=	receiver load resistance
SMK	k	=	Boltzsmann's constant
H	h	=	Planck's constant
Q	q	=	electronic charge
C	c	=	velocity of light
TE	T_e	=	receiver temperature
USBQ	$(\mu_S, B)_{Req}$	=	number of signal photoelectrons required per bit
UNBQ	$(\mu_N, B)_{Req}$	=	number of noise photoelectrons required per bit

Computer Symbol	Text Symbol		Description
USS	$\mu_{S, S}$	=	number of signal photoelectrons per second
UNS	$\mu_{N, S}$	=	number of noise photoelectrons per second
SN	$\left(\frac{S}{N}\right)$	=	receiver output power signal-to-noise ratio
RB	R_B	=	information rate in bits per second
CP	C_P	=	constant relating shot noise powers due to signal and background radiation

APPENDIX A2.2

INPUT DATA PROGRAM

FUNCTION

The function of the input data program is to provide parametric computer plots of the system burdens as a function of the major system parameters.

DESCRIPTION

Exhibit A2.2-1 is a flow chart of the Input Data Program. The input independent variables are listed below:

transmission wavelength (microns) λ [$\lambda_1, \dots, \lambda_5$]
information rate (bits per second) R_B [$10^1, 10^2, \dots, 10^{10}$]
transmitter aperture diameter (cm) d_T [1, 2, 5, 10, 20, 50, 100]
receiver aperture diameter (cm) d_R [10, 20, 50, 100, 200, 500, 1000]
transmitter power (watts) P_T [1, 2, 5, 10, 20, 50, 100]
receiver field of view (rad.) θ_R [$0.1 \times 10^{-3}, 0.2 \times 10^{-3},$
 $0.5 \times 10^{-3}, 1.0 \times 10^{-3}$]

Exhibit A2.2-2 contains a typical listing of the required system burdens data. Exhibit A2.2-3 contains a listing of the plots generated by the computer. Exhibit A2.2-4 contains a listing of the Fortran IV Input Data Program.

EXHIBIT A2.2-1

OPTIMIZATION METHODOLOGY INPUT DATA PROGRAM

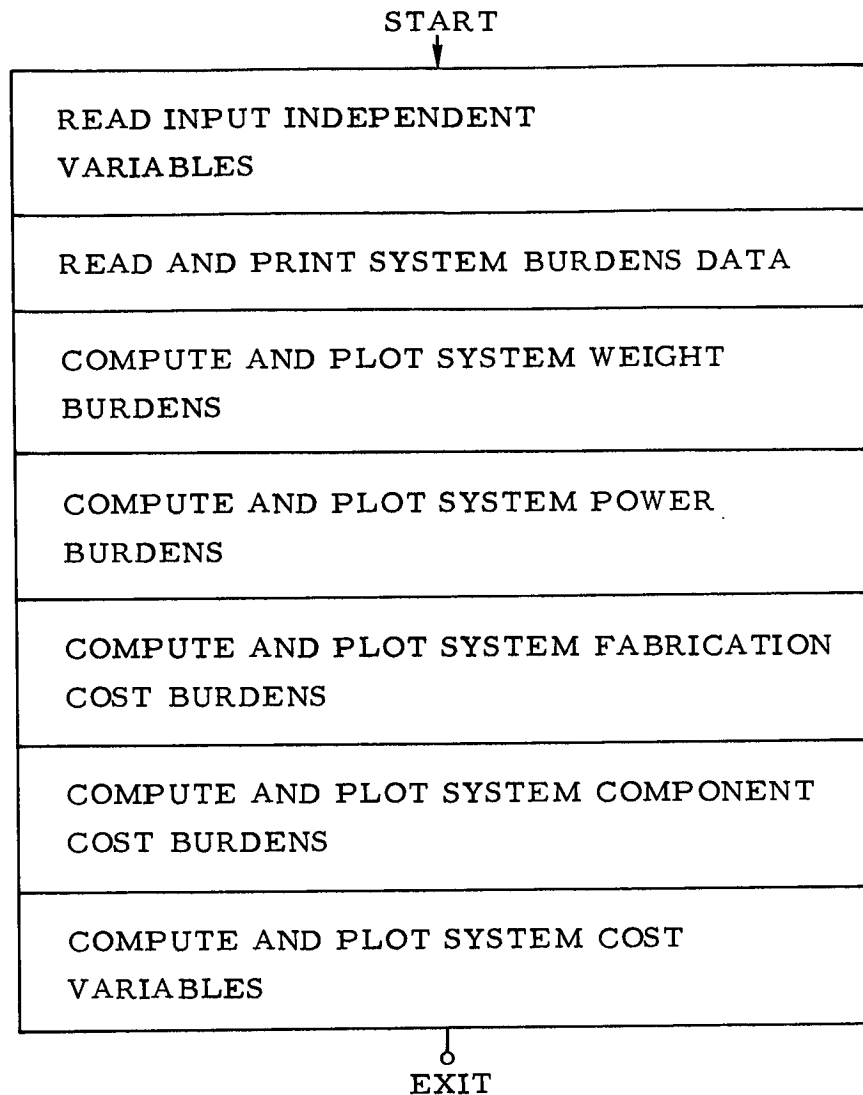


EXHIBIT A2.2-2 SYSTEM BURDENS INPUT DATA

Component	Parameter	Unit	Wavelength				Component	Parameter	Unit	Wavelength			
			0.5μ	0.63μ	0.84μ	3.39μ				0.5μ	0.63μ	0.84μ	3.39μ
Transmitter Antenna	K _{PT}	\$ ¹	14	—	—	—	Modulation Equipment	K _{PM}	\$/bit	7.5 x 10 ⁻⁵	7.5 x 10 ⁻⁵	0	—
	K _{QT}	lb ¹	0.01	—	—	—		K _M	lb/bit	5 x 10 ⁻⁸	5 x 10 ⁻⁸	0	—
	C _{KT}	\$	2 x 10 ⁴	—	—	—		K _{PM}	watt/lb	3.33	—	—	—
	W _{KT}	lb	25	—	—	—		CKM	\$	7500	7500	—	—
	m _T	—	2	—	—	—		W _{KM}	lb	5	5	—	—
Receiver Antenna	n _T	—	2	—	—	—	Demodulation Equipment	K _{FD}	\$/bit	5 x 10 ⁻⁵	5 x 10 ⁻⁵	—	—
	K _{QR}	\$ ²	8.75	—	—	—		K _D	lb/bit	10 ⁻⁷	10 ⁻⁷	—	—
	K _{GR}	lb ³	2.3 x 10 ⁻²	—	—	—		K _{PD}	watt/lb	3.33	—	—	—
	C _{KR}	\$	2.5 x 10 ⁴	—	—	—		CKD	\$	15,000	15,000	—	—
	W _{KR}	lb	20	—	—	—		W _{KD}	lb	30	30	—	—
Transmitter Acquisition and Track System	m _R	—	2	—	—	—	Transmitter Power Supply	K _{ST}	\$/watt	1250	—	—	—
	n _R	—	2	—	—	—		K _{WST}	lb/watt	0.125	—	—	—
	K _{AT}	\$ ⁴	80	—	—	—		CKE	\$	10 ⁴	—	—	—
	K _{WAT}	lb ¹	2.22	—	—	—		W _{KE}	lb	10	—	—	—
	K _{PQT}	watt/lb	0.66	—	—	—	Receiver Power Supply	K _{SR}	\$/watt	250	—	—	—
Receiver Acquisition and Track System	C _{AT}	\$	10,000	—	—	—		K _{WSR}	lb/watt	0.125	—	—	—
	W _{BT}	lb	460	—	—	—		CKF	\$	10 ⁴	—	—	—
	q _T	—	2	—	—	—		W _{KF}	lb	10	—	—	—
	K _{AR}	\$ ²	80	—	—	—		K _S	\$/lb	1640	—	—	—
	K _{WAR}	lb ³	2.22	—	—	—	General	K _{GT}	lb	5000	—	—	—
Transmitter	K _{POR}	watt/lb	0.66	—	—	—		K _{BT}	lb	6.5 x 10 ⁵	3200	100	—
	C _{AR}	\$	10,000	—	—	—		K _{JT}	\$	1.59 x 10 ⁶	3.28 x 10 ⁶	1.64 x 10 ⁴	—
	W _{BR}	lb	350	—	—	—		K _{MT}	lb	14	—	—	—
	q _R	—	2	—	—	—		K _{RT}	lb	74.1	—	—	—
	K _{PT}	\$ ⁵	5000	3200	100	27,700		K _{QT}	lb	1.57 x 10 ⁶	1.27 x 10 ⁶	9.5 x 10 ⁵	—
Transmitter	K _{WT}	lb ⁵	400	2000	10	5900	General	K _{MR}	lb	8.75	—	—	—
	K _{IT}	\$/watt	10	—	—	—		K _{GR}	lb	8.42	—	—	—
	K _X	lb/watt	0.07	—	—	—		K _{QR}	lb	80	—	—	—
	K _e	—	1 x 10 ⁻³	—	—	—							
	C _{KP}	\$	5000	2000	0.1	4 x 10 ⁻⁴							
Transmitter	C _{KH}	\$	0	—	—	—	General	K _{GT}	lb	1.57 x 10 ⁶	1.27 x 10 ⁶	9.5 x 10 ⁵	—
	W _{KP}	lb	100	100	25	100		K _{MT}	lb	14	—	—	—
	W _{KH}	lb	0	—	—	—		K _{RT}	lb	74.1	—	—	—
	P _{KT}	watt	10	—	—	—		K _{QT}	lb	1.57 x 10 ⁶	1.27 x 10 ⁶	9.5 x 10 ⁵	—
	q _T	—	2	—	—	—		K _{MR}	lb	8.75	—	—	—
Transmitter	b _T	—	1	—	—	—		K _{GR}	lb	80	—	—	—

¹Per unit of d_T
²Per 0 R unit
³Per unit of d_P
⁴Per 0_T unit
⁵Per P_T unit

EXHIBIT A2. 2-3

INPUT DATA PROGRAM COMPUTER PLOTS

All plots versus transmission wavelength.

System Weight Burdens

W_{d_T} vs d_T

W_{d_R} vs d_R

W_{QT} vs d_T

W_{QR} vs d_R

W_T vs P_T

W_H vs P_T

W_M vs R_B

W_D vs R_B

W_{ST} vs P_T $R_B = 10^8$, $d_T = 10$ cm

W_{ST} vs P_T $R_B = 10^8$, $d_T = 20$ cm

W_{ST} vs P_T $R_B = 10^8$, $d_T = 50$ cm

W_{SR} vs d_R $R_B = 10^8$

System Power Burdens

P_{QT} vs d_T

P_{QR} vs d_R

P_{PT} vs P_T

P_M vs R_B

P_D vs R_B

EXHIBIT A2.2-3 (continued)

System Fabrication Cost Burdens

C_{θ_T}	vs	d_T	
C_{θ_R}	vs	d_R	
C_{NT}	vs	d_T	
C_{NR}	vs	θ_R	
C_{FL}	vs	P_T	
C_H	vs	P_T	
C_{FM}	vs	R_B	
C_{FD}	vs	R_B	
C_{FT}	vs	P_T	$R_B = 10^8, d_T = 10 \text{ cm}$
C_{FT}	vs	P_T	$R_B = 10^8, d_T = 20 \text{ cm}$
C_{FT}	vs	P_T	$R_B = 10^8, d_T = 50 \text{ cm}$
C_{FR}	vs	d_R	$R_B = 10^8$

System Component Cost Burdens

C_{d_T}	vs	d_T	
C_{d_R}	vs	d_R	
C_{QT}	vs	d_T	
C_{QR}	vs	d_R	
C_{P_T}	vs	P_T	
C_M	vs	R_B	
C_D	vs	R_B	
C_{ST}	vs	P_T	$R_B = 10^8, d_T = 10 \text{ cm}$
C_{ST}	vs	P_T	$R_B = 10^8, d_T = 20 \text{ cm}$

EXHIBIT A2. 2-3 (continued)

$$\begin{array}{lll} C_{ST} & \text{vs} & P_T \\ C_{SR} & \text{vs} & d_R \end{array} \quad R_B = 10^8, d_T = 50 \text{ cm}$$
$$R_B = 10^8$$

System Cost Variables

$$\begin{array}{lll} C_T & \text{vs} & d_T \\ C_R & \text{vs} & d_R \\ C_G & \text{vs} & P_T \\ C_Q & \text{vs} & \theta_R \end{array}$$

EXHIBIT A2.2-4

\$JOB	CF	56030,2113A,01140,5,1000	C.E.RADFORD	
\$IBJOB	CER	GO,MAP		
\$IBFTC	MAIN	LIST,DECK		0020
	COMMON	/CURVE / LAM(10), KE(10), DT(10), THER(10), PL(10), DR(10)		0030
*		/FOFDT / WDT(10), WQT(10), PQT(10), CTHT(10), CNT(10),		0040
*		CDT(10), CQT(10), CT(10)		0050
*		/FOFDR / WDR(10), WQR(10), WSR(10), PQR(10), CTHR(10),		0060
*		CFR(10), CDR(10), CQR(10), CSR(10), CR(10),		0070
*		BD(10)		0080
*		/FOFPL / WT(10), WH(10), WST1(10), WST2(10), WST3(10),		0090
*		PPT(10), CFL(10), CFT1(10), CFT2(10), CFT3(10),		0100
*		CG(10), CH(10), CPT(10), CST1(10), CST2(10), CST3(10)		0110
*		/FOFBD / WM(10), WD(10), PM(10), PD(10), CFM(10),		0120
*		CFD(10), CM(10), CD(10)		0130
*		/FOFTHR/ CNR(10), CTH(10)		0140
*		/FREQ / NOLAM, NODT, NOTHR, NOPL, NODR, NOBD		0150
	COMMON	/TANTNA/ KTHT, KDT, CKT, WKT, MT, NT		0160
*		/RANTNA/ KTHR, KDR, CKR, WKR, MR, NR		0170
*		/TACTRS/ KAT, KWAT, KPQT, CAT, CTT, WBT, QT		0180
*		/RACTRS/ KAR, KWAR, KPQR, CAR, CTR, WBR, QR		0190
*		/XMITER/ KPT(10), KWT(10), KH, KX, CKP(10), CKH,		0200
*		WKP, WKH, PKT, GT, HT		0210
*		/MOD / KFM(10), KM(10), KPM, CKM(10), WKM(10)		0220
*		/DMOD / KFD(10), KD(10), KPD, CKD(10), WKD(10)		0230
*		/TPOWER/ KST, KWST, CKE, WKE		0240
*		/RPOWER/ KSR, KWSR, CKF, WKF		0250
*		/GEN / KS		0260
1000	FORMAT(1H1 ////)			0270
10	CONTINUE			0280
	CALL INPUT			0290
	DO 20I = 1,NOLAM			0300
	WRITE(2,1000)			0310
	CALL COST(I)			0320
	CALL OUTPUT(I)			0330
20	CONTINUE			0340
	GO TO 10			0350
	END			0360
\$IBFTC	INPUT	DECK		0370
	SUBROUTINE	INPUT		0380
	REAL	KE, KTHT, KDT, MT, NT, KTHR, KDR, MR, NR, KAT, KWAT, KPQT,		0390
*		KAR, KWAR, KPQR, KPT, KWT, KH, KX, KFM, KM, KPM, KFD, KD, KPD,		0400
*		KST, KWST, KSR, KWSR, KS, LAM		0410
	COMMON	/CURVE / LAM(10), KE(10), DT(10), THER(10), PL(10), DR(10)		0420
*		/FOFDT / WDT(10), WQT(10), PQT(10), CTHT(10), CNT(10),		0430
*		CDT(10), CQT(10), CT(10)		0440
*		/FOFDR / WDR(10), WQR(10), WSR(10), PQR(10), CTHR(10),		0450
*		CFR(10), CDR(10), CQR(10), CSR(10), CR(10),		0460
*		BD(10)		0470
*		/FOFPL / WT(10), WH(10), WST1(10), WST2(10), WST3(10),		0480
*		PPT(10), CFL(10), CFT1(10), CFT2(10), CFT3(10),		0490
*		CG(10), CH(10), CPT(10), CST1(10), CST2(10), CST3(10)		0500
*		/FOFBD / WM(10), WD(10), PM(10), PD(10), CFM(10),		0510
*		CFD(10), CM(10), CD(10)		0520
*		/FOFTHR/ CNR(10), CTH(10)		0530
*		/FREQ / NOLAM, NODT, NOTHR, NOPL, NODR, NOBD		0540
	COMMON	/TANTNA/ KTHT, KDT, CKT, WKT, MT, NT		0550
*		/RANTNA/ KTHR, KDR, CKR, WKR, MR, NR		0560
				0570

EXHIBIT A2.2-4 (continued)

```

*      /TACTRS/  KAT, KWAT, KPQT, CAT, CTT, WBT, QT      0580
*      /RACTRS/  KAR, KWAR, KPQR, CAR, CTR, WBR, QR      0590
*      /XMITER/  KPT(10), KWT(10), KH, KX, CKP(10), CKH,  0600
*                  WKP, WKH, PKT, GT, HT                  0610
*      /MOD      /  KFM(10), KM(10), KPM, CKM(10), WKM(10)  0620
*      /DMOD     /  KFD(10), KD(10), KPD, CKD(10), WKD(10)  0630
*      /TPOWER/  KST, KWST, CKE, WKE                      0640
*      /RPOWER/  KSR, KWSR, CKF, WKF                      0650
*      /GEN      /  KS                                     0660
2000  FORMAT( 5I15 )                                       0670
2010  FORMAT( 5E15.7 )                                       0680
      READ( 1,2000 ) NOLAM, NODT, NOTHR, NOPL, NODR, NOBD  0690
      READ( 1,2010 ) ( LAM(I), I= 1,NOLAM )                0700
      READ( 1,2010 ) ( KE(I), I= 1,NOLAM )                 0710
      READ( 1,2010 ) ( KPT(I), I= 1,NOLAM )                 0720
      READ( 1,2010 ) ( KWT(I), I= 1,NOLAM )                 0730
      READ( 1,2010 ) ( CKP(I), I= 1,NOLAM )                 0740
      READ( 1,2010 ) ( KFM(I), I= 1,NOLAM )                 0750
      READ( 1,2010 ) ( KM(I), I= 1,NOLAM )                  0760
      READ( 1,2010 ) ( CKM(I), I= 1,NOLAM )                 0770
      READ( 1,2010 ) ( WKM(I), I= 1,NOLAM )                 0780
      READ( 1,2010 ) ( KFD(I), I= 1,NOLAM )                 0790
      READ( 1,2010 ) ( KD(I), I= 1,NOLAM )                  0800
      READ( 1,2010 ) ( CKD(I), I= 1,NOLAM )                 0810
      READ( 1,2010 ) ( WKD(I), I= 1,NOLAM )                 0820
      READ( 1,2010 ) ( DT(I), I= 1,NODT )                   0830
      READ( 1,2010 ) ( THER(I), I= 1,NOTHR )                 0840
      READ( 1,2010 ) ( PL(I), I= 1,NOPL )                   0850
      READ( 1,2010 ) ( DR(I), I= 1,NODR )                   0860
      READ( 1,2010 ) ( BD(I), I= 1,NOBD )                   0870
      READ( 1,2010 ) KTHT, KDT, CKT, WKT, MT,              0880
*                  NT, KTHR, KDR, CKR, WKR,                0890
*                  MR, NR, KAT, KWAT, KPQT,                 0900
*                  CAT, CTT, WBT, QT, KAR,                  0910
*                  KWAR, KPQR, CAR, CTR, WBR,               0920
*                  QR, KH, KX, CKH, WKP,                    0930
*                  WKH, PKT, GT, HT, KPM,                   0940
*                  KPD, KST, KWST, CKE, WKE,                 0950
*                  KSR, KWSR, CKF, WKF, KS                  0960
      CALL PDUMP( LAM(1), KS, 1 )                            0970
      RETURN                                                  0980
      END                                                    0990
$IBFTC COST LIST,REF,DECK                                  1000
      SUBROUTINE COST( K )                                    1010
      REAL KQT, KMT, KNT, KMR, KNR, KQR, KGT, KHT, KJT      1020
      REAL KE, KTHT, KDT, MT, NT, KTHR, KDR, MR, NR, KAT, KWAT, KPQT,
*      KAR, KWAR, KPQR, KPT, KWT, KH, KX, KFM, KM, KPM, KFD, KD, KPD,
*      KST, KWST, KSR, KWSR, KS, LAM                        1050
      COMMON /CURVE / LAM(10), KE(10), DT(10), THER(10), PL(10), DR(10)
*      /FOFDT / WDT(10), WQT(10), PQT(10), CTHT(10), CNT(10),
*      CDT(10), CQT(10), CT(10)                            1080
*      /FOFDR / WDR(10), WQR(10), WSR(10), PQR(10), CTHR(10),
*      CFR(10), CDR(10), CQR(10), CSR(10), CR(10),         1100
*      BD(10)                                                1110
*      /FOFPL / WT(10), WH(10), WST1(10), WST2(10), WST3(10),
*      PPT(10), CFL(10), CFT1(10), CFT2(10), CFT3(10),     1130
*      CG(10), CH(10), CPT(10), CST1(10), CST2(10), CST3(10) 1140

```

EXHIBIT A2.2-4 (continued)

```

*      /FOFBD / WM(10), WD(10), PM(10), PD(10), CFM(10),      1150
*      CFM(10), CM(10), CD(10)                                1160
*      /FOFTHR/ CNR(10), CTH(10)                               1170
*      /FREQ / NOLAM, NODT, NOTHR, NOPL, NODR, NOBD           1180
COMMON /TANTNA/ KTHT, KDT, CKT, WKT, MT, NT                    1190
*      /RANTNA/ KTHR, KDR, CKR, WKR, MR, NR                    1200
*      /TACTRS/ KAT, KWAT, KPQT, CAT, CTT, WBT, QT             1210
*      /RACTRS/ KAR, KWAR, KPQR, CAR, CTR, WBR, QR             1220
*      /XMITER/ KPT(10), KWT(10), KH, KX, CKP(10), CKH,        1230
*      WKP, WKH, PKT, GT, HT                                    1240
*      /MOD / KFM(10), KM(10), KPM, CKM(10), WKM(10)           1250
*      /DMOD / KFD(10), KD(10), KPD, CKD(10), WKD(10)         1260
*      /TPOWER/ KST, KWST, CKE, WKE                             1270
*      /RPOWER/ KSR, KWSR, CKF, WKF                             1280
*      /GEN / KS                                                 1290
EQUIVALENCE ( KMT,KTHT), ( KMR,KTHR), ( KQR,KAR)              1300
KGT = KPT(K)                                                    1310
KQT = KAT / LAM(K) **QT                                          1320
KNT = KDT * ( KS * ( 1.+KWAT ) + KPQT * KWAT * ( KST + KS * KWST )) 1330
KNR = KDR * ( KS * ( 1.+KWAR ) + KPQR * KWAR * ( KSR + KS * KWSR )) 1340
KHT = KS * KWT( K )                                              1350
KJT = KS * ( KWST/ KE(K) + KX * ( 1./KE(K)-1. ) ) + KST /KE(K) 1360
*      + KH * ( 1./KE(K)-1. )                                     1370
DO 10I = 1,NODT                                                  1380
    DTNT = DT(I) **NT                                             1390
    WDT(I) = KDT * DTNT + WKT                                       1400
    WQT(I) = WBT + KWAT * KDT * DTNT                               1410
    PQT(I) = KPQT * ( WBT + KWAT * KDT * DTNT )                    1420
    CTHT(I) = KTHT * DT(I) **MT + CKT                             1430
    CNT(I) = CAT + KAT / LAM(K) **QT * DT(I) **QT                1440
    CDT(I) = CTHT + KS * WDT(I)                                     1450
    CQT(I) = CAT + CTT + KS * WQT(I)                               1460
    CT(I) = KQT * DT(I) **QT + KMT * DT(I) **MT + KNT * DTNT     1470
10 CONTINUE                                                       1480
DO 20I = 1,NODR                                                  1490
    DRNR = DR(I) **NR                                              1500
    WDR(I) = KDR * DRNR + WKR                                       1510
    WQR(I) = WBR + KWAR * KDR * DRNR                               1520
    HOLD= KPD*( KD(K) *1.E8 + WKD(K) ) + KPQR * ( WBR + KWAR *   1530
*      KDR * DRNR )                                               1540
    WSR(I) = KWSR * HOLD + WKF                                       1550
    PQR(I) = KPQR * ( WBR + KWAR * KDR * DRNR )                    1560
    CTHR(I) = KTHR * DR(I) **MR + CKR                               1570
    CFR(I) = KSR * HOLD + CKF                                       1580
    CDR(I) = CTHR(I) + KS * WDR(I)                                   1590
    CQR(I) = CAR + CTR + KS * WQR(I)                               1600
    CSR(I) = CFR(I) + KS * WSR(I)                                   1610
    CR(I) = KMR * DR(I) **MR + KNR * DRNR                          1620
20 CONTINUE                                                       1630
DO 30I = 1,NOPL                                                  1640
    WT(I) = KWT(K) * PL(I) **HT + WKP                             1650
    WH(I) = KX * ( 1./KE(K)-1. ) * PL(I) + WKH                    1660
    WST1(I) = KWST * ( KPM * KM(K) *1.E8 + PL(I) / KE(K) + KPQT * 1670
*      ( WBT + KWAT * KDT * (10.) **NT ) ) + WKE                 1680
*      WST2(I) = KWST * ( KPM * KM(K) *1.E8 + PL(I) / KE(K) + KPQT * 1690
*      ( WBT + KWAT * KDT * (20.) **NT ) ) + WKE                 1700
*      WST3(I) = KWST * ( KPM * KM(K) *1.E8 + PL(I) / KE(K) + KPQT * 1710

```

EXHIBIT A2.2-4 (continued)

```

*      ( WBT + KWAT * KDT * (50.) **NT ) ) + WKE      1720
PPT(I) = PL(I) /KE(K) + PKT      1730
CFL(I) = KPT(K) * PL(I) **GT + CKP(K)      1740
CH(I) = KH * ( 1./KE(K)-1. ) * PL(I) + CKH      1750
CFT1(I) = KST * ( KPM * KM(K) * 1.E8 + PL(I)/KE(K) + KPQT *      1760
*      ( WBT + KWAT * KDT * (10.) **NT ) ) + CKE      1770
CFT2(I) = KST * ( KPM * KM(K) * 1.E8 + PL(I) /KE(K) + KPQT *      1780
*      ( WBT + KWAT * KDT * (20.) **NT ) ) + CKE      1790
CFT3(I) = KST * ( KPM * KM(K) * 1.E8 + PL(I) /KE(K) + KPQT *      1800
*      ( WBT + KWAT * KDT * (50.) **NT ) ) + CKE      1810
CPT(I) = CFL(I) + CH(J) + KS * ( WT(I)+WH(I) )      1820
CST1(I) = CFT1(I) + KS * WST1(I)      1830
CST2(I) = CFT2(I) + KS * WST2(I)      1840
CST3(I) = CFT3(I) + KS * WST3(I)      1850
CG(I) = KGT * PL(I) **GT + KHT * PL(I) **HT + KJT * PL(I)      1860
30  CONTINUE      1870
DO 40I = 1,NOBD      1880
    WM(I) = KM(K) * BD(I) + WKM(K)      1890
    WD(I) = KD(K) * BD(I) + WKD(K)      1900
    PM(I) = KPM * (KM(K) * BD(I) + WKM(K) )      1910
    PD(I) = KPD * ( KD(K) * BD(I) + WKD(K) )      1920
    CFM(I) = KFM(K) * BD(I) + CKM(K)      1930
    CFD(I) = KFD(K) * BD(I) + CKD(K)      1940
    CM(I) = CFM(I) + KS * WM(I)      1950
    CD(I) = CFD(I) + KS * WD(I)      1960
40  CONTINUE      1970
DO 50I = 1,NOTHR      1980
    CNR(I) = CAR + KAR / THER(I) **QR      1990
    CTH(I) = KQR / THER(I) **QR      2000
50  CONTINUE      2010
    RETURN      2020
    END      2030
$IBFTC OUTPUT LIST,DECK      2040
    SUBROUTINE OUTPUT( K )      2050
    COMMON /CURVE / LAM(10), KE(10), DT(10), THER(10), PL(10), DR(10)      2060
*      /FOFDT / WDT(10), WQT(10), PQT(10), CTHT(10), CNT(10),      2070
*      CDT(10), CQT(10), CT(10)      2080
*      /FOFDR / WDR(10), WQR(10), WSR(10), PQR(10), CTHR(10),      2090
*      CFR(10), CDR(10), CQR(10), CSR(10), CR(10),      2100
*      BD(10)      2110
*      /FOFPL / WT(10), WH(10), WST1(10), WST2(10), WST3(10),      2120
*      PPT(10), CFL(10), CFT1(10), CFT2(10), CFT3(10),      2130
*      CG(10), CH(10), CPT(10), CST1(10), CST2(10), CST3(10)      2140
*      /FOFBD / WM(10), WD(10), PM(10), PD(10), CFM(10),      2150
*      CFD(10), CM(10), CD(10)      2160
*      /FOFTHR/ CNR(10), CTH(10)      2170
*      /FREQ / NOLAM, NODT, NOTHR, NOPL, NODR, NOBD      2180
COMMON /TANTNA/ KTHR, KDT, CKT, WKT, MT, NT      2190
*      /RANTNA/ KTHR, KDR, CKR, WKR, MR, NR      2200
*      /TACTRS/ KAT, KWAT, KPQT, CAT, CTT, WBT, QT      2210
*      /RACTRS/ KAR, KWAR, KPQR, CAR, CTR, WBR, QR      2220
*      /XMITER/ KPT(10), KWT(10), KH, KX, CKP(10), CKH,      2230
*      WKP, WKH, PKT, GT, HT      2240
*      /MOD / KFM(10), KM(10), KPM, CKM(10), WKM(10)      2250
*      /DMOD / KFD(10), KD(10), KPD, CKD(10), WKD(10)      2260
*      /TPOWER/ KST, KWST, CKE, WKE      2270
*      /RPOWER/ KSR, KWSR, CKF, WKF      2280

```


EXHIBIT A2.2-4 (continued)

```

*          /GEN  /  KS
*          DIMENSION HOLD(10), HOLD1(10), HOLD2(10), HOLD3(10)
3000  FORMAT(14X 2HDT 18X 3HWDT 17X 3HWQT 17X 3HPQT 17X 4HCTHT 16X 3HCNT
*          *///(E23.8, 5E20.8) )
3010  FORMAT(///14X2HDT18X 3HCDT 17X 3HCQT 18X 2HCT //(E23.8, 3E20.8) )
3020  FORMAT(///14X2HDR18X 3HWDR 17X 3HWQR 17X 3HWSR 17X 3HPQR 17X 4HCTHR
*          */// (E23.8, 5E20.8) )
3030  FORMAT(///14X2HDR18X 3HCFR 17X 3HCDR 17X 3HCQR 17X 3HCSR 18X 2HCR
*          */// (E23.8, 5E20.8) )
3040  FORMAT(///14X2HPL18X 2HWT 18X 2HWH 18X 4HWST1 16X 4HWST2 16X 4HWST3
*          */// (E23.8,5E20.8) )
3050  FORMAT(///14X2HPL18X 3HPPT 17X 3HCFL 17X 2HCH 18X 4HCFT1 16X 4HCFT2
*          */// (E23.8,5E20.8) )
3060  FORMAT(///14X2HPL18X 4HCFT3 16X 3HCPT 17X 4HCST1 16X 4HCST2 16X
*          * 4HCST3 // (E23.8, 5E20.8) )
3070  FORMAT(///14X2HPL18X 2HCG // (E23.8,E20.8) )
3080  FORMAT(///14X2HBD18X 2HWM 18X 2HWD 18X 2HPM 18X 2HPD //(E23.8,
*          * 4E20.8) )
3090  FORMAT(///14X2HBD18X 3HCFM 17X 3HCFD 17X 2HCM 18X 2HCD //
*          *( / E23.8, 4E20.8) )
3100  FORMAT(///14X4HTHER16X 3HCNR 17X 3HCTH //(E23.8,2E20.8) )
3110  FORMAT( /// 14X 3HLAM 17X 3HKPT 17X 3HKWT 17X 3HKFD 17X 2HKE
*          * 18X 3HCKP // E23.8, 5E20.8 /// 14X 2HKD 18X 3HKFM 17X 2HKM
*          * 18X 3HCKD 17X 3HCKM 17X 3HWKM // E23.8, 5E20.8 /// 14X 4HWKD=
*          * E16.8 )
*          WRITE( 2,3110 ) LAM(K), KPT(K), KWT(K), KFD(K), KE(K), CKP(K),
*          *          KD(K), KFM(K), KM(K), CKD(K), CKM(K), WKM(K),
*          *          WKD(K)
*          WRITE( 2,3000 ) ( DT(I), WDT(I), WQT(I), PQT(I), CTHT(I),
*          *          CNT(I), I = 1,NODT )
*          WRITE( 2,3010) ( DT(I), CDT(I), CQT(I), CT(I), I = 1,NODT )
*          WRITE( 2,3020) ( DR(I), WDR(I), WQR(I), WSR(I), PQR(I), CTHR(I),
*          *          I = 1,NODR )
*          WRITE( 2,3030) ( DR(I), CFR(I), CDR(I), CQR(I), CSR(I), CR(I),
*          *          I = 1,NODR )
*          WRITE( 2,3040) ( PL(I), WT(I), WH(I), WST1(I), WST2(I), WST3(I),
*          *          I = 1,NOPL )
*          WRITE( 2,3050) ( PL(I), PPT(I), CFL(I), CH(I), CFT1(I), CFT2(I),
*          *          I = 1,NOPL )
*          WRITE( 2,3060) ( PL(I), CFT3(I), CPT(I), CST1(I), CST2(I), CST3(I)
*          *          , I = 1,NOPL )
*          WRITE( 2,3070) ( PL(I), CG(I), I= 1,NOPL )
*          WRITE( 2,3080) ( BD(I), WM(I), WD(I), PM(I), PD(I), I = 1,NOBD )
*          WRITE( 2,3090) ( BD(I), CFM(I), CFD(I), CM(I), CD(I),I=1,NOBD )
*          WRITE( 2,3100) ( THER(I), CNR(I), CTH(I), I = 1,NOTHR )
*          IF( K .GT. 1 ) RETURN
*          DO 10I = 1,NODT
*          HOLD(I) = DT(I)
*          HOLD1(I) = DT(I)
10  CONTINUE
*          CALL CPlot( 4,HOLD,20.,2HDT,NODT,WDT,8.,3HWDT,NODT,WQT,8.,3HWQT,
*          *          NODT,PQT,8.,3HPQT,NODT,CTHT,8.,4HCTHT)
*          CALL CPlot( 4,HOLD1,20.,2HDT,NODT,CNT,8.,3HCNT,NODT,CDT,8.,3HCDT,
*          *          NODT,CQT,8.,3HCQT,NODT,CT,8.,2HCT )
*          DO 20I = 1,NODR
*          HOLD(I) = DR(I)
*          HOLD1(I) = DR(I)

```

EXHIBIT A2.2-4 (continued)

```

20  CONTINUE
    CALL CPLOT(5,HOLD,20.,2HDR,NODR,WDR,8.,3HWDR,NODR,WQR,8.,3HWQR,
*      NODR,WSR,8.,3HWSR,NODR,PQR,8.,3HPQR,
*      NODR,CTHR,8.,4HCTHR )
    CALL CPLOT(5,HOLD1,20.,2HDR,NODR,CFR,8.,3HCFR,NODR,CDR,8.,3HCDR,
*      NODR,CQR,8.,3HCQR,NODR,CSR,8.,3HCSR,
*      NODR,CR,8.,2HCR )
    DO 30I = 1,NOPL
        HOLD(I) = PL(I)
        HOLD1(I) = PL(I)
        HOLD2(I) = PL(I)
        HOLD3(I) = PL(I)
30  CONTINUE
    CALL CPLOT(6,HOLD,20.,2HPL,NOPL,CFT1,8.,4HCFT1,NOPL,CFT2,8.,4HCFT2
*      ,NOPL,CFT3,8.,4HCFT3,NOPL,CST1,8.,4HCST1,
*      NOPL,CST2,8.,4HCST2,NOPL,CST3,8.,4HCST3 )
    CALL CPLOT(3,HOLD1,20.,2HPL,NOPL,WST1,8.,4HWST1,NOPL,WST2,8.,
*      4HWST2,NOPL,WST3,8.,4HWST3 )
    CALL CPLOT(4,HOLD2,20.,2HPL,NOPL,WT,8.,2HWT,NOPL,WH,8.,2HWH,
*      NOPL,CFL,8.,3HCFL,NOPL,CH,8.,2HCH )
    CALL CPLOT(3,HOLD3,20.,2HPL,NOPL,PPT,8.,3HPPT,NOPL,CPT,8.,3HCPT,
*      NOPL,CG,8.,2HCG )
    DO 40I = 1,NOBD
        HOLD(I) = BD(I)
        HOLD1(I) = BD(I)
40  CONTINUE
    CALL CPLOT(4,HOLD,20.,2HBD,NOBD,WM,8.,2HWM,NOBD,WD,8.,2HWD,
*      NOBD,PM,8.,2HPM,NOBD,PD,8.,2HPD )
    CALL CPLOT(4,HOLD1,20.,2HBD,NOBD,CFM,8.,3HCFM,NOBD,CFD,8.,3HCFD,
*      NOBD,CM,8.,2HCM,NOBD,CD,8.,2HCD )
    DO 50I = 1,NOTHR
        HOLD(I) = THER
50  CONTINUE
    CALL CPLOT(2,HOLD,20.,4HTHER,NOTHR,CNR,8.,3HCNR,NOTHR,CTH,8.,
*      3HCTH )
    RETURN
    END

$DATA
      5          7          4          7          7
      10
      .51E-4      .63E-4      .84E-4      3.39E-4      10.6E-4
      1.E-3       2.E-3       1.E-4       4.E-4       1.E-1
      5.E3        3.2E3       1.E2       27.7E3      1.43
      400.        2.0E3       10.0       5.9E3       2.
      5.E3        2.0E3       2.E3       2.0E3       2.E3
      7.5E-5      7.5E-5      0.00     1.5E-4      0.00
      5.0E-8      5.0E-8      0.00     9.0E-8      0.00
      7.5E+3      7.5E+3      7.5E3     1.0E+4      3.E4
      5.0E+0      5.0E+0      5.0E0     7.5E+0      20.0
      5.0E-5      5.0E-5      5.E-5     1.0E-4      1.E-4
      1.0E-7      1.0E-7      1.E-7     2.0E-7      2.E-7
      15.0E3      15.0E3      15.E3     25.E+3      27.5E3
      3.0E+1      3.0E+1      3.0E1     5.0E+1      5.5E1
      1.0         2.0         5.0       10.        20.
      50.         100.        5.0E-3    1.E-3       3400
      .1E-3       .2E-3       5.0       10.        3410
      1.0         2.0         5.0       10.        20.

```

EXHIBIT A2.2-4 (continued)

50.	100.			3430
10.	20.	50.	100.	200. 3440
500.	1.E3			3450
10.	1.E2	1.E3	1.E4	1.E5 3460
1.E6	1.E7	1.E8	1.E9	1.E10 3470
14.	.01	2.E4	25.	2. 3480
2.	8.75	2.3E-2	2.5E4	20. 3490
2.	2.	.21E-5	2.22	.66 3500
4.E6	0.	460.	1.	.039 3510
2.22	.66	2.E6	0.	350. 3520
1.	10.	.07	0.	100. 3530
0.	10.	2.	1.	3.33 3540
3.33	1250.	.125	1.E4	10. 3550
250.	.125	1.E4	10.	40. 3560

APPENDIX A2.3

OUTPUT DATA PROGRAM

FUNCTION

The function of the Output Data Program is to provide parametric plots as a function of transmission wavelength and information rate of the optimum values of the major system parameters and the corresponding system weight, power, fabrication cost and component cost burdens.

DESCRIPTION

Exhibit A2.3-1 is a flow chart of the Output Data Program.

The input information required for the program is the systems burdens data and the optimum value of the major system parameters, d_{TO} , d_{RO} , P_{TO} , θ_{RO} , as a function of information rate as determined by an optimization program.

Exhibit A2.3-2 contains a listing of the plots generated by the computer.

Exhibit A2.3-3 contains a listing of the Fortran Output Data Program.

OUTPUT DATA PROGRAM

START



READ AND PRINT SYSTEMS BURDENS DATA
READ AND PRINT OPTIMUM SYSTEM PARAMETERS $d_{TO}, d_{RO}, P_{TO}, \theta_{RO}$
<p>COMPUTE, PLOT, AND PRINT OPTIMUM WEIGHT BURDENS</p> $W_{d_T} = K_{d_T} (d_{TO})^{n_T} + W_{KT}$ $W_{d_R} = K_{d_R} (d_{RO})^{n_R} + W_{KR}$ $W_{QT} = W_{BT} + K_{W_{AT}} K_{d_T} (d_{TO})^{n_T}$ $W_{QR} = W_{BR} + K_{W_{AR}} K_{d_R} (d_{RO})^{n_R}$ $W_T = K_{W_T} (P_{TO})^{h_T} + W_{KP}$ $W_H = K_X \left(\frac{1 - k_e}{k_e} \right) P_{TO} + W_{KH}$ $W_M = K_{M^R_B} + W_{KM}$ $W_D = K_{D^R_B} + W_{KD}$ $W_{ST} = K_{W_{ST}} \left\{ K_P K_{M^R_B} + K_P W_{K_M} + \frac{P_{TO}}{k_e} \right. \\ \left. + K_{P_{QT}} \left[W_{BT} + K_{W_{AT}} K_{d_T} (d_{TO})^{n_T} \right] \right\} + W_{KE}$ $W_{SR} = K_{W_{SR}} \left\{ K_P K_{D^R_B} + K_P W_{K_D} \right. \\ \left. + K_{P_{QR}} \left[W_{BR} + K_{W_{AR}} K_{d_R} (d_{RO})^{n_R} \right] \right\} + W_{KF}$

$$W_A = W_{dT} + W_{QT} + W_T + W_H + W_M + W_{ST}$$

$$W_B = W_{dR} + W_{QR} + W_D + W_{SR}$$

COMPUTE, PLOT, AND PRINT OPTIMUM POWER BURDENS

$$P_{QT} = K_P \left[W_{BT} + K_{W_{AT}} K_{d_T} (d_{TO})^{n_T} \right]$$

$$P_{QR} = K_P \left[W_{BR} + K_{W_{AR}} K_{d_R} (d_{RO})^{n_R} \right]$$

$$P_{PT} = \frac{P_{TO}}{k_e} + P_{KT}$$

$$P_M = K_P K_M R_B + K_P W_{KM}$$

$$P_D = K_P K_D R_B + K_P W_{KD}$$

$$P_A = P_{QT} + P_{PT} + P_M$$

$$P_B = P_{QR} + P_D$$

COMPUTE, PLOT, AND PRINT OPTIMUM FABRICATION COST BURDENS

$$C_{\theta_T} = K_{\theta_T} (d_{TO})^{m_T} + C_{KT}$$

$$C_{\theta_R} = K_{\theta_R} (d_{RO})^{m_R} + C_{KR}$$

$$C_{NT} = C_{AT} + \frac{K_{AT}}{(A)^{q_T}} (d_{TO})^{q_T}$$

$$C_{NR} = C_{AR} + K_{AR} (\theta_{RO})^{-q_R}$$

$$C_{FL} = K_P (P_{TO})^{q_T} + C_{KP}$$

$$C_H = K_H \left(\frac{1 - k_e}{k_e} \right) P_{TO} + C_{KH}$$

$$C_{FM} = K_{FM} R_B + C_{KM}$$

$$C_{FD} = K_{FD} R_B + C_{KD}$$

$$C_{FT} = K_{ST} \left\{ K_P K_M R_B + K_P W_{KM} + \frac{P_{TO}}{k_e} + K_P \left[W_{BT} + K_{W_{AT}} K_{d_T} (d_{TO})^{n_T} \right] \right\} + C_{KE}$$

$$C_{FR} = K_{SR} \left\{ K_P K_D R_B + K_P W_{KD} + K_P \left[W_{BR} + K_{W_{AR}} K_{d_R} (d_{RO})^{n_R} \right] \right\} + C_{KF}$$

$$C_{FA} = C_{\theta_T} + C_{NT} + C_{FL} + C_H + C_{FM} + C_{FT}$$

$$C_{FB} = C_{\theta_R} + C_{NR} + C_{FD} + C_{FR}$$

COMPUTE, PLOT, AND PRINT OPTIMUM SYSTEM COMPONENT COST BURDENS

$$C_{dT} = C_{\theta_T} + K_S W_{dT}$$

$$C_{dR} = C_{\theta_R} + K_S W_{dR}$$

$C_{QT} = C_{AT} + K_S W_{QT}$ $C_{QR} = C_{AR} + K_S W_{QR}$ $C_{PT} = C_{FL} + C_H + K_S W_T + K_S W_H$ $C_M = C_{FM} + K_S W_M$ $C_D = C_{FD} + K_S W_D$ $C_{ST} = C_{FT} + K_S W_{ST}$ $C_{SR} = C_{FR} + K_S W_{SR}$	<p>COMPUTE, PLOT, AND PRINT OPTIMUM SYSTEM COST BURDENS</p> $K_{gT} = K_{pT}$ $K_{hT} = K_S W_T$ $K_{iT} = K_S \left\{ \frac{K_{W_{ST}}}{k_e} + K_X \left(\frac{1-k}{k_e} \right) \right\} + \frac{K_{ST}}{k_e} + K_H \left(\frac{1-k}{k_e} \right)$ $K_{mT} = K_{\theta T}$ $K_{nT} = K_{dT} \left\{ K_S \left[1 + K_{W_{AT}} \right] + K_{p_{QT}} K_{W_{AT}} \left[K_{ST} + K_S W_{ST} \right] \right\}$ $K_{qT} = \frac{K_{AT}}{(\lambda)^n T}$ $K_{mR} = K_{\theta R}$ $K_{nR} = K_{dR} \left\{ K_S \left[1 + K_{W_{AR}} \right] + K_{p_{OR}} K_{W_{AR}} \left[K_{SR} + K_S W_{SR} \right] \right\}$ $K_{qR} = K_{AR}$ $C_{TO} = K_{qT} (d_{TO})^q + K_{mT} (d_{TO})^m + K_{nT} (d_{TO})^n$ $C_{RO} = K_{mR} (d_{RO})^m + K_{nR} (d_{RO})^n$ $C_{QO} = K_{qR} (\theta_{RO})^{-q_R}$ $C_{GO} = K_{gT} (P_{TO})^g + K_{hT} (P_{TO})^h + K_{iT} (P_{TO})^i$ $C_V = C_{GO} + C_{TO} + C_{QO} + C_{RO}$ $C_S = C_V + C_{FA} + C_{FB}$ $C_A = C_{GO} + C_{TO} + C_{FA}$ $C_B = C_{QO} + C_{RO} + C_{FB}$
---	--

EXHIBIT A2.3-2

OUTPUT DATA PROGRAM COMPUTER PLOTS

All plots versus transmission wavelength.

System Weight Burdens W_{dT} vs R_B W_{dR} vs R_B W_{QT} vs R_B W_{QR} vs R_B W_T vs R_B W_H vs R_B W_M vs R_B W_D vs R_B W_{ST} vs R_B W_{SR} vs R_B W_A vs R_B W_B vs R_B System Fabrication Cost Burdens $C_{\theta T}$ vs R_B $C_{\theta R}$ vs R_B C_{NT} vs R_B C_{NR} vs R_B C_{FL} vs R_B C_H vs R_B C_{FM} vs R_B C_{FD} vs R_B C_{FT} vs R_B C_{FR} vs R_B C_{FA} vs R_B C_{FB} vs R_B System Power Burdens P_{QT} vs R_B P_{QR} vs R_B P_{PT} vs R_B P_M vs R_B P_D vs R_B P_A vs R_B P_B vs R_B System Component Cost Burdens C_{dT} vs R_B C_{dR} vs R_B C_{QT} vs R_B C_{QR} vs R_B C_{PT} vs R_B C_M vs R_B C_D vs R_B C_{ST} vs R_B C_{SR} vs R_B

EXHIBIT A2.3-2 (continued)

System Cost Variables

C_T vs R_B

C_R vs R_B

C_G vs R_B

C_Q vs R_B

C_V vs R_B

C_A vs R_B

C_B vs R_B

C_S vs R_B

EXHIBIT A2.3-3

C OUTPUT OPTIMIZATION METHODOLOGY, OUTPUT DATA PROGRAM

```

SUBROUTINE OUTPUT(DTO,DRO,PTO,THERO,RR)
REAL KTHT, KDT, MT, NT, KTHR, KDR, MR, NR, KAT, KWAT, KPQT, KAR
REAL KVAR, KPQR, KPT, KWT, KH, KX, KE, KFM, KM, KPM, KFD, KD
REAL KPD, KST, KWST, KSR, KWSR, KS, KHT, KJT, KGT, KMT, KNT, KQT
REAL KMR, KNR, KQR, LAMBDA, LMBDI, K, KN
COMMON/TRAN/ KTHT, KDT, CKT, WKT, MT, NT
COMMON/PCANT/ KTHR, KDR, CKR, WKR, MR, NR
COMMON/TACTS/ KAT, KWAT, KPQT, CAT, WBT, QT
COMMON/RACTS/ KAR, KVAR, KPQR, CAR, WBR, QR
COMMON/TRNSM/ KPT, KWT, KH, KX, KE, CKP, CKH, WKP, WKH, PKT, GT, HT
COMMON/EQMOD/ KFM, KM, KPM, CKM, WKM
COMMON/EQDMD/ KFD, KD, KPD, CKD, WKD
COMMON/TRNPS/ KST, KWST, CKF, WKF
COMMON/RCVPS/ KSR, KWSR, CKF, WKF
COMMON/GENRL/ KS, LAMBDA, LMBDI, R, TAUT, TAUR, TAU, ETA, SN, QB
COMMON/OUTPT/ KHT, KJT, KGT, KMT, KNT, KQT, KMR, KNR, KQR
WRITE(6,1) RR, DTO, DRO, PTO, THERO
WDT = KDT*DTO**MT + WKT
WDR = KDR*DRO**NR + WKR
WQT = WBT + KWAT*KDT *DTO**NT
WQR = WBR + KVAR*KDR *DRO**NR
WT = KWT*PTO**HT + WKP
WH = PTO*KX * (1.-KE)/KE + WKH
WM = KM*RB + WKM
WD = KD*RB + WKD
WST = KWST*(KPM*KM*RB + KPM*WKM + PTO/KE + KPQT*(WBT + KWAT*KDT
* *DTO**NT)) + WKF
WSR = KWSR*(KPD*KD*RB + KPD*WKD + KPQR*(WBR + KVAR*KDR*DRO**NR))
* + WKF
WA = WDT + WQT + WT + WH + WM + WST
WB = WDR + WQR + WD + WSR
WRITE(6,2) WDT, WDR, WQT, WQR, WT, WH, WM, WD, WST, WSR, WA, WB
PQT = KPQT*(WBT + KWAT*KDT*DTO**NT)
PQR = KPQR*(WBR + KVAR*KDR*DRO**NR)
PPT = PTO/KE + PKT
PM = KPM*(KM*RB + WKM)
PD = KPD*(KD*RB + WKD)
PA = PQT + PPT + PM
PB = PQR + PD
WRITE(6,3) PQT, PQR, PPT, PM, PD, PA, PB
CTHT = KTHT * DTO**MT + CKT
CTHR = KTHR * DRO**MR + CKR
CNT = CAT + KAT*(DTO/LAMBDA)**QT
CNR = CAR + KAR*THERO**(-QR)
CFL = KPT*PTO**GT + CKP
CH = PTO*KH*(1.-KE)/KE + CKH
CFM = KFM*RB + CKM
CFD = KFD*RB + CKD
CFT = KST*(KPM*(KM*RB + WKM) + PTO/KE + KPQT*(WBT + KWAT*DTO**NT))
* + CKF
CFR = KSR*(KPD*(KD*RB + WKD) + KPQR*(WBR + KVAR*KDR*DRO**NR)) + CKF
CFA = CTHT + CNT + CFL + CH + CFM + CFT
CFB = CTHR + CNR + CFD + CFR
WRITE(6,4) CTHT, CTHR, CNT, CNR, CFL, CH, CFM, CFD, CFT, CFR, CFA, CFB

```

EXHIBIT A2. 3-3 (continued)

```

CDT = CTHT + KS*WDT
CDR =          CTHR + KS*WDR
CQT = CAT + KS*WQT
CQR = CAR + KS*WQR
CPT = CFL + CH +KS*(WT + WH)
CM = CFM + KS*WM
CD = CFD + KS*WD
CST = CFT + KS*WST
CSR = CFR + KS*WSP
WRITE(6,5) CDT,CDR,CQT,CQR,CPT,CM,CD,CST,CSR
KHT = KS*KWT
KJT =(KS*KNST + KST)/KF + (KS*KX + KH)*(1.-KF)/KF
KGT = KPT
KMT = KTHT
KNT = KDT*(KS*(1. + KWAT) + KPQT*KWAT*(KST + KS*KWST))
KQT = KAT/LAMBDA**QT
KMR = KTHR
KNR = KDR*(KS*(1. + KWAR) + KPQR*KWAR*(KSR + KS*KWSP))
KQR = KAR
CTO = KQT*DTO**QT +KMT*DTO**MT + KNT*DTO**NT
CRO = KMR*DRO**MR + KNR*DRO**NR
CQO = KQR/THERO**QP
CGO = KGT*PTO**GT + KHT*PTO**HT +KJT*PTO
CV = CGO +CTO + CQO + CRO
CS = CV + CFA +CFR
CA = CGO +CTO + CFA
CB = CQO + CRO +CFR
WRITE(6,6) CTO,CRO,CQO,CGO,CV,CS,CA,CB
1 FORMAT(35H OPTIMUM SYSTEM PARAMETERS      RB = ,E12.5,9H   DTO = ,
  *E12.5,9H   DRO ,E12.5,9H   PTO = ,E12.5,10H   THERO = ,E12.5//)
2 FORMAT( 23H OPTIMUM WEIGHT BURDENS, 5H   WDT,E15.6,5H   WDR,E15.6
  *,5H   WQT,E15.6,5H   WQR,E15.6,5H   WT,E15.6/23X,          5H   WH,
  *E15.6,5H   WM,E15.6,5H   WD,E15.6,5H   WST,E15.6,5H   WSR,E15.6/23X,
  * 5H   WA,E15.6,5H   WB,E15.6//)
3 FORMAT( 23H OPTIMUM POWER BURDENS , 5H   PQT,E15.6,5H   PQR,E15.6
  *,5H   PPT,E15.6,5H   PM,E15.6,5H   PD,E15.6/23X,5H   PA,E15.6,5H
  *PR,E15.6//)
4 FORMAT(33H OPTIMUM FABRICATION COST BURDENS,10X,5H   CTHT,E15.6,5H   C
  *THR,E15.6,5H   CNT,E15.6,5H   CNR,E15.6/23X,5H   CFL,E15.6,5H   CH,
  *E15.6,5H   CFM,E15.6,5H   CFD,E15.6,5H   CFT,E15.6/5H   CFR,E15.6,5H
  *CFA,E15.6,5H   CFB,E15.6//)
5 FORMAT(38H OPTIMUM SYSTEM COMPONENT COST BURDENS,5X,5H   CDT,E15.6,
  *5H   CDR,E15.6,5H   CQT,E15.6,5H   CQR,E15.6/23X,5H   CPT,E15.6,5H   C
  *M,E15.6,5H   CD,E15.6,5H   CST,E15.6,5H   CSR,E15.6//)
6 FORMAT(28H OPTIMUM SYSTEM COST BURDENS,15X,5H   CTO,E15.6,5H   CRO,
  *E15.6,5H   CQO,E15.6,5H   CGO,E15.6/23X,5H   CV,E15.6,5H   CS,E15.6,
  *5H   CA,E15.6,5H   CB,E15.6//)
RETURN
END

```

APPENDIX A2.5

THERMAL NOISE LIMITED DIRECT DETECTION OPTICAL RECEIVER OPTIMIZATION PROGRAM (TOP) WITHOUT COMPONENT STOPS

FUNCTION

The function of the TOP program is to determine the optimum values of the major system parameters as a function of information rate for a thermal noise limited direct detection optical receiver.

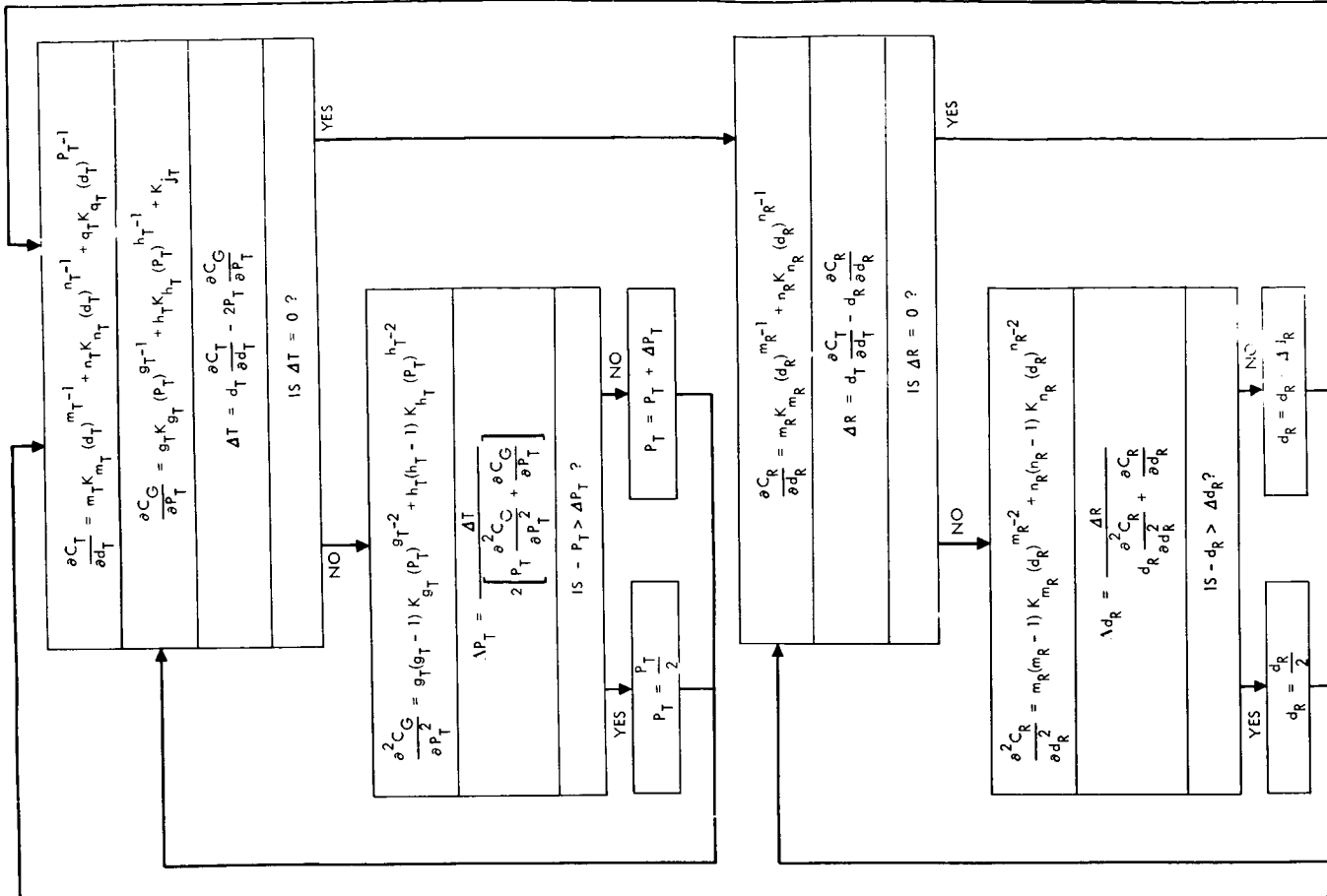
DESCRIPTION

Exhibit A2.5-1 is a detailed flow chart of the TOP optimization program. The input information required for the TOP program is the systems burden data, the system parametric data, and the initial conditions data. Exhibit A2.5-2 contains a listing of the Fortran IV TOP program.

TOP PROGRAM

START

READ SYSTEMS BURDEN DATA
PRINT SYSTEMS BURDEN DATA
READ SYSTEMS PARAMETRIC DATA
PRINT SYSTEMS PARAMETRIC DATA
$K_M = \left(\frac{0.3 T_r T_o T_r}{hc \lambda R^e} \right)^2 \frac{2R_L}{kT_e \left(\frac{S}{N} \right)}$
$K_{mT} = K_{\theta T}$
$K_{nT} = K_d \left[K_S \left[1 + K_{WAT} \right] + K_P K_{WAT} \left[K_{ST} + K_S K_{WST} \right] \right]$
$K_{qT} = \frac{K_{AT}}{(\lambda) q_T}$
$K_{mR} = K_{\theta R}$
$K_{nR} = K_d \left[K_S \left[1 + K_{WAR} \right] + K_P K_{WAR} \left[K_{SR} + K_S K_{WSR} \right] \right]$
$K_{qR} = K_{AR}$
$K_{gT} = K_{PT}$
$K_{hT} = K_S K_{WT}$
$K_{JT} = K_S \left[\frac{K_{WST}}{k_e} + K_X \left(\frac{1-k_e}{k_e} \right) \right] + \frac{K_{ST}}{k_e} + K_H \left(\frac{1-k_e}{k_e} \right)$
PRINT $K_M, K_{mT}, K_{nT}, K_{qT}, K_{mR}, K_{nR}, K_{qR}, K_{hT}, K_{JT}$
READ INITIAL CONDITIONS DATA
PRINT INITIAL CONDITIONS DATA



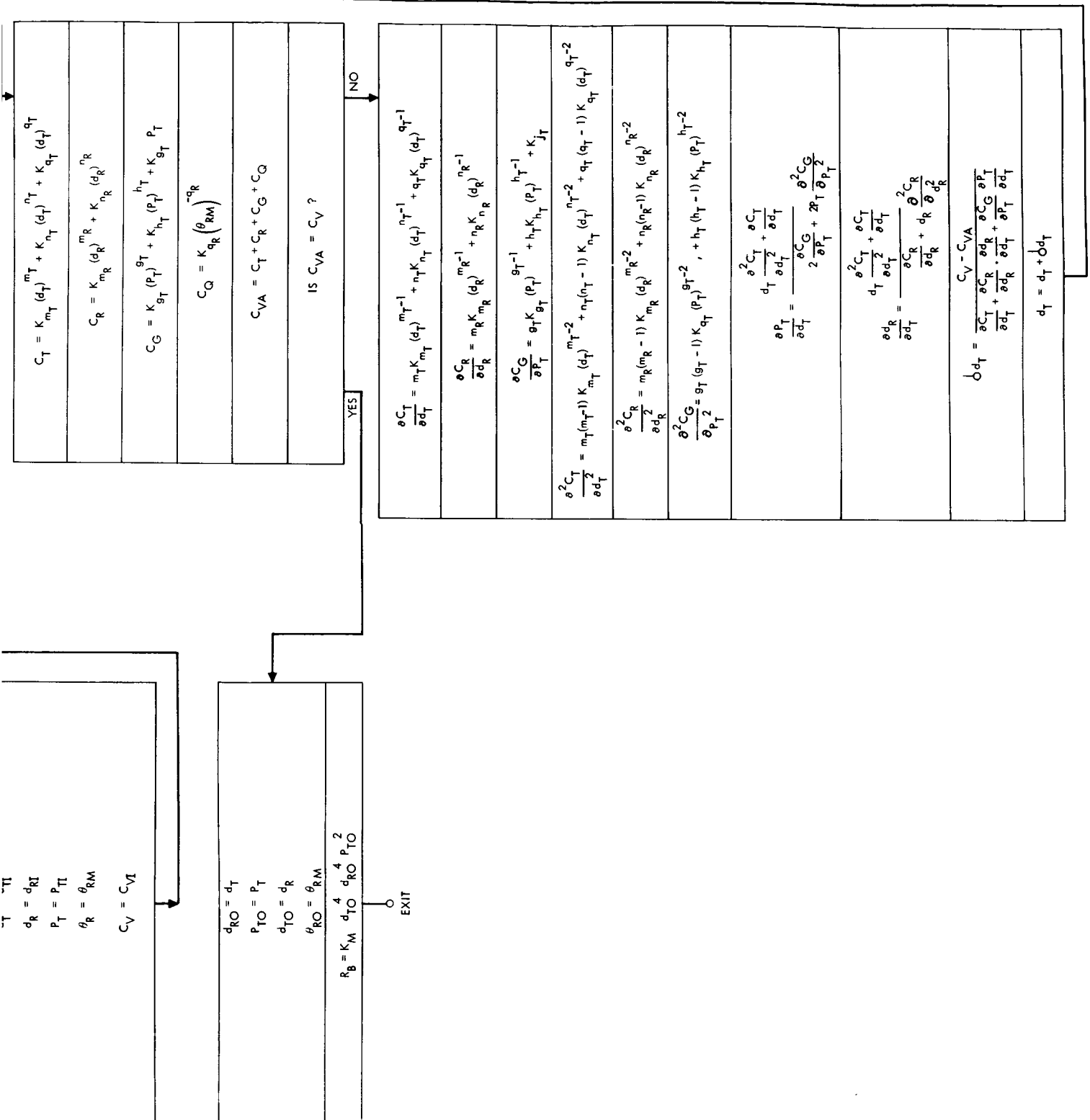


EXHIBIT A2.5-2

CTOP OPTIMIZATION METHODOLOGY TOP PROGRAM

```

REAL KTHT, KDT, MT, NT, KTHR, KDR, MR, NR, KAT, KWAT, KPQT, KAR
REAL KWAR, KPQR, KPT, KWT, KH, KX, KE, KFM, KM, KPM, KFD, KD
REAL KPD, KST, KWST, KSR, KWSR, KS, KHT, KJT, KGT, KMT, KNT, KQT
REAL KMR, KNR, KQR, LAMBDA, LMBDI, K, KN
COMMON/TRAN/ KTHT, KDT, CKT, WKT, MT, NT
COMMON/RCANT/ KTHR, KDR, CKR, WKR, MR, NR
COMMON/TACTS/ KAT, KWAT, KPQT, CAT, WBT, QT
COMMON/RACTS/ KAR, KWAR, KPQR, CAR, WBR, QR
COMMON/TRNSM/ KPT, KWT, KH, KX, KE, CKP, CKH, WKP, WKH, PKT, GT, HT
COMMON/ECMOD/ KFM, KM, KPM, CKM, WKM
COMMON/EQDMD/ KFD, KD, KPD, CKD, WKD
COMMON/TRNPS/ KST, KWST, CKE, WKE
COMMON/RCVPS/ KSR, KWSR, CKF, WKF
COMMON/GENRL/ KS, LAMBDA, LMBDI, R, TAUT, TAUR, TAUA, ETA, SN, QB
COMMON/OUTPT/ KHT, KJT, KGT, KMT, KNT, KQT, KMR, KNR, KQR
READ(5,1100) KTHT, KDT, CKT, WKT, MT, NT
WRITE(6,1200) KTHT, KDT, CKT, WKT, MT, NT
READ(5,1100) KTHR, KDR, CKR, WKR, MR, NR
WRITE(6,1201) KTHR, KDR, CKR, WKR, MR, NR
READ(5,1100) KAT, KWAT, KPQT, CAT, WBT, QT
WRITE(6,1202) KAT, KWAT, KPQT, CAT, WBT, QT
READ(5,1100) KAR, KWAR, KPQR, CAR, WBR, QR
WRITE(6,1203) KAR, KWAR, KPQR, CAR, WBR, QR
READ(5,1100) KPT, KWT, KH, KX, KE, CKP, CKH, WKP, WKH, PKT, GT, HT
WRITE(6,1204) KPT, KWT, KH, KX, KE, CKP, CKH, WKP, WKH, PKT, GT, HT
READ(5,1100) KFM, KM, KPM, CKM, WKM
WRITE(6,1205) KFM, KM, KPM, CKM, WKM
READ(5,1100) KFD, KD, KPD, CKD, WKD
WRITE(6,1206) KFD, KD, KPD, CKD, WKD
READ(5,1100) KST, KWST, CKE, WKE
WRITE(6,1207) KST, KWST, CKE, WKE
READ(5,1100) KSR, KWSR, CKF, WKF
WRITE(6,1208) KSR, KWSR, CKF, WKF
WRITE(6,1210) H, C, Q, SMK, TE, RL
READ(5,1100) H, C, Q, SMK, TE, RL
READ(5,1100) KS, LAMBDA, LMBDI, R, TAUT, TAUR, TAUA, ETA, SN, QB
WRITE(6,1209) KS, LAMBDA, LMBDI, R, TAUT, TAUR, TAUA, ETA, SN, QB
KM = (.3*ETA*TAUT*TAUA*TAUR*Q/((H*R**2)*C*LAMBDA))**2
*
*
KMT = KTHT
KNT = KDT*(KS*(1.+KWAT)+ KPQT*KWAT*(KST+KS*KWST))
KQT = KAT/LAMBDA**QT
KMR = KTHR
KNR = KDR*(KS*(1.+KWAR)+KPQR*KWAR*(KSR+KS*KWSR))
KGT = KPT
KHT = KS*KWT
KJT = KS*(KWST/KE + KX*(1.-KE)/KE) + KST/KE + KH*(1.-KE)/KE
KQR = KAR
WRITE(6,2000) KN, K, KMT, KNT, KQT, KMR, KNR, KQR, KGT, KHT, KJT
READ(5,1100) DTI, DRI, PTI, THERI, CVI, CVMIN
CV = CVI
DELCV = CV/10.
DT = DTI
PT = PTI

```

0

EXHIBIT A2. 5-2 (continued)

```

DR = DRI
THER = THERI
WRITE (6,2001) THER,DT,DR,PT,CV
8 PCIPDT = (MT*KMT*DT**MT + NT*KNT*DT**NT + QT*KQT*DT**QT)/DT
10 PCGPPT = (GT*KGT*PT**GT + HT*KHT*PT**HT)/PT + KJT
F1 = DT*PCIPDT
F2 = 2.*PT * PCGPPT
T = F1 - F2
IF((F1/F2) .GT. .999995 .AND. (F1/F2) .LT. 1.000005 ) GO TO 60
PCGPT2 = (GT*(GT-1.)*KGT*PT**GT + HT*(HT-1.)*KHT*PT**HT)/PT**2
DELPDT = T/(2.*(PT*PCGPT2 + PCGPPT))
XXX = PT + DELPDT
IF(XXX .LT. 0.) XXX = PT/2.
PT = XXX
GO TO 10
60 CONTINUE
80 PCRPPDR = (MR*KMR*DR**MR + NR*KNR*DR**NR)/DR
F1 = DT*PCIPDT
F2 = DR*PCRPPDR
W = F1 - F2
IF((F1/F2) .GT. .999995 .AND. (F1/F2) .LT. 1.000005 ) GO TO 100
PCRDR2 = (MR*(MR-1.)*KMR*DR**MR + NR*(NR-1.)*KNR*DR**NR)/DR**2
DELDLDR = W/(DR*PCRDR2 + PCRPPDR)
XXX = DR + DELDLDR
IF( XXX .LT. 0. ) XXX = DR/2.
DR = XXX
GO TO 80
100 CT = KMT*DT**MT + KNT*DT**NT + KQT*DT**QT
CR = KMR*DR**MR + KNR*DR**NR
CG = KGT*PT**GT + KHT*PT**HT + KJT*PT
CQ = KOR*THER*(-QD)
CVA = CT + CR + CG + CQ
IF((CV/CVA) .GT. .999995 .AND. (CV/CVA) .LT. 1.000005 ) GO TO 280
PCIPDT = (MT*KMT*DT**MT + NT*KNT*DT**NT + QT*KQT*DT**QT)/DT
PCRPPDR = (MR*KMR*DR**MR + NR*KNR*DR**NR)/DR
PCGPPT = (GT*KGT*PT**GT + HT*KHT*PT**HT)/PT + KJT
PCTDT2 = (MT*KMT*(DT-1.)*DT**MT + NT*(NT-1.)*KNT*DT**NT + QT*
* (QT-1.)*KQT*DT**QT)/DT**2
PCRDR2 = (MR*(MR-1.)*KMR*DR**MR + NR*(NR-1.)*KNR*DR**NR)/DR**2
PCGPT2 = (GT*(GT-1.)*KGT*PT**GT + HT*(HT-1.)*KHT*PT**HT)/PT**2
PPTPDT = (DT*PCTDT2 + PCIPDT)/(2.*PCGPPT + 2.*PT*PCGPT2)
PDRPDT = (DT*PCTDT2 + PCIPDT)/(PCRPPDR + DR*PCRDR2)
DELDLDT = (CV-CVA)/( PCTPDT + PCRPPDR*PDRPDT + PCGPPT*PPTPDT)
XXX = DELDLDT + DT
IF( XXX .LT. 0. ) XXX = DT/2.
DT = XXX
GO TO 8
280 DTD = DT
PTD = PT
DRO = DR
THERO = THER
RB = KN*DTD**2 *DRO**2 *PTD
CALL OUTPUT(DTD,DRO,PTD,THERO,RB)
IF(CV .LE. CVMIN) GO TO 370
IF(CV .EQ. DELCV) DELCV = DELCV/10.
CV = CV - DELCV
GO TO 8

```


EXHIBIT A2. 5-2 (continued)

```

370 STOP
1100 FORMAT (6E12.5)
1200 FORMAT (15H1 TRANSMITTER ,5H KTHT,E13.5,5H KDT ,E13.5,5H CKT ,E13
*.5,5H WKT ,E13.5,5H MT ,E13.5,5H NT ,E13.5/15H ANTENNA //)
1201 FORMAT (15H RECEIVER ,5H KTHR,E13.5,5H KDR ,E13.5,5H CKR ,E13
*.5,5H WKR ,E13.5,5H MR ,E13.5,5H NR ,E13.5/15H ANTENNA //)
1202 FORMAT (15H TRANSMITTER ,5H KAT ,E13.5,5H KWAT,E13.5,5H KPQT,E13
*.5,5H CAT ,E13.5,5H WPT ,E13.5,5H QT ,E13.5/15H ACQUISITION /
* 15H AND TRACK /
* 15H SYSTEM //)
1203 FORMAT (15H RECEIVER ,5H KAR ,E13.5,5H KWAR,E13.5,5H KPQR,E13
*.5,5H CAR ,E13.5,5H WBR ,E13.5,5H QR ,E13.5/15H ACQUISITION /
* 15H AND TRACK
* /15H SYSTEM //)
1204 FORMAT (15H TRANSMITTER ,5H KPT ,E13.5,5H KWT ,E13.5,5H KH ,E13
*.5,5H KX ,E13.5,5H KE ,E13.5,5H CKP ,E13.5/15X,5H CKH ,E13.5,5H
*WKP ,E13.5,5H WKH ,E13.5,5H PKT ,E13.5,5H GT ,E13.5,5H HT ,E13.5
* //)
1205 FORMAT (15H MODULATION ,5H KFM ,E13.5,5H KM ,E13.5,5H KPM ,E13
*.5,5H CKM ,E13.5,5H WKM ,E13.5/15H EQUIPMENT //)
1206 FORMAT (15H DEMODULATION ,5H KFD ,E13.5,5H KD ,E13.5,5H KPD ,E13
*.5,5H CKD ,E13.5,5H WKD ,E13.5/15H EQUIPMENT //)
1207 FORMAT (15H TRANSMITTER ,5H KST ,E13.5,5H KWST,E13.5,5H CKE ,E13
*.5,5H WKE ,E13.5/15H POWER SUPPLY //)
1208 FORMAT (15H RECEIVER ,5H KSR ,E13.5,5H KWSR,E13.5,5H CKF ,E13
*.5,5H WKF ,E13.5/15H POWER SUPPLY //)
1209 FORMAT ( 7H KS = ,E13.5,11H LAMBDA = ,F13.5,13H LAMBDA I = ,E13
*.5,6H R = ,E13.5,10H TAU T = ,E13.5//10H TAU R = ,E13.5,10H TA
*U A = ,E13.5, 8H ETA = ,E13.5,11H (S/N) = ,E13.5,7H QB = ,E13.
*5/2H1 )
1210 FORMAT(7H H = ,E13.5,7H C = ,E13.5,7H Q = ,E13.5,7H SMK = ,
*E13.5,7H TE = ,E13.5,7H RL = ,E13.5//)
2000 FORMAT( 7H1 KN = ,E18.8,7H K = ,E18.8,7H KMT = ,E18.8,7H KNT = ,
* E18.8,7H KQT = ,E18.8/ 7H KMR = ,E18.8,7H KNR = ,E18.8,7H KQR = ,
* E18.8,7H KGT = ,E18.8, 7H KHT = ,E18.8/7H KJT = ,E18.8//)
2001 FORMAT(53X,23HINITIAL CONDITIONS DATA//11H THETA-R = ,E12.5,
* 6H DT = ,E12.5,6H DR = ,E12.5,6H PT = ,E12.5,6H CV = ,E12.5// )
END

```

APPENDIX A2.6

HETERODYNE DETECTION OPTICAL RECEIVER OPTIMIZATION PROGRAM WITHOUT COMPONENT STOPS (HOP)

FUNCTION

The function of the HOP program is to determine the optimum values of the major system parameters as a function of information rate for a heterodyne detection optical receiver.

DESCRIPTION

Exhibit A2.6-1 is a detailed flow chart of the HOP optimization program. The input information required for the HOP program is the systems burden data, the system parametric data, and the initial conditions data. Exhibit A2.6-2 contains a listing of the Fortran IV HOP program.

HOP PROGRAM

START

READ SYSTEMS BURDEN DATA

PRINT SYSTEMS BURDEN DATA

READ SYSTEMS PARAMETRIC DATA

PRINT SYSTEMS PARAMETRIC DATA

$$K_N = \frac{0.37 T_f \tau_0 \tau_f}{h c (S/N) R^2}$$

$$K_{m_T} = K_{\theta_T}$$

$$K_{n_T} = K_{d_T} \left\{ K_S \left[1 + K_{W_{AT}} \right] + K_P K_{W_{AT}} \left[K_{ST} + K_{S_{W_{ST}}} \right] \right\}$$

$$K = \frac{K_{AT}}{q_T (\lambda)^{q_T}}$$

$$K_{mR} = K_{\theta R}$$

$$K_{n_r} = K_{d_r} \left\{ K_S \left[1 + K_{W_{AR}} \right] + K_P K_{W_{AR}} \right\} \left[K_{SR} + K_S K_{W_{SR}} \right]$$

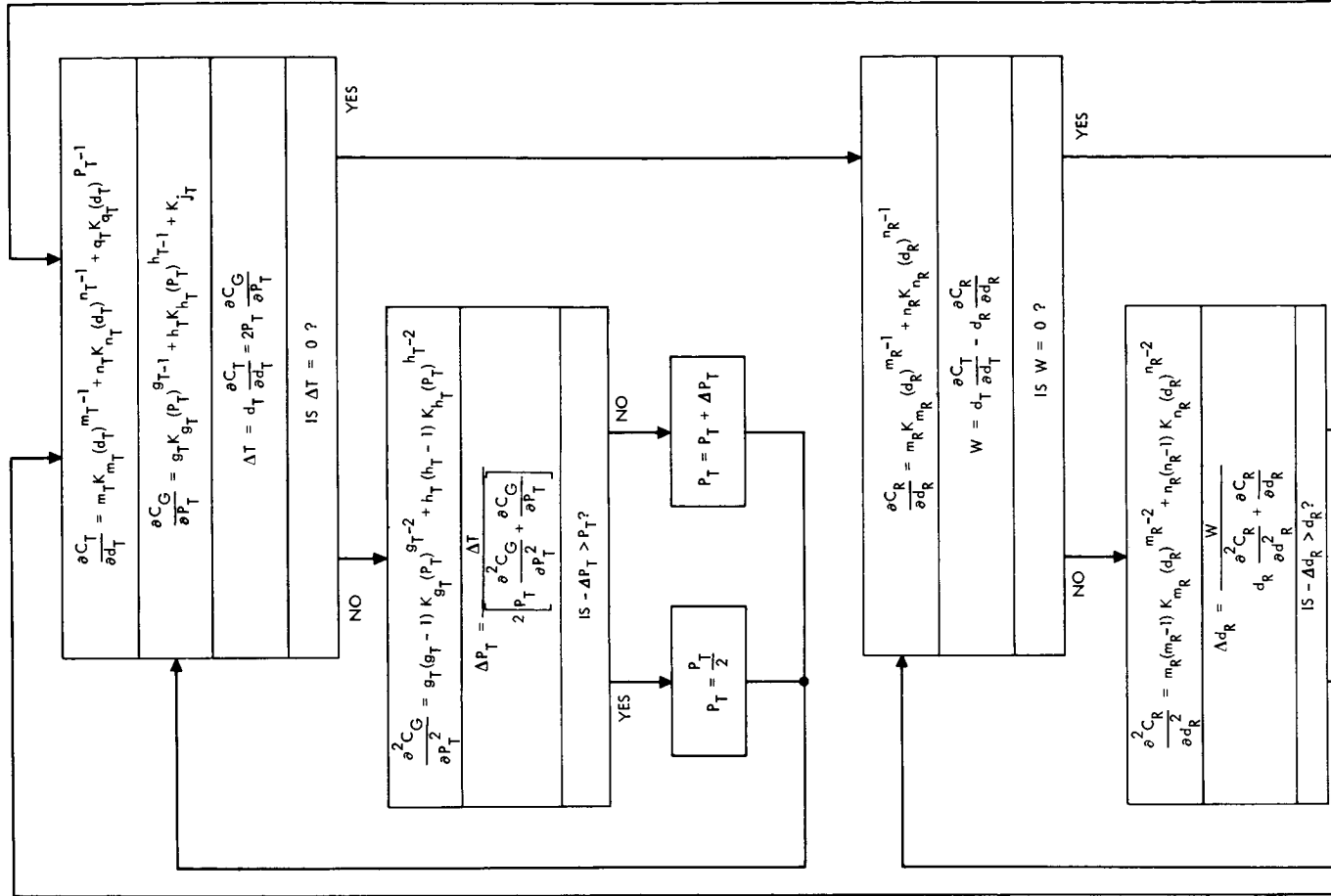
$$K_{qR} = K_{AR}$$

$$K_{g_r} = K_{p_T}$$

$$K_{h_T} = K_S K_{W_T}$$

$$\kappa_{JT} = \kappa_S \left\{ \frac{\kappa_{ST}^w}{k_e} + \kappa_X \left(\frac{1 - k_e}{k_e} \right) \right\} + \frac{\kappa_{ST}}{k_e} + \kappa_H \left(\frac{1 - k_e}{k_e} \right)$$

```
PRINT KN1, K2, K3, K4, K5, K6, K7, K8, K9, K10, K11, K12, K13, K14, K15, K16, K17, K18, K19, K20, K21, K22, K23, K24, K25, K26, K27, K28, K29, K30, K31, K32, K33, K34, K35, K36, K37, K38, K39, K40, K41, K42, K43, K44, K45, K46, K47, K48, K49, K50, K51, K52, K53, K54, K55, K56, K57, K58, K59, K60, K61, K62, K63, K64, K65, K66, K67, K68, K69, K70, K71, K72, K73, K74, K75, K76, K77, K78, K79, K80, K81, K82, K83, K84, K85, K86, K87, K88, K89, K90, K91, K92, K93, K94, K95, K96, K97, K98, K99, K100, K101, K102, K103, K104, K105, K106, K107, K108, K109, K110, K111, K112, K113, K114, K115, K116, K117, K118, K119, K120, K121, K122, K123, K124, K125, K126, K127, K128, K129, K130, K131, K132, K133, K134, K135, K136, K137, K138, K139, K140, K141, K142, K143, K144, K145, K146, K147, K148, K149, K150, K151, K152, K153, K154, K155, K156, K157, K158, K159, K160, K161, K162, K163, K164, K165, K166, K167, K168, K169, K170, K171, K172, K173, K174, K175, K176, K177, K178, K179, K180, K181, K182, K183, K184, K185, K186, K187, K188, K189, K190, K191, K192, K193, K194, K195, K196, K197, K198, K199, K200, K201, K202, K203, K204, K205, K206, K207, K208, K209, K210, K211, K212, K213, K214, K215, K216, K217, K218, K219, K220, K221, K222, K223, K224, K225, K226, K227, K228, K229, K230, K231, K232, K233, K234, K235, K236, K237, K238, K239, K240, K241, K242, K243, K244, K245, K246, K247, K248, K249, K250, K251, K252, K253, K254, K255, K256, K257, K258, K259, K260, K261, K262, K263, K264, K265, K266, K267, K268, K269, K270, K271, K272, K273, K274, K275, K276, K277, K278, K279, K280, K281, K282, K283, K284, K285, K286, K287, K288, K289, K290, K291, K292, K293, K294, K295, K296, K297, K298, K299, K300, K301, K302, K303, K304, K305, K306, K307, K308, K309, K310, K311, K312, K313, K314, K315, K316, K317, K318, K319, K320, K321, K322, K323, K324, K325, K326, K327, K328, K329, K330, K331, K332, K333, K334, K335, K336, K337, K338, K339, K340, K341, K342, K343, K344, K345, K346, K347, K348, K349, K350, K351, K352, K353, K354, K355, K356, K357, K358, K359, K360, K361, K362, K363, K364, K365, K366, K367, K368, K369, K370, K371, K372, K373, K374, K375, K376, K377, K378, K379, K380, K381, K382, K383, K384, K385, K386, K387, K388, K389, K390, K391, K392, K393, K394, K395, K396, K397, K398, K399, K400, K401, K402, K403, K404, K405, K406, K407, K408, K409, K410, K411, K412, K413, K414, K415, K416, K417, K418, K419, K420, K
```



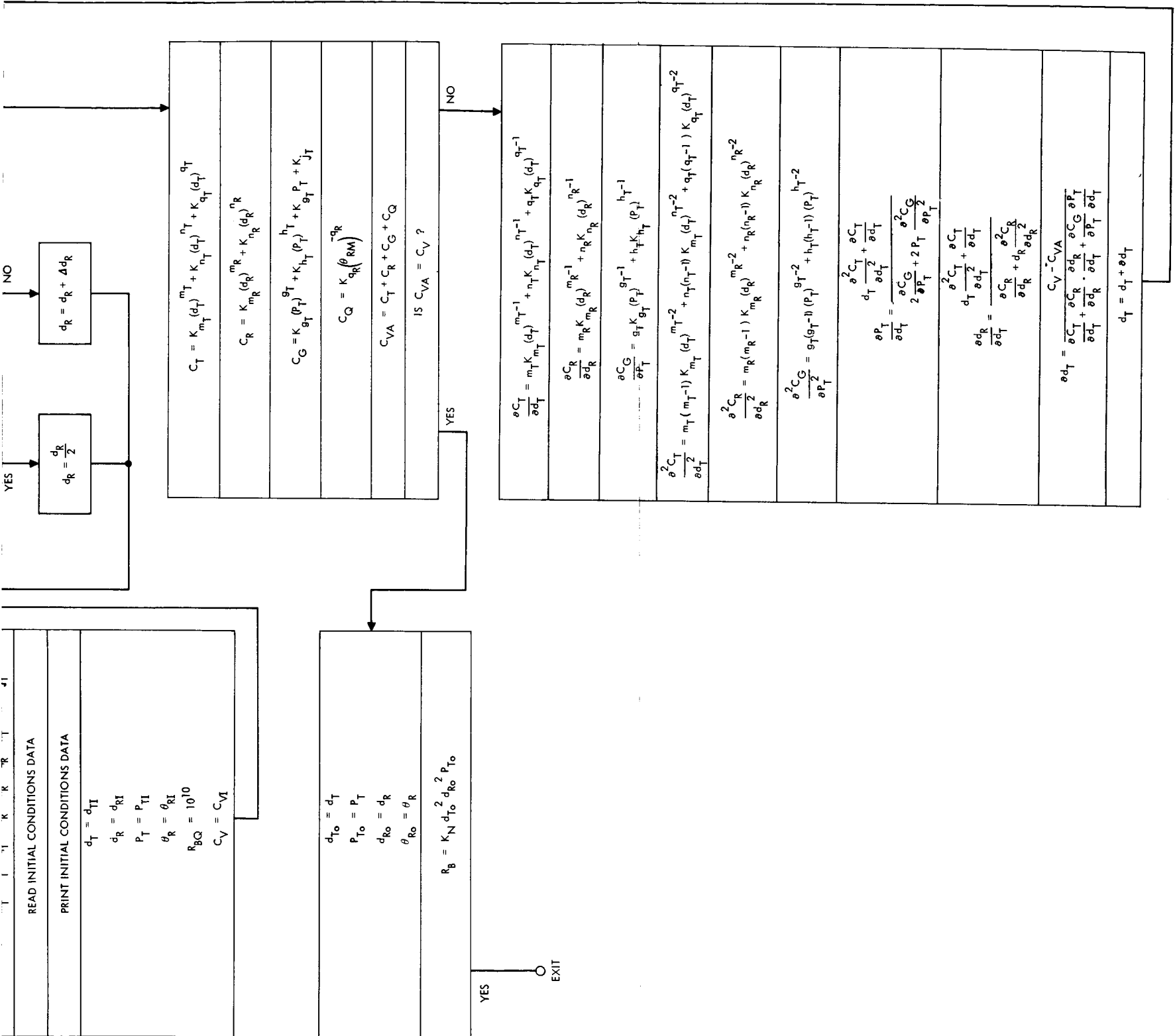


EXHIBIT A2.6-2

CHGP

OPTIMIZATION METHODOLOGY HOP PROGRAM

```

REAL KTHT, KDT, MT, NT, KTHR, KDR, MR, NR, KAT, KWAT, KPQT, KAR
REAL KWAR, KPQR, KPT, KNT, KH, KX, KE, KFM, KM, KPM, KFD, KD
REAL KPD, KST, KWST, KSR, KWSR, KS, KHT, KJT, YGT, KMT, KNT, KQT
REAL KMR, KNR, KQR, LAMBDA, LMRDI, K, KN
COMMON/TRANT/ KTHT, KDT, CKT, WKT, MT, NT
COMMON/PCANT/ KTHR, KDR, CKR, WKR, MR, NR
COMMON/TACTS/ KAT, KWAT, KPQT, CAT, WBT, QT
COMMON/RACTS/ KAR, KWAR, KPQR, CAR, WBR, QR
COMMON/TRNSM/ KPT, KWT, KH, KX, KE, CKP, CKH, WKP, WKH, PKT, GT, HT
COMMON/EQMOD/ KFM, KM, KPM, CKM, WKM
COMMON/EQDMD/ KFD, KD, KPD, CKD, WKD
COMMON/TRNPS/ KST, KWST, CKE, WKE
COMMON/RCVPS/ KSR, KWSR, CKF, WKF
COMMON/GENRL/ KS, LAMBDA, LMRDI, R, TAUT, TAUR, TAUA, ETA, SN, QB
COMMON/OUTPT/ KHT, KJT, KGT, KMT, KNT, KQT, KMR, KNR, KQR
READ(5,1100) KTHT, KDT, CKT, WKT, MT, NT
WRITE(6,1200) KTHT, KDT, CKT, WKT, MT, NT
READ(5,1100) KTHR, KDR, CKR, WKR, MR, NR
WRITE(6,1201) KTHR, KDR, CKR, WKR, MR, NR
READ(5,1100) KAT, KWAT, KPQT, CAT, WBT, QT
WRITE(6,1202) KAT, KWAT, KPQT, CAT, WBT, QT
READ(5,1100) KAR, KWAR, KPQR, CAR, WBR, QR
WRITE(6,1203) KAR, KWAR, KPQR, CAR, WBR, QR
READ(5,1100) KPT, KWT, KH, KX, KE, CKP, CKH, WKP, WKH, PKT, GT, HT
WRITE(6,1204) KPT, KWT, KH, KX, KE, CKP, CKH, WKP, WKH, PKT, GT, HT
READ(5,1100) KFM, KM, KPM, CKM, WKM
WRITE(6,1205) KFM, KM, KPM, CKM, WKM
READ(5,1100) KFD, KD, KPD, CKD, WKD
WRITE(6,1206) KFD, KD, KPD, CKD, WKD
READ(5,1100) KST, KWST, CKE, WKE
WRITE(6,1207) KST, KWST, CKE, WKE
READ(5,1100) KSR, KWSR, CKF, WKF
WRITE(6,1208) KSR, KWSR, CKF, WKF
READ(5,1100) H, C
WRITE(6,1210) H, C
READ(5,1100) KS, LAMBDA, LMRDI, R, TAUT, TAUR, TAUA, ETA, SN, QB
WRITE(6,1209) KS, LAMBDA, LMRDI, R, TAUT, TAUR, TAUA, ETA, SN, QB
KN = .3*ETA*TAUT*TAUA*TAUR/((R**2 * H)*C *LAMBDA*SN)
K = (1.22E-23*R**2)* QB*LAMBDA*LMRDI/TAUT
KMT = KTHT
KNT = KDT*(KS*(1.+KWAT)+ KPQT*KWAT*(KST+KS*KWST))
KQT = KAT/LAMBDA**QT
KMR = KTHR
KNR = KDR*(KS*(1.+ KWAR) +KPQR*KWAR*(KSR + KS*KWSR))
KGT = KPT
KHT = KS*KWT
KJT = KS*(KWST/KE + KX*(1.-KE)/KE) + KST/KE + KH*(1.-KE)/KE
KQR = KAR
WRITE(6,2000) KN, K, KMT, KNT, KQT, KMR, KNR, KQR, KGT, KHT, KJT
READ(5,1100) DTI, DRI, PTI, THERI, CVI, CVMIN
CV = CVI
DFLCV = CV/10.
DT = DTI
PT = PTI

```

EXHIBIT A2.6-2 (continued)

```

DR = DRI
THER = THERI
WRITE (6,2001) THER,DT,DR,PT,CV
8 PCTPDT = (MT*KMT*DT**MT + NT*KNT*DT**NT + QT*KQT*DT**QT)/DT
10 PCGPPT = (GT*KGT*PT**GT + HT*KHT*PT**HT)/PT + KJT
F1 = DT*PCTPDT
F2 = 2.*PT * PCGPPT
T = F1 - F2
IF((F1/F2) .GT. .999995 .AND. (F1/F2) .LT. 1.000005 ) GO TO 60
PCGPT2 = (GT*(GT-1.)*KGT*PT**GT + HT*(HT-1.)*KHT*PT**HT)/PT**2
DELPT = T/(2.*(PT*PCGPT2 + PCGPPT))
XXX = PT + DELPT
IF(XXX .LT. 0.) XXX = PT/2.
PT = XXX
GO TO 10
60 CONTINUE
80 PCRPDR = (MR*KMR*DR**MR + NR*KNR*DR**NR)/DR
F1 = DT*PCTPDT
F2 = DR*PCRPDR
W = F1 - F2
IF((F1/F2) .GT. .999995 .AND. (F1/F2) .LT. 1.000005 )GO TO 100
PCRPDR2 = (MR*(MR-1.)*KMR*DR**MR + NR*(NR-1.)*KNR*DR**NR)/DR**2
DELDLDR = W/(DR*PCRPDR2 + PCRPDR)
XXX= DR + DELDLDR
IF( XXX .LT. 0. ) XXX = DR/2.
DR = XXX
GO TO 80
100 CT = KMT*DT**MT + KNT*DT**NT + KQT*DT**QT
CR = KMR*DR**MR + KNR*DR**NR
CG = KGT*PT**GT + KHT*PT**HT + KJT*PT
CQ = KQR*THER**(-QR)
CVA = CT+ CR + CG + CQ
IF((CV/CVA) .GT. .99995 .AND. (CV/CVA) .LT. 1.00005 ) GO TO 280
PCTPDT = (MT*KMT*DT**MT + NT*KNT*DT**NT + QT*KQT*DT**QT)/DT
PCRPDR = (MR*KMR*DR**MR + NR*KNR*DR**NR )/DR
PCGPPT = (GT*KGT*PT**GT + HT*KHT*PT**HT )/PT + KJT
PCTDT2 = (MT*KMT*(MT-1.)*DT**MT + NT*(NT-1.)*KNT*DT**NT + QT*
* (QT-1.)*KQT*DT**QT)/DT**2
PCRPDR2 = (MR*(MR-1.)*KMR*DR**MR + NR*(NR-1.)*KNR*DR**NR)/DR**2
PCGPT2 = (GT*(GT-1.)*KGT*PT**GT + HT*(HT-1.)*KHT*PT**HT)/PT**2
PPTPDT = (DT*PCTDT2 + PCTPDT)/(2.*PCGPPT+ 2.*PT*PCGPT2)
PDRPDT = (DT*PCTDT2 + PCTPDT)/(PCRPDR + DR*PCRPDR2)
DELDLDT = (CV-CVA)/( PCTPDT +PCRPDR*PDRPDT +PCGPPT*PPTPDT)
XXX = DELDLT +DT
IF( XXX .LT. 0. ) XXX = DT/2.
DT = XXX
GO TO 8
280 DTO = DT
PTO = PT
DRO = DR
THERO = THER
RB = KM*DTO**4*DRO**4*PTO**2
CALL OUTPUT(DTO,DRO,PTO,THERO,RB)
IF(CV .LE. CVMIN) GO TO 370
IF(CV .EQ. DELCV) DELCV = DELCV/10.
CV = CV - DELCV
GO TO 8

```

EXHIBIT A2.6-2 (continued)

```

370 STOP
1100 FORMAT (6F12.5)
1200 FORMAT (15H1 TRANSMITTER ,5H KTHT,F13.5,5H KDT ,E13.5,5H CKT ,F13
*,5,5H WKT ,E13.5,5H MT ,E13.5,5H NT ,E13.5/15H ANTENNA //)
1201 FORMAT (15H RECEIVER ,5H KTHR,F13.5,5H KDR ,E13.5,5H CKR ,F13
*,5,5H WKR ,E13.5,5H MR ,E13.5,5H NR ,E13.5/15H ANTENNA //)
1202 FORMAT (15H TRANSMITTER ,5H KAT ,E13.5,5H KWAT,E13.5,5H KPQT,F13
*,5,5H CAT ,E13.5,5H WBT ,F13.5,5H QT ,E13.5/15H ACQUISITION /
* 15H AND TRACK /
* 15H SYSTEM //)
1203 FORMAT (15H RECIVER ,5H KAR ,E13.5,5H KWAR,E13.5,5H KPQR,F13
*,5,5H CAR ,E13.5,5H WPR ,F13.5,5H QR ,E13.5/15H ACQUISITION /
* 15H AND TRACK
* /15H SYSTEM //)
1204 FORMAT (15H TRANSMITTER ,5H KPT ,E13.5,5H KWT ,E13.5,5H KH ,F13
*,5,5H KX ,E13.5,5H KE ,E13.5,5H CKP ,E13.5/15X,5H CKH ,F13.5,5H
*WKP ,E13.5,5H WKH ,E13.5,5H PKT ,E13.5,5H GT ,E13.5,5H HT ,E13.5
* //)
1205 FORMAT (15H MODULATION ,5H KFM ,E13.5,5H KM ,E13.5,5H KPM ,E13
*,5,5H CKM ,E13.5,5H WKM ,F13.5/15H EQUIPMENT //)
1206 FORMAT (15H DEMODULATION ,5H KFD ,E13.5,5H KD ,E13.5,5H KPD ,F13
*,5,5H CKD ,F13.5,5H WKD ,F13.5/15H EQUIPMENT //)
1207 FORMAT (15H TRANSMITTER ,5H KST ,E13.5,5H KWST,F13.5,5H CKF ,F13
*,5,5H WKF ,F13.5/15H POWER SUPPLY //)
1208 FORMAT (15H RECIVER ,5H KSR ,E13.5,5H KWSR,E13.5,5H CKF ,F13
*,5,5H WKF ,E13.5/15H POWER SUPPLY //)
1209 FORMAT ( 7H KS = ,E13.5,11H LAMBDA = ,F13.5,13H LAMBDA I = ,E13
*,5,6H R = ,E13.5,10H TAU T = ,E13.5//10H TAU R = ,E13.5,10H TA
*U A = ,E13.5, 8H ETA = ,E13.5,11H (S/N) = ,E13.5,7H QR = ,E13.
*5/2H1 )
1210 FORMAT(7H H = ,E13.5,7H C = ,E13.5//)
2000 FORMAT( 7H1 KN = ,E18.8,7H K = ,F18.8,7H KMT = ,F18.8,7H KNT = ,
* F18.8,7H KQT = ,E18.8/ 7H KMR = ,F18.8,7H KNR = ,E18.8,7H KQR = ,
* F18.8,7H KGT = ,E18.8, 7H KHT = ,F18.8/7H KJT = ,E18.8//)
2001 FORMAT(53X,23HINITIAL CONDITIONS DATA//11H THETA-R = ,F12.5,
* 6H DT = ,F12.5,6H DR = ,F12.5,6H PT = ,E12.5,6H CV = ,F12.5// )
END

```

APPENDIX A2.7

RADIO RECEIVER OPTIMIZATION PROGRAM WITHOUT COMPONENT STOPS (ROP)

FUNCTION

The function of the ROP program is to determine the optimum values of the major system parameters as a function of information rate for a radio receiver.

DESCRIPTION

Exhibit A2.7-1 is a detailed flow chart of the ROP optimization program. The input information required for the program is the systems burdens data, the systems parametric data, and the initial conditions data. Exhibit A2.7-2 contains a listing of the Fortran IV ROP program.

ROP PROGRAM

START

READ SYSTEMS BURDEN DATA

PRINT SYSTEMS BURDEN DATA

READ SYSTEMS PARAMETRIC DATA

PRINT SYSTEMS PARAMETRIC DATA

$$K_R = \frac{0.3 T_1 T_o T_r}{\lambda^2 R^2 T_e (S/N)}$$

$$K_{m_T} = K_{\theta_T}$$

$$K_{n_T} = K_{d_T} \left[K_S \left[1 + K_{W_{AT}} \right] + K_{P_{QT}} K_{W_{AT}} \left[K_{ST} + K_{S_{W_{ST}}} \right] \right]$$

$$K_{q_T} = \frac{K_{AT}}{(\lambda)^{q_T}}$$

$$K_{m_R} = K_{h_R}$$

$$K_{n_R} = K_{d_R} \left[K_S \left[1 + K_{W_{AR}} \right] + K_{P_{QR}} K_{W_{AR}} \left[K_{SR} + K_{S_{W_{SR}}} \right] \right]$$

$$K_{q_R} = K_{AR}$$

$$K_{\theta_T} = K_{P_T}$$

$$K_{h_T} = K_{S_{W_T}}$$

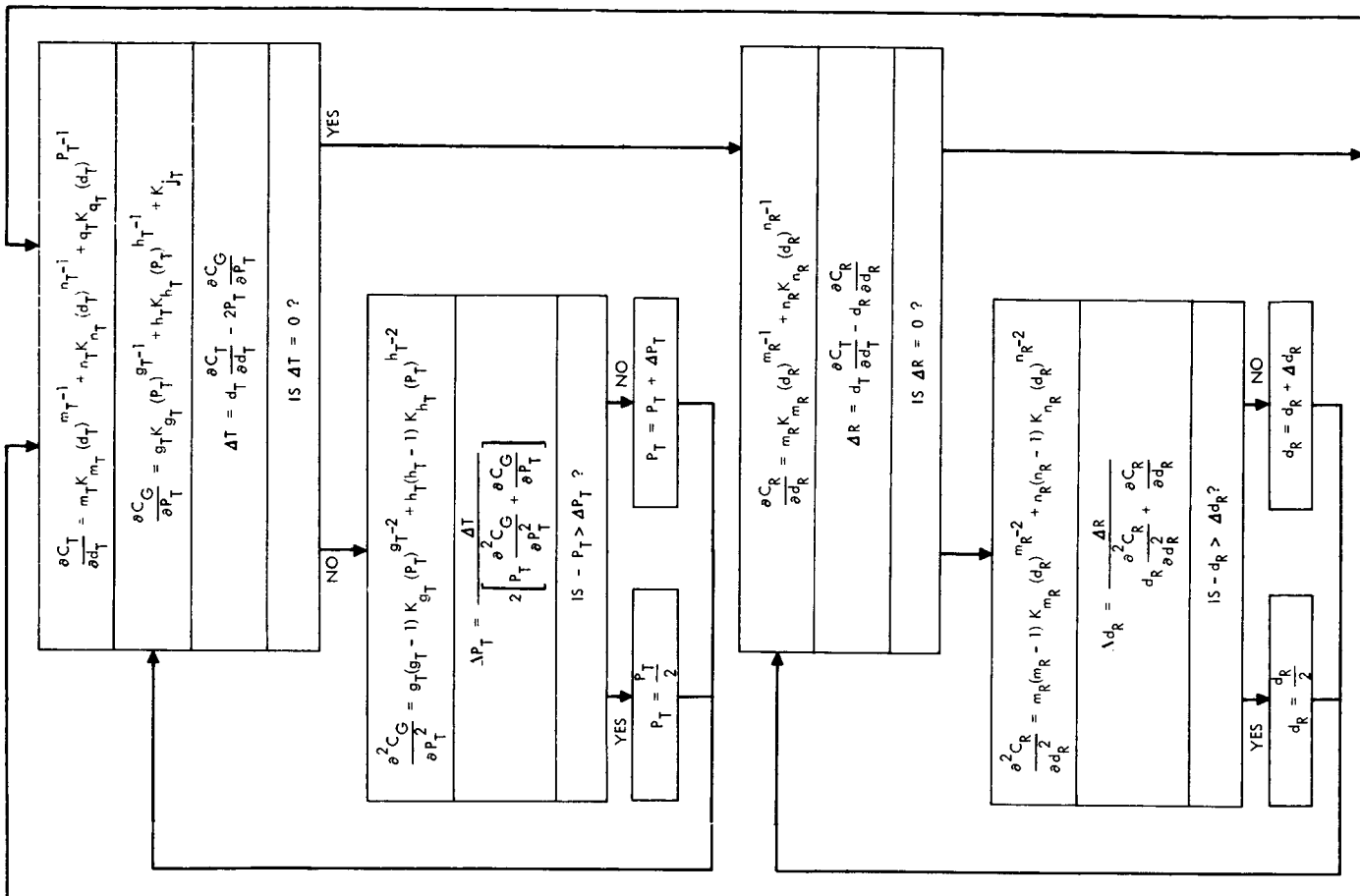
$$K_{J_T} = K_S \left[\frac{K_{W_{ST}}}{k_e} + K_X \left(\frac{1-k}{k_e} \right) \right] + \frac{K_{ST}}{k_e} + K_H \left(\frac{1-k}{k_e} \right)$$

PRINT K_{m_T} , K_{n_T} , K_{q_T} , K_{m_R} , K_{n_R} , K_{q_R} , K_{h_T} , K_{h_R} , K_{J_T}

READ INITIAL CONDITIONS DATA

PRINT INITIAL CONDITIONS DATA

$$d_T = d_{T1}$$



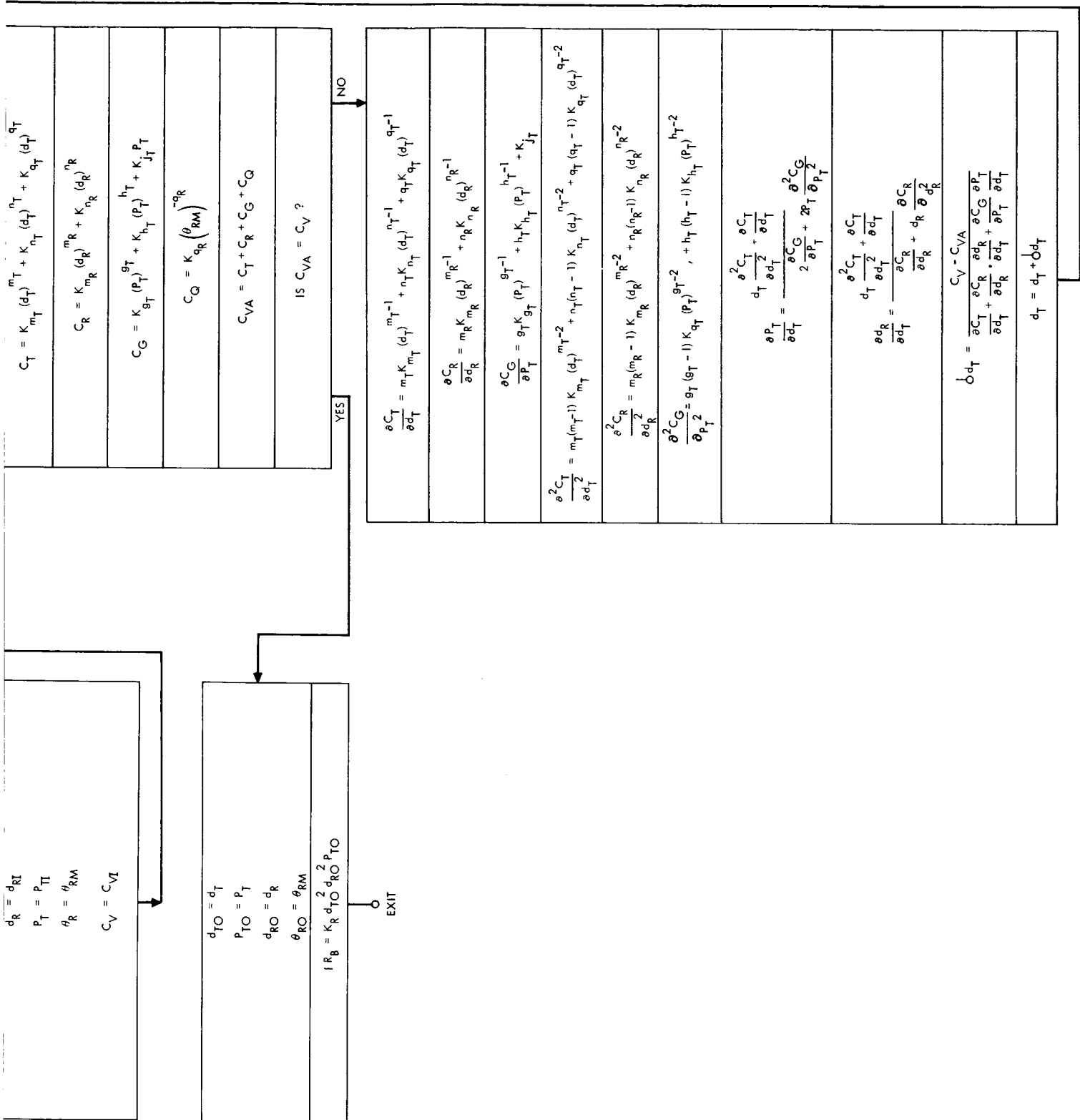


EXHIBIT A2. 7-2

CHCP OPTIMIZATION METHODOLOGY FOR PROGRAM

```

REAL KTHT, KDT, MT, NT, KTHR, KDR, MR, NR, KAT, KWAT, KPQT, KAR
REAL KWAR, KPQR, KPT, KMT, KH, KX, KE, KFM, KM, KPM, KFD, KD
REAL KPD, KST, KWST, KSR, KWSR, KS, KHT, KJT, KGT, KNT, KQT
REAL KMR, KNR, KQP, LAMBDA, LMBDI, K, KN
COMMON/TRANI/ KTHT, KDT, CKT, WKT, MT, NT
COMMON/RCANT/ KTHR, KDR, CKR, WKR, MR, NR
COMMON/TACTS/ KAT, KWAT, KPQT, CAT, WBT, QT
COMMON/PACTS/ KAR, KWAR, KPQR, CAR, WBR, QR
COMMON/TRNSM/ KPT, KWT, KH, KX, KE, CKP, CKH, WKP, WKH, PKT, GT, HT
COMMON/ECMOD/ KFM, KM, KPM, CKM, WKM
COMMON/EGDMD/ KFD, KD, KPD, CKD, WKD
COMMON/TPNPS/ KST, KWST, CKF, WKE
COMMON/RCVPS/ KSR, KWSR, CKF, WKF
COMMON/GENRL/ KS, LAMBDA, LMBDI, R, TAUT, TAUR, TAUA, ETA, SN, QB
COMMON/OUTPT/ KHT, KJT, KGT, KMT, KNT, KQT, KMR, KNR, KQR
READ(5,1100) KTHT, KDT, CKT, WKT, MT, NT
WRITE(6,1200) KTHT, KDT, CKT, WKT, MT, NT
READ(5,1100) KTHR, KDR, CKR, WKR, MR, NR
WRITE(6,1201) KTHR, KDR, CKR, WKR, MR, NR
READ(5,1100) KAT, KWAT, KPQT, CAT, WBT, QT
WRITE(6,1202) KAT, KWAT, KPQT, CAT, WBT, QT
READ(5,1100) KAR, KWAR, KPQR, CAR, WBR, QR
WRITE(6,1203) KAR, KWAR, KPQR, CAR, WBR, QR
READ(5,1100) KPT, KWT, KH, KX, KE, CKP, CKH, WKP, WKH, PKT, GT, HT
WRITE(6,1204) KPT, KWT, KH, KX, KE, CKP, CKH, WKP, WKH, PKT, GT, HT
READ(5,1100) KFM, KM, KPM, CKM, WKM
WRITE(6,1205) KFM, KM, KPM, CKM, WKM
READ(5,1100) KFD, KD, KPD, CKD, WKD
WRITE(6,1206) KFD, KD, KPD, CKD, WKD
READ(5,1100) KST, KWST, CKF, WKE
WRITE(6,1207) KST, KWST, CKF, WKE
READ(5,1100) KSR, KWSR, CKF, WKF
WRITE(6,1208) KSR, KWSR, CKF, WKF
READ(5,1100) SMK, TE
WRITE(6,1210) SMK, TE
READ(5,1100) KS, LAMBDA, LMBDI, R, TAUT, TAUR, TAUA, ETA, SN, QB
WRITE(6,1209) KS, LAMBDA, LMBDI, R, TAUT, TAUR, TAUA, ETA, SN, QB
KR = (.3*TAUR*TAUA*TAUT)/(LAMBDA**2 *(R**2 * SMK) * TE * SN)
KMT = KTHT
KNT = KDT*(KS*(1.+KWAT)+ KPQT*KWAT*(KST+KS*KWST))
KQT = KAT/LAMBDA**QT
KMR = KTHP
KNR = KDR*(KS*(1.+ KWAR) +KPQR*KWAR*(KSR + KS*KWSR))
KGT = KPT
KHT = KS*KWT
KJT = KS*(KWST/KE + KX*(1.-KF)/KF) + KST/KE + KH*(1.-KF)/KE
KQR = KAR
WRITE(6,2000) KN, K, KMT, KNT, KQT, KMR, KNR, KQR, KGT, KHT, KJT
READ(5,1100) DTI, DRI, PTI, THERI, CVI, CVMIN
CV = CVI
DELCV = CV/10.
DT = DTI
PT = PTI
DR = DRI

```

EXHIBIT A2.7-2 (continued)

```

THER = THERI
WRITE (6,2001) THER,DT,DR,PT,CV
8 PCTPDT = (MT*KMT*DT**MT + NT*KNT*DT**NT + QT*KQT*DT**QT)/DT
10 PCGPPT = (GT*KGT*PT**GT + HT*KHT*PT**HT)/PT + KJT
F1 = DT*PCTPDT
F2 = 2.*PT * PCGPPT
T = F1 - F2
IF((F1/F2) .GT. .999995 .AND. (F1/F2) .LT. 1.000005 ) GO TO 60
PCGPT2 = (GT*(GT-1.)*KGT*PT**GT + HT*(HT-1.)*KHT*PT**HT)/PT**2
DELP T = T/(2.*(PT*PCGPT2 + PCGPPT))
XXX = PT + DELPT
IF(XXX .LT. 0.) XXX = PT/2.
PT = XXX
GO TO 10
60 CONTINUE
80 PCRPDR = (MR*KMR*DR**MR + NR*KNR*DR**NR)/DR
F1 = DT*PCTPDT
F2 = DR*PCRPDR
W = F1 - F2
IF((F1/F2) .GT. .999995 .AND. (F1/F2) .LT. 1.000005 ) GO TO 100
PCDR2 = (MR*(MR-1.)*KMR*DR**MR + NR*(NR-1.)*KNR*DR**NR)/DR**2
DELD R = W/(DR*PCDR2 + PCRPDR)
XXX = DR + DELDR
IF( XXX .LT. 0. ) XXX = DR/2.
DR = XXX
GO TO 80
100 CT = KMT*DT**MT + KNT*DT**NT + KQT*DT**QT
CR = KMR*DR**MR + KNR*DR**NR
CG = KGT*PT**GT + KHT*PT**HT + KJT*PT
CQ = KQP*THER**(-OR)
CVA = CT + CR + CG + CQ
IF((CV/CVA) .GT. .99995 .AND. (CV/CVA) .LT. 1.00005 ) GO TO 280
PCTPDT = (MT*KMT*DT**MT + NT*KNT*DT**NT + QT*KQT*DT**QT)/DT
PCRPDR = (MR*KMR*DR**MR + NR*KNR*DR**NR)/DR
PCGPPT = (GT*KGT*PT**GT + HT*KHT*PT**HT)/PT + KJT
PCTDT2 = (MT*KMT*(MT-1.)*DT**MT + NT*(NT-1.)*KNT*DT**NT + QT*
* (QT-1.)*KQT*DT**QT)/DT**2
PCDR2 = (MR*(MR-1.)*KMR*DR**MR + NR*(NR-1.)*KNR*DR**NR)/DR**2
PCGPT2 = (GT*(GT-1.)*KGT*PT**GT + HT*(HT-1.)*KHT*PT**HT)/PT**2
PPTPDT = (DT*PCTDT2 + PCTPDT)/(2.*PCGPPT + 2.*PT*PCGPT2)
PDRPDT = (DT*PCTDT2 + PCTPDT)/(PCRPDR + DR*PCDR2)
DELD T = (CV-CVA)/( PCTPDT + PCRPDR*PDRPDT + PCGPPT*PPTPDT)
XXX = DELDT + DT
IF( XXX .LT. 0. ) XXX = DT/2.
DT = XXX
GO TO 8
280 DTO = DT
PTO = PT
DRO = DR
THERO = THER
RB = KR*DTO**2 *DRO**2 *PTO
CALL OUTPUT(DTO,DRO,PTO,THERO,RB)
IF(CV .LE. CVMIN) GO TO 370
IF(CV .EQ. DELCV) DELCV = DELCV/10.
CV = CV - DELCV
GO TO 8
370 STOP

```

EXHIBIT A2.7-2 (continued)

```

1100 FORMAT (6E12.5)
1200 FORMAT (15H1 TRANSMITTER ,5H KTHT,E13.5,5H KDT ,E13.5,5H CKT ,E13
*.5,5H WKT ,E13.5,5H MT ,E13.5,5H NT ,E13.5/15H ANTENNA //)
1201 FORMAT (15H RECEIVER ,5H KTHR,E13.5,5H KDR ,E13.5,5H CKR ,E13
*.5,5H WKR ,E13.5,5H MR ,E13.5,5H NR ,E13.5/15H ANTENNA //)
1202 FORMAT (15H TRANSMITTER ,5H KAT ,E13.5,5H KWAT,E13.5,5H KPQT,E13
*.5,5H CAT ,E13.5,5H WBT ,E13.5,5H QT ,E13.5/15H ACQUISITION /
* 15H AND TRACK /
* 15H SYSTEM //)
1203 FORMAT (15H RECEIVER ,5H KAR ,E13.5,5H KWAR,E13.5,5H KPQR,E13
*.5,5H CAR ,E13.5,5H WBR ,E13.5,5H QR ,E13.5/15H ACQUISITION /
* 15H AND TRACK
* /15H SYSTEM //)
1204 FORMAT (15H TRANSMITTER ,5H KPT ,E13.5,5H KWT ,E13.5,5H KH ,E13
*.5,5H KX ,E13.5,5H KE ,E13.5,5H CKP ,E13.5/15X,5H CKH ,E13.5,5H
*WKP ,E13.5,5H WKH ,E13.5,5H PKT ,E13.5,5H GT ,E13.5,5H HT ,E13.5
* //)
1205 FORMAT (15H MODULATION ,5H KFM ,E13.5,5H KM ,E13.5,5H KPM ,E13
*.5,5H CKM ,E13.5,5H WKM ,E13.5/15H EQUIPMENT //)
1206 FORMAT (15H DEMODULATION ,5H KFD ,E13.5,5H KD ,E13.5,5H KPD ,E13
*.5,5H CKD ,E13.5,5H WKD ,E13.5/15H EQUIPMENT //)
1207 FORMAT (15H TRANSMITTER ,5H KST ,E13.5,5H KWST,E13.5,5H CKE ,E13
*.5,5H WKE ,E13.5/15H POWER SUPPLY //)
1208 FORMAT (15H RECEIVER ,5H KSR ,E13.5,5H KWSR,E13.5,5H CKF ,E13
*.5,5H WKF ,E13.5/15H POWER SUPPLY //)
1209 FORMAT ( 7H KS = ,E13.5,11H LAMBDA = ,E13.5,13H LAMBDA I = ,E13
*.5,6H R = ,E13.5,10H TAU T = ,E13.5//10H TAU R = ,E13.5,10H TA
*U A = ,E13.5, 8H ETA = ,E13.5,11H (S/N) = ,E13.5,7H QB = ,E13.
*5/2H) )
1210 FORMAT(7H SMK = ,E13.5,7H TE = ,E13.5)
2000 FORMAT( 7H1 KN = ,E18.8,7H K = ,E18.8,7H KMT = ,E18.8,7H KNT = ,
* E18.8,7H KQT = ,E18.8/ 7H KMR = ,E18.8,7H KNR = ,E18.8,7H KQR = ,
* E18.8,7H KGT = ,E18.8, 7H KHT = ,E18.8/7H KJT = ,E18.8//)
2001 FORMAT(53X,23HINITIAL CONDITIONS DATA//11H THETA-R = ,E12.5,
* 6H DT = ,E12.5,6H DR = ,E12.5,6H PT = ,E12.5,6H CV = ,E12.5// )
END

```

14.0 HEAT REJECTION SYSTEMS

14.1 INTRODUCTION

The spacecraft thermal control system requirements imposed by the communication system and the resulting cost, weight, and area burdens are presented in this section. The communication system characteristics which determine the thermal control requirements are the output power, efficiency, and operating temperature of the transmitting source. In addition, the thermal control system burden is also influenced by the mission thermal environment and the spacecraft configuration.

14.2 COMMUNICATION SYSTEM HEAT REJECTION REQUIREMENTS

14.2.1 General Considerations

Since operation of the transmitter will not be continuous throughout the mission, the steady state thermal control of the spacecraft must of necessity be independent of rejected transmitter heat. Thus, essentially all the heat produced by intermittent operation of the transmitter must be rejected from the spacecraft. The power to be rejected, W , is then

$$W = P_T \frac{1 - k_e}{k_e}$$

where

P_T = transmitter output power

k_e = transmitter efficiency

This approximation of rejected heat burden is totally conservative since it is assumed that none of the power rejected by the transmitter may be put to effective use in thermal control.

The system parameters of most significance in determining the radiator burden for a given transmitted power are the operating temperature of the transmitting source and its efficiency. Operating temperatures range from less than 100° F for some laser sources to 400 to 500° F for TWT microwave sources. The efficiencies vary even more widely. If the transmitter power and efficiency have been specified and if its operating temperature is known, the associated radiator weight, area, and cost burdens are essentially determined.

14.2.2 Transmitter Source Characteristics

Microwave Sources. The microwave source of greatest interest for long space missions is the traveling-wave amplifier tube (TWT), Figure 14-1. The greatest heat is generated at the collector surface of the TWT. These parts may reach temperatures as high as 400 to 500° F in present long life tubes. For lower power levels (less than 100 to 200 watts output) it is customary to conductively cool the collector by thermally connecting it to a heat sink, which conducts to an external radiating surface. Higher power tubes are customarily cooled by flowing a coolant fluid through integral passages in the collector and other critical parts. The upper limit in outlet fluid temperature is imposed by the collector temperature limitations although it is typically somewhat lower as a result of temperature drops in other parts of the internal tube coolant circuit.

For power levels beyond 1 kw, TWTs are generally built in a different configuration from that used at lower powers. The high power configuration uses a cavity resonator which requires a solenoid to provide the necessary magnetic field. The solenoid must be cooled as well in this case. With modern high temperature insulating materials the solenoid operating temperatures may be comparable with the collector temperature.

Traveling wave tubes operate at efficiencies as high as 30 percent including power supply losses. For high power tubes, the solenoid cooling requirement is reflected in the efficiency.

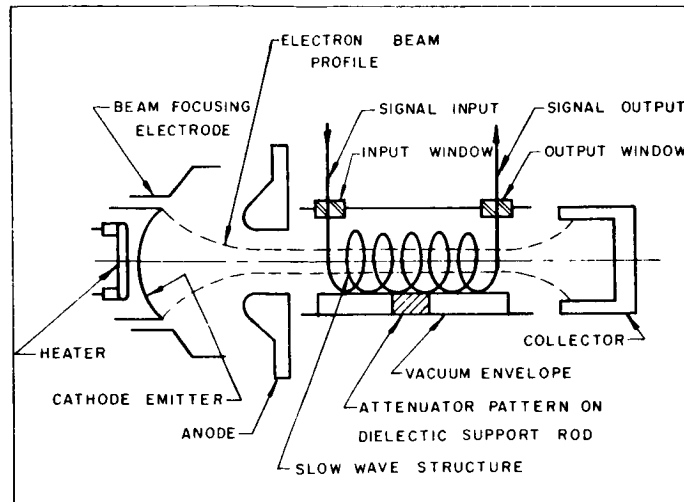


Figure 14-1. Schematic diagram showing basic parts of a traveling-wave tube.

Optical Transmitting Sources. The two optical sources of primary interest here are the CO_2 laser (10.6μ wavelength) and the Argon laser (0.5145μ wavelength). They differ drastically in operating efficiency and operating temperature requirements.

The CO_2 laser operates at efficiencies as high as 15 percent. To achieve this high efficiency, the gas mixture must be kept at temperatures of 20°C or less. Efficiency drops off rapidly at higher temperatures. For a typical low power device, output was reduced from 1.5 watts at 20°C to 0.7 watt at 60°C and 0.25 watt at 100°C . To maintain the required temperatures, most laboratory versions use water as a coolant, flowing it between the walls of the discharge tube and an outer concentric jacket. For the high power levels envisioned for space transmitting sources, an active fluid cooling system is virtually a necessity.

The Argon laser is characterized by efficiencies of the order of 0.1 percent or less. The very large fraction of input power which must be rejected as a result of this inefficiency demands liquid cooling for all power levels under consideration. Efficiency is not a critical function of the operating temperature as is the case with the CO_2 laser.

The upper limit in operating temperature is imposed by the limits for safe operation of the solenoid which surrounds the discharge tube and provides the pumping magnetic field. The pumping solenoid generates a large amount of heat and both it and the discharge tube must be cooled. The most effective way to achieve this is to flow the coolant fluid through the annular passage between them. Maximum operating temperatures imposed by solenoid temperature as limited by modern high temperature insulating materials may be as high as 200 to 300° F.

14.3 GENERAL HEAT REJECTION SYSTEM CONSIDERATIONS

Heat rejection systems may be classified as active or passive. In the most general sense, an active system is one which embodies moving parts (e.g., a coolant fluid or a thermal switch) while a passive system does not. In typical active systems heat is conveyed to the radiating surface by first transferring it to a fluid medium which is then physically transported to the radiator where its heat is rejected. In a passive system heat is conveyed to a radiating surface and dissipated from it by purely static processes. Passive systems usually are limited to dissipation of relatively small quantities of heat per volume in cases where an excellent thermal conductive path exists between the heat source and radiating surface.

14.4 ACTIVE HEAT REJECTION SYSTEMS

In general, the active heat rejection system consists of a heat exchanger to transfer heat from the transmitting source to the cooling fluid, the necessary plumbing to convey the fluid to the radiator, and the radiator itself. Of these, the radiator proper is the major contributor to the thermal control system cost, weight, and area burdens. The heat exchanger at the transmitting source is an integral part of the source and is characteristic of it. The burdens associated with transferring heat from the source to the cooling system are thus included in the transmitting source burdens and cannot meaningfully be divorced from them. The remaining system components — plumbing, pumps, controls and the coolant itself — are of less significance than the radiator

with respect to cost, weight, and volume. They are, in any event, so peculiar to a specific vehicle and communication system configuration as to preclude meaningful treatment here.

Both condensing and non-condensing heat rejection systems will be discussed. Condensing (two phase) systems are most applicable to dynamic power systems and so are included as a matter of general interest. Non-condensing (single phase) systems appear more applicable to cooling transmitting sources since boiling of the coolant fluid in condensing systems introduces vapor pockets and would lead to local hot spots in critical areas.

The design of optimum fin and tube radiators is a fairly complicated process which has been adapted to computer optimization. Input variables typically include radiator and heat sink temperatures, power capacity, coolant pressure drops in the tubes and headers, and susceptibility to meteoroid damage during a given mission. The optimum configuration may then be determined in terms of tube length, number of tubes, fin length, fin diameter, and tube wall thickness. Optimization may be with respect to radiator specific weight (lbs/ft^2), specific heat rejection (watts/ft^2), or specific cost (dollars/ft^2), depending on the particular constraints of the mission.

14.4.1 Radiative Heat Transfer

For typical spacecraft fin and tube radiators the controlling thermal resistance is conduction and radiation in the radiator fin. Therefore, the preliminary designer need only consider heat transfer in the fin. Heat transfer from the working fluid to the fin is a second-order effect and must eventually be treated in some detail.

Radiant heat transfer from a flat surface at temperature, T , to a sink at absolute zero is described by the Stefan-Boltzmann equation:

$$Q = \epsilon \sigma T^4 \quad (14-1)$$

where

Q = radiative power (watts/ft²)

ϵ = surface emissivity

σ = Stefan-Boltzmann constant = 5×10^{-10} watts/ft² °R⁴

T = radiating surface temperature (°R)

For a non-zero sink temperature, this expression becomes

$$Q = \sigma \epsilon (T^4 - T_s^4) \quad (14-2)$$

where

T_s = sink temperature (°R)

If solar illumination is incident on the radiator, it must also be rejected, reducing the effective radiative heat flux (i.e., dissipation of heat produced by an on-board source) to

$$Q = \epsilon \sigma (T^4 - T_s^4) - \alpha_s H \cos \theta \quad (14-3)$$

where

α_s = surface absorptivity to solar illumination

H = solar illumination intensity (watts/ft²)

θ = angle between the incident solar illumination and the normal to the radiator surface

ϵ = surface emissivity

A quantity termed the fin effectiveness is introduced to assist in the evaluation of the performance of a finned radiator. It is defined as the ratio of the heat rejected by the fin to that which would be rejected

if the entire fin were maintained at the base temperature. Expressed mathematically:

$$\eta = \frac{\int_0^{\frac{B}{2}} T_x^4 dx}{\frac{B}{2} T^4} \quad (14-4)$$

where

η = fin effectiveness

B = tube spacing

T_x = temperature at a point on the fin

x = distance along fin

T = fin base temperature

This equation was derived by Coombs¹ et al., and was solved numerically on an IBM-704 computer. The results are given in Figure 14-2 as a function of the dimensionless radiation modulus M_r , defined as:

$$M_r = \frac{B^2 \epsilon \sigma T^3}{kt} \quad (14-5)$$

where

k = conductivity of fin material

t = fin thickness

By using the curve in Figure 14-2 the fin effectiveness may be evaluated for a given material, geometry, and base temperature (T). Equation (14-1) is plotted in Figure 14-3 for various values of the product $\epsilon \eta$ which constitutes an effective emissivity.

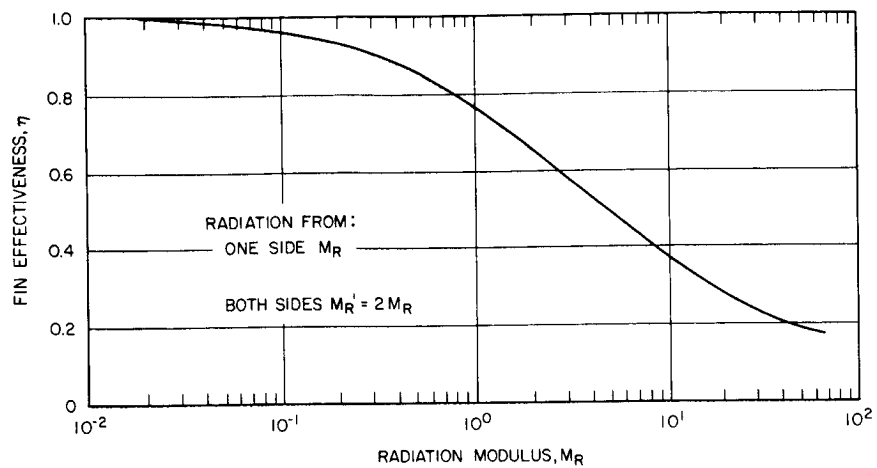


Figure 14-2. Fin effectiveness versus radiation modulus.

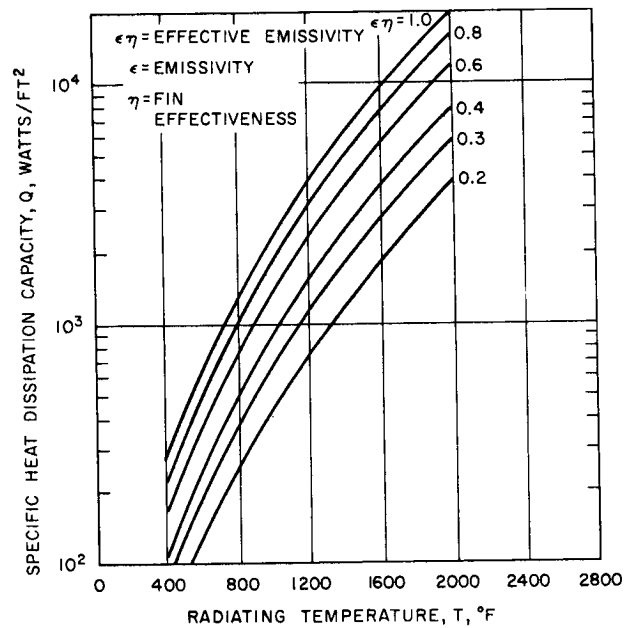


Figure 14-3. Specific heat dissipation capacity versus radiator temperature.

14.4.2 Radiator Area Requirements

Condensing Systems. For condensing radiators, the tube temperature remains constant until the fluid is completely condensed as long as the static pressure drop is kept small. This follows since the condensate and condensing vapor are always in thermal equilibrium. If this condition is met, the area requirements for the condensing portion of the radiator can be obtained by combining Equation (14-3) with the definition of fin effectiveness.

$$Q = \epsilon \sigma \eta \left(T^4 - T_s^4 \right) - \alpha_s H \cos \theta \quad (14-6)$$

Figure 14-3 can be used directly to obtain the required area if the ϵ as shown is considered to be equal to the product, $\epsilon \eta$.

Non-condensing Systems. In non-condensing systems the radiant heat rejection is accompanied by a sensible heat loss of the fluid. The temperature decrease of the fluid results in temperature gradients both perpendicular and parallel to the direction of fluid flow. This complicates the analysis, but by combining the model of the condensing (constant temperature) fin with that of a radiator which experiences a coolant temperature drop, an expression can be derived to give the area requirements for the tube-fin configuration.² The result is given by:

$$Q = \eta \sigma \epsilon T_{\text{eff}}^4 \quad (14-7)$$

where

Q = radiative power (watts/ft²)

T_{in} = fluid temperature into radiator (°R)

T_{out} = fluid temperature out of radiator (°R)

$$T_{\text{eff}} = \left[\frac{3 T_{\text{in}}^3 T_{\text{out}}^3}{T_{\text{in}}^2 + T_{\text{in}} T_{\text{out}} + T_{\text{out}}^2} \right]^{1/4}$$

and

η = fin effectiveness (evaluated at T_{eff})

Equation (14-7) is plotted in Figure 14-4 for various values of T_{in} and $\Delta T = T_{\text{in}} - T_{\text{out}}$. This figure can be used to determine the area requirements for the non-condensing radiator. Using fin effectiveness and emissivity typical of non-condensing low temperature aluminum fin and tube radiators the area requirements become³

$$A = \frac{25.5 W}{\left(\frac{T}{100}\right)^4} \text{ square feet} \quad (14-8)$$

for the zero sink temperature characteristic of deep space and

$$A = \frac{25.5 W}{\left(\frac{T}{100}\right)^4 - 320} \text{ square feet} \quad (14-9)$$

for a sink temperature of -40°F , typical of near earth orbits.

Fin and Tube Radiator Weight and Cost Burdens. According to AiResearch Corporation,⁴ low temperature radiator specific weight, assuming aluminum construction and structural rigidity as required for radiator areas greater than 50 ft^2 , is approximately 0.95 lb/ft^2 . For smaller radiator areas, depending on the amount of structural rigidity required, the specific weight may be as low as 0.045 lb/ft^2 . Radiator heat dissipation capability versus weight is plotted in Figure 14-5 based on 0.95 lb/ft^2 . Typical costs as quoted by the same source indicate development costs of \$50,000, exclusive of environmental

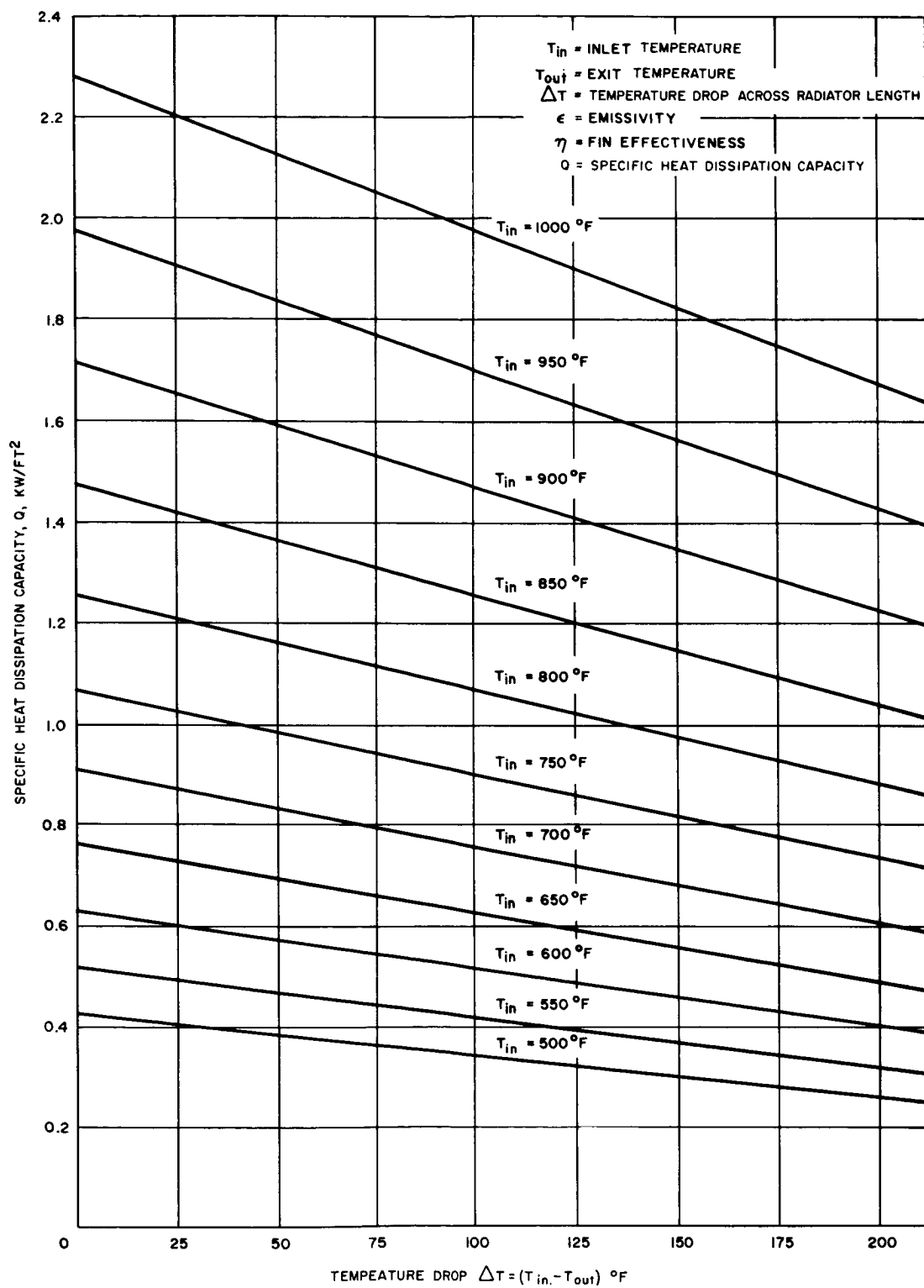


Figure 14-4. Area requirements for non-condensing radiator.

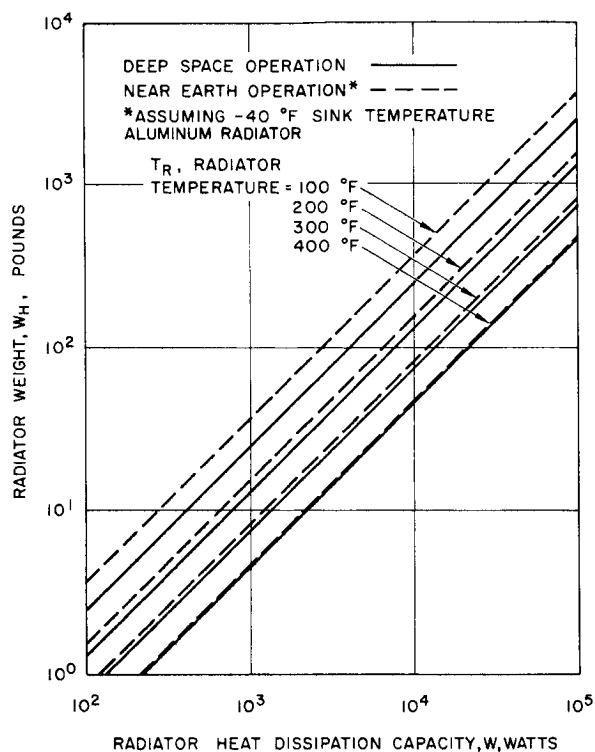


Figure 14-5. Fin and tube radiator weight, W_H (pounds), versus heat dissipation capacity at various radiator temperatures, T_R .

testing, for one 10 to 30 ft² space qualified radiator. For production of a number of identical radiators with the above development cost amortized over five units, an approximate functional relationship between radiator cost C_H and area of

$$C_H = \$13,750 + \$75 A \quad (14-10)$$

can be inferred. For large production runs, with the development cost amortized over one hundred units, the radiator cost is reduced to

$$C_H = \$2,750 + 25 A \quad (14-11)$$

Radiator heat dissipation capability versus cost for a five unit production run is plotted in Figure 14-6.

14.4.3 Pressure Drops

Condensing Systems. For both condensing and non-condensing radiators, determination of pressure drop in the coolant loop is necessary to determine the optimum tradeoff between piping diameter and coolant pump size. The design of a minimum weight condensing radiator requires an accurate prediction of the pressure drop associated with condensing in the radiator tubes. This must be done with some precision since a loss of static pressure in the condenser tubes lowers the (saturation) temperature of the working fluid, resulting in a drop in radiating power.

Viscous drag is the mechanism by which condensate is removed from a radiator-condenser. The working fluid enters the radiator-condenser as saturated vapor, and is condensed at substantially constant temperature by being subjected to a constant heat flux throughout the length of the tube. After the working fluid has been completely condensed it may be subcooled to reduce the possibility of pump cavitation, and in the case of turboelectric systems, to provide a low-temperature bearing and alternator coolant.

Many investigators have correlated pressure drop data for two-phase flow in tubes with that for single phase flow. Of these, the correlation of Lockhart and Martinelli⁵ is probably the best and most widely used. They were able to correlate pressure drop for two-phase, two-component flow in the non-dimensional form:

$$\left(\frac{dP}{dL}\right)_{\text{TPF}} = \varphi_g^2 \left(\frac{dP}{dL}\right)_g, \quad (14-12)$$

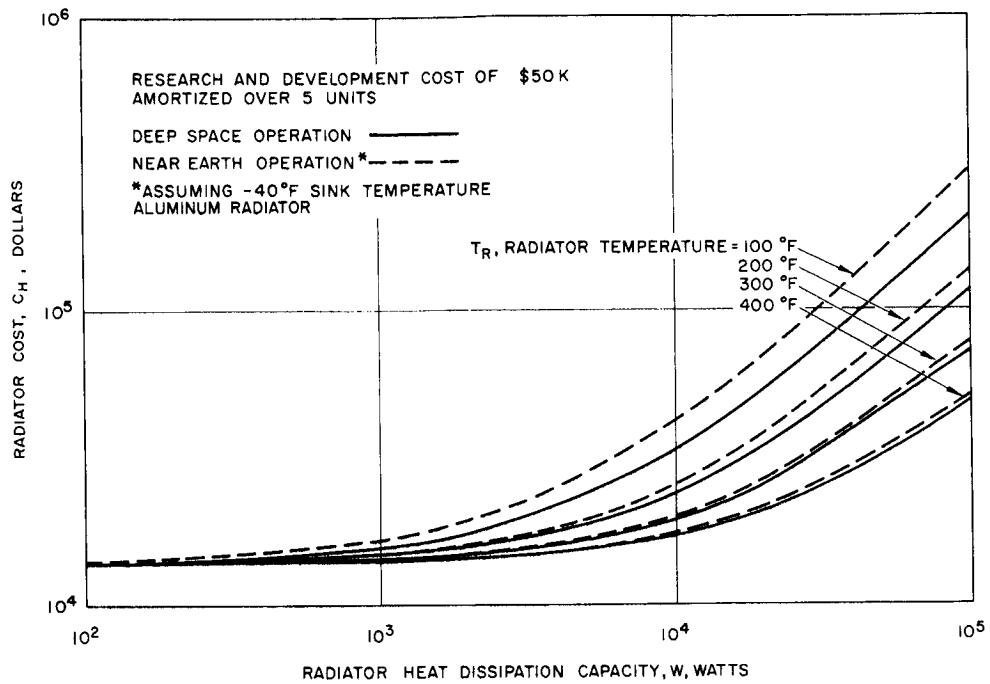


Figure 14-6. Fin and tube radiator cost, C_H , versus heat dissipation capacity at various radiator temperatures, T_R .

where

$$\left(\frac{dP}{dL}\right)_{\text{TPF}} = \text{two-phase frictional pressure gradient}$$

$$\left(\frac{dP}{dL}\right)_g = \text{pressure gradient per unit tube length of the gas (vapor) phase alone}$$

$$\left(\frac{dP}{dL}\right)_l = \text{pressure gradient per unit tube length of the liquid phase alone}$$

$$\varphi_g = \text{dimensionless parameter}$$

The experimental data of Lockhart and Martinelli were plotted in terms of φ_g and

$$\sqrt{\frac{\left(\frac{dP}{dL}\right)_l}{\left(\frac{dP}{dL}\right)_g}}$$

for different combinations of flow regimes, e. g. , viscous liquid-turbulent gas and turbulent liquid-turbulent gas. While these correlations were for two-component flow, extension of these correlations to boiling or condensing (i. e. , two-phase one-component flow) has been suggested by Martinelli and Nelson⁶ and has been tested with some success. In support of this extrapolation, McAdams⁷ has found that friction arising from transfer of momentum between phases of a one-component system was of little importance under his experimental conditions. Furthermore, Lockhart and Martinelli stated that their correlation was independent of flow mechanism, whether mist, annular or stratified flow existed. Experimental work indicates that these correlations predict reasonable values for condensing pressure drop in tubes.

The Lockhart and Martinelli correlation for viscous-turbulent flow is reproduced in Figure 14-7. In the range of interest it can be represented by

$$\phi_g = 1.76 X^{0.0825} \quad (14-13)$$

where

$$X = \sqrt{\frac{\left(\frac{dP}{dL}\right)_l}{\left(\frac{dP}{dL}\right)_g}} \quad (14-14)$$

By combining Equations (14-12), (14-13), and (14-14) with the appropriate values of $(dP/dL)_g$ and integrating the resulting expression to account for the changing flow conditions throughout the length of the tube, an expression for the frictional pressure drop can be derived.⁸ The result is given by:

$$\left(\frac{\Delta P}{L}\right)_{TPF} = \frac{0.402 W_T^{1.684} \mu_g^{0.316}}{N^{1.684} D^{4.684} \rho_g g_c} \left(\frac{\rho_g \mu_l}{\rho_l \mu_g}\right)^{0.0825} \quad (14-15)$$

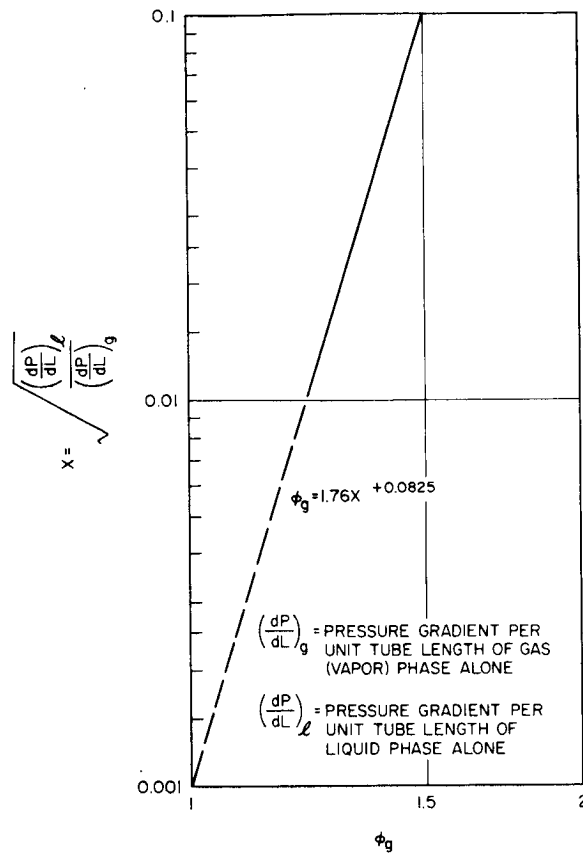


Figure 14-7. Coefficient relating the pressure gradient for two-phase flow with those for single-phase flows.

where

W_T = weight flow

μ_g = viscosity of vapor

μ_l = viscosity of liquid

N = number of tubes

D = inside tube diameter

ρ_g = density of vapor

ρ_l = density of liquid

g = gravitational constant

Any consistent system of units may be used.

In addition to the frictional pressure drop given by Equation (14-15), there is a pressure rise due to the momentum loss of the high velocity vapor as it traverses the condenser tube. Since the fluid velocity is essentially zero at the exit of the condenser this is given by

$$\Delta P_M = \int_{\text{inlet}}^{\text{outlet}} \rho u du = - \rho_g U_o^2 \quad (14-16)$$

ρ = density at two phase mixture

u = velocity of two-phase mixture flow

U_o = vapor velocity at condenser inlet

or for parallel flow through N tubes

$$\Delta P_M = \left(\frac{1.62 W_T^2}{\rho_g g D^4 N^2} \right) \quad (14-17)$$

where the negative sign indicates a pressure rise. Equations (14-15) and (14-17) can be used to calculate the pressure drop in condensing radiators.

Non-condensing Systems. In non-condensing systems, which reject heat by cooling a liquid, the pressure drop is predicted by the Fanning friction equation:

$$\frac{dP}{dL} = \frac{2f u^2 \rho}{g D} \quad (14-18)$$

where the friction factor, f , is given by

$$f = 0.079 R_e^{-0.25} \quad (14-19)$$

where R_e is the Reynolds number. For flow through N tubes in parallel:

$$\frac{\Delta P}{L} = 0.242 \frac{W_T^{1.75} \mu^{0.25}}{N^{1.75} D^{4.75} \rho g} \quad (14-20)$$

Equation (14-20) gives the pressure drop for a non-condensing radiator.

14.5 PASSIVE HEAT REJECTION SYSTEMS

Passive heat rejection systems are preferable when they can meet the requirements because of their extreme simplicity and concomitant lighter weight, lower cost, and higher reliability. They consist merely of a conducting path between the heat source and an external radiating surface, often a part of the spacecraft structure, having a highly emissive surface coating with low solar absorptivity. The limitation on their utility is almost always excessive temperature gradients in the conducting path as a result of thermal resistance. If the radiator is a flat surface having a uniform temperature, the heat dissipation capability is

$$Q = \epsilon \sigma (T^4 - T_s^4) - \alpha_s H \cos \theta \quad (14-21)$$

where

Q = radiative power (watts/ft²)

ϵ = surface emissivity

- σ = Stefan-Boltzmann constant = 5×10^{-10} watts/ft² - °R⁴
 T = radiating surface temperature (°R)
 T_s = sink temperature (°R)
 α_s = surface absorptivity to solar illumination
 H = solar illumination intensity (watts/ft²)
 θ = angle between the incident solar illumination and the normal to the radiator surface

Equation (14-21) is plotted in Figure 14-8 for various solar distances and normally incident solar illumination with $\alpha_s = 0.18$ and $\epsilon = 0.87$.*

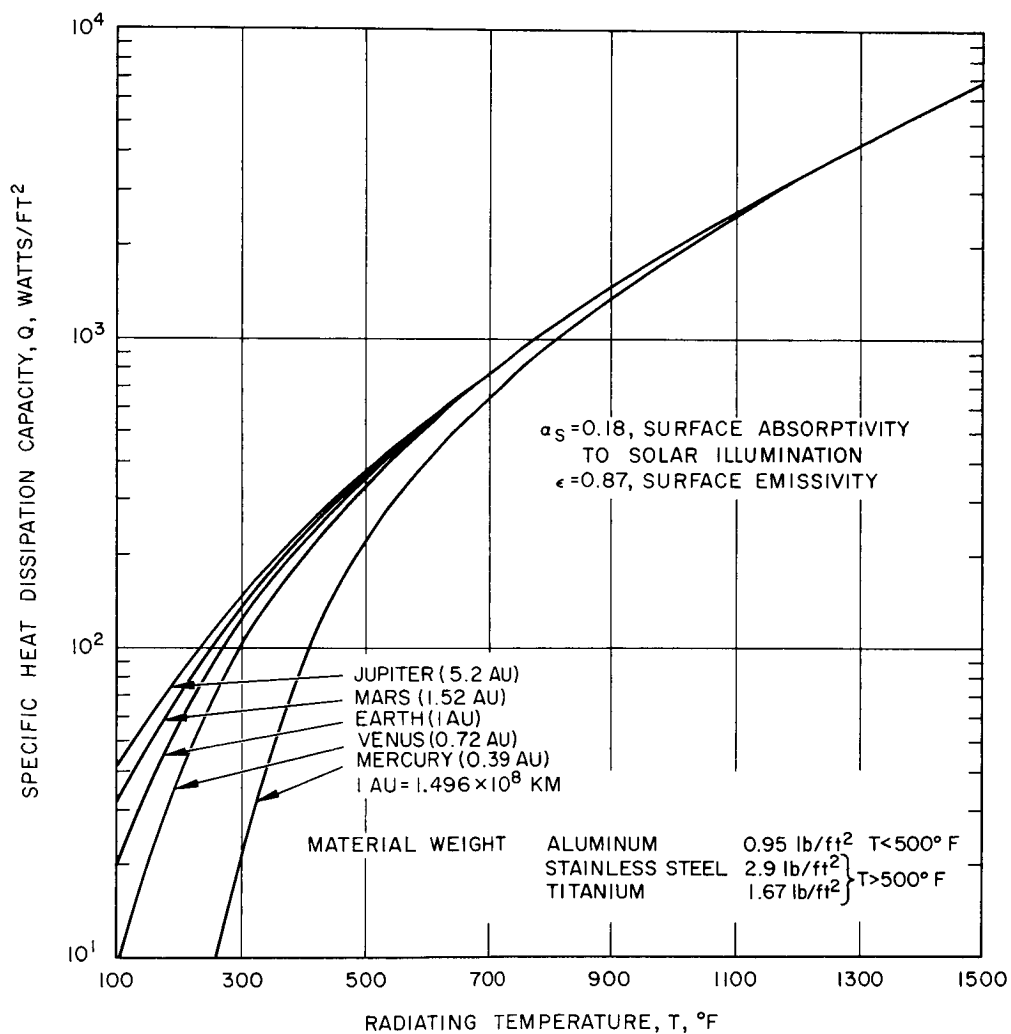


Figure 14-8. Specific heat dissipation capacity versus temperature of radiators in direct sunlight at various solar distances.

*Typical of Hughes B6003 inorganic white paint.

14.6 NOMENCLATURE

A	radiator area
B	tube spacing
C_H	radiator cost
D	inside tube diameter
f	friction factor = $0.079 R_e^{-0.25}$
g	gravitational constant
H	solar illumination (watts/ft ²)
k	conductivity of fin material
K_e	transmitter efficiency
L	length along tube
M_r	radiation modulus = $B^2 \epsilon \sigma T^3/kt$
N	number of tubes
P	pressure
ΔP_M	pressure rise due to momentum loss
Q	heat dissipation capacity (watts/ft ²)
R_e	Reynolds number
T	radiating surface temperature
T_{eff}	radiator effective temperature
T_{in}	radiator inlet temperature
T_{out}	radiator outlet temperature
ΔT	$T_{in} - T_{out}$
T_R	radiator temperature
T_s	sink temperature
T_x	temperature point on radiating fin

t	fin thickness
U_o	vapor velocity at condenser inlet
u	velocity of two-phase mixture flow in condenser
W	total heat dissipated
W_H	radiator weight
W_T	mass flow rate
X	$\sqrt{\frac{\left(\frac{dP}{dL}\right)_l}{\left(\frac{dP}{dL}\right)_g}}$
x	distance along fin from base
α_s	surface absorptivity to solar illumination
ϵ	surface emissivity
η	fin effectiveness
θ	angle between incident solar illumination and normal to the radiator surface
μ	micron
μ_g	vapor viscosity
μ_l	liquid viscosity
ρ	two-phase mixture density
ρ_g	vapor density
ρ_l	liquid density
σ	Stefan-Boltzmann constant
φ_g	dimensionless parameter which correlates pressure gradients for two-phase flow and single-phase flow, viz. , $(dP/dL)_{TPF} = \varphi^2 (dP/dL)_g$
$(dP/dL)_g$	pressure gradient per unit tube length for gas (vapor) phase alone

$(dP/dL)_\ell$	pressure gradient per unit tube length for liquid phase alone
$(dP/dL)_{TPF}$	two-phase flow frictional pressure gradient per unit tube length

14.7 REFERENCES

1. M.G. Coombs, R. A. Stone, and T. Kapus, "The SNAP 2 Radiative Condenser Analysis," NAA-SR-5317, July 1960.
2. Energy Conversion Systems Reference Handbook, Volume X, Reactor System Design, Electro-Optical Systems, September 1960.
3. Personal Communication, AiResearch Corporation.
4. Ibid.
5. R. W. Lockhart and R. C. Martinelli, "Chemical Engineering Progress," 45, pp. 39-48 (1949).
6. R. C. Martinelli and D. B. Nelson, "Transactions of the ASME," 70, pp. 695-702 (1948).
7. W.H. McAdams, W.K. Woods, and R. L. Bryan, "Transactions of the ASME," 63, pp. 545-552 (1941).
8. Energy Conversion Systems Reference Handbook, Volume X, Reactor System Design, Electro-Optical Systems, September 1960.

SIXTH QUARTERLY REPORT
CONTRACT NO. NAS 5-9637

PARAMETRIC ANALYSIS OF MICROWAVE AND LASER SYSTEMS FOR COMMUNICATION AND TRACKING

6 MARCH 1967

AEROSPACE GROUP

HUGHES

HUGHES AIRCRAFT COMPANY
CULVER CITY, CALIFORNIA

FACILITY FORM 102

05

ACCESSION NUMBER	THRU
PAGES	(CODE)
CR 8577	(CATEGORY)
NASA CR OR TRX OR AD NUMBER	